# NACA

# RESEARCH MEMORANDUM

INVESTIGATION OF THE I-40 JET-PROPULSION ENGINE IN THE

CLEVELAND ALTITUDE WIND TUNNEL

I - PERFORMANCE AND WINDMILLING DRAG CHARACTERISTICS

By Stanley L. Gendler and William K. Koffel

Flight Propulsion Research Laboratory
Cleveland, Ohio

CLASSIFICATION CHANGED TO
UNCLASSIFIED
AUTHORITY CROWLEY CHANGE #1951
DATE 12-14-53            T.C.F.

# NATIONAL ADVISORY COMMITTEE
# FOR AERONAUTICS
WASHINGTON
August 24, 1948

NATIONAL ADVISORY COMMITTEE FOR AERONAUTICS

RESEARCH MEMORANDUM

INVESTIGATION OF THE I-40 JET-PROPULSION ENGINE IN THE

CLEVELAND ALTITUDE WIND TUNNEL

I - PERFORMANCE AND WINDMILLING DRAG CHARACTERISTICS

By Stanley L. Gendler and William K. Koffel

SUMMARY

The performance characteristics of the I-40 jet-propulsion engine are presented and analyzed for a range of altitudes from 10,000 to 40,000 feet and a range of ram pressure ratios from 0.98 to 1.76.

At an engine speed of 11,500 rpm, the net thrust and the net-thrust horsepower decreased about 25 percent at any airspeed with each 10,000-foot increase in altitude. At an altitude of 30,000 feet and an engine speed of 11,500 rpm, the net thrust increased from 1525 to 1890 pounds with an increase of airspeed from 235 to 640 miles per hour. At a constant engine speed of 11,500 rpm, the specific fuel consumption based on net-thrust horsepower showed no apparent altitude effect and decreased from 2.10 pounds to 0.80 pound of fuel per horsepower hour as the airspeed increased from 235 to 640 miles per hour.

The use of generalizing factors for estimating altitude performance of the engine gave only fair results; for example, the performance at 40,000 feet may be calculated from data obtained at 20,000 feet with an accuracy within about 9 percent at a corrected engine speed of 11,500 rpm.

At an altitude of 20,000 feet, the internal drag when the engine was windmilling at airspeeds from 235 to 550 miles per hour is shown to increase from 2.6 to 13.7 percent of the net thrust developed by the engine operating at 11,500 rpm at the same respective airspeeds. At an airspeed of 400 miles per hour the windmilling drag decreased from 8.4 percent of the net thrust developed by the engine operating at 11,500 rpm at 10,000 feet to 5.6 percent at 40,000 feet.

# INTRODUCTION

An investigation has been conducted in the Cleveland altitude wind tunnel to determine the performance and operational characteristics of the I-40 jet-propulsion engine and its components. The over-all performance and the windmilling drag characteristics of the engine over a range of altitudes from 10,000 to 40,000 feet and ram pressure ratios from 0.98 to 1.76 are presented. These ram pressure ratios correspond to true airspeeds of about 0 to 640 miles per hour.

A preliminary presentation of general effects observed in altitude investigations of several jet-propulsion engines including the I-40 was given in reference 1. The I-40 performance data presented herein supersede those in reference 1 where slight differences exist between corresponding curves.

Efficiencies of the engine components are presented as an aid in interpreting the engine-performance curves. An induction-system efficiency of 100 percent was used in calculating the net thrust and the airspeeds. The free-stream total pressure was assumed to be equal to the total pressure at the compressor inlets in order that the performance data may be applied to the installation of the I-40 engine in any airplane in which the induction-system efficiency is known. Gas flow and thrust were calculated from survey-rake measurements at the tail-pipe-nozzle outlet. The reliability of the use of generalizing factors in estimating engine performance at any altitude from experimental data obtained at another altitude was examined.

Several types of fuel system were investigated on the engine in an effort to improve the engine operation. Because none of the revised systems materially changed the engine performance, the performance of the engine with the original fuel system including a barometric control and 40-gallon-per-hour fuel nozzles is presented.

# DESCRIPTION OF ENGINE

The I-40 jet-propulsion engine is $102\frac{7}{8}$ inches in length from the front of the accessory section to the rear of the exhaust cone, 48 inches in diameter, and weighs approximately 1850 pounds. The power ratings of the engine for static sea-level operation are:

629

|                                                        | Military take-off | Normal | Idling |
|--------------------------------------------------------|-------------------|--------|--------|
| Engine speed, (rpm)                                    | 11,500            | 11,000 | 3500   |
| Thrust, (lb)                                           | 3,750             | 3,200  | 200    |
| Maximum exhaust temperature, (°F)                      | 1,200             | 1,100  | ------ |
| Thrust specific fuel consumption, (lb/(hr)(lb thrust)) | 1.20              | 1.20   | ------ |
| Fuel flow, (lb/hr)                                     | --------          | ------ | 880    |

The engine consists of five component sections: compressor, combustion chambers, turbine, accessory section, and exhaust cone and tail pipe. The total area of the compressor inlets, including the 5-mesh screen covering the openings, is 6.53 square feet. The compressor casing contains an aluminum impeller of the double-entry centrifugal type, which is 30 inches in diameter. Air discharges from the impeller into the diffuser, which guides and diffuses the air into the air adapters connected to each of the 14 combustion-chamber inlets.

The compressor impeller is bolted between two flanged shafts that rotate on a ball thrust bearing at the front and a roller bearing at the rear. The rear shaft is coupled to the turbine shaft by a splined coupling and the front shaft drives the accessory train. The turbine shaft also rotates on a ball thrust bearing at the front of the shaft and a roller bearing immediately ahead of the turbine.

The burner section is composed of 14 combustion chambers of the through-flow type into which the air and the fuel are introduced at the front and from which the hot products of combustion are discharged from the rear. Each combustion chamber contains a perforated and truncated combustion liner that divides the combustion zone from the tapered annular passage through which the secondary air flows. The upstream end of the combustion liner is covered with a dome having perforations for admittance of primary air into the combustion zone. Each dome contains a 40-gallon-per-hour fuel nozzle with an 80° spray cone. Fuel is directed downstream along the axis of the combustion chamber. Ignition for starting is provided by spark plugs that project through the air adapters and the combustion-chamber domes into the fuel sprays of two combustion chambers. All combustion chambers are interconnected with cross-ignition tubes, which ignite the remaining combustion chambers.

The combustion chambers discharge into a collector that forms the nozzle box for the turbine. Exhaust gases leaving the turbine

pass through the annular space formed between the inner and outer
exhaust cones. The inner cone is supported by four vanes, which
also reduce the rotation of the gases before they are discharged
into the exhaust pipe.

In the standard fuel system, fuel is supplied to each fuel-
injection nozzle from a common fuel manifold at pressures ranging
from 10 to 180 pounds per square inch, depending on engine speed
and altitude. The main fuel pump is a positive-displacement pump
driven by the engine. Fuel is pumped to the fuel-nozzle manifold
at high pressure. Fuel flow is regulated by three controls: a
manual control valve, a "barometric," and a governor. The manual-
control valve consists of a poppet-type shut-off valve closed to
stop the engine and a sliding-cylinder throttling valve set by the
pilot for the desired operating speed. The barometric and the
governor bypass the fuel from the high-pressure line between the
fuel pump and the nozzles back to the pump inlet. The function of
the barometric is to maintain constant engine speed for a given
cockpit throttle setting, regardless of changes in altitude and
airspeed. The governor limits the maximum engine speed to
11,500 rpm.

All bearings on the impeller and turbine shafts and the splined
coupling are lubricated by jets of oil pumped from the accessory
section. The oil drains from the bearings into a sump and is pumped
back into the oil-supply reservoir in the accessory case. The
accessory case is mounted on the front of the engine and supports
the engine accessories. The gears and the bearings in the accessory
drive assembly are splash-lubricated from the gear that drives the
oil pump.

Some of the air approaching the rear impeller inlet of the com-
pressor is used for engine cooling air. A cooling-air fan mounted
on the front side of the turbine wheel pumps cooling air through the
engine as shown in figure 1. A baffle on the engine is sealed to
the nacelle wall to limit the cooling-air flow. The maximum cooling-
air flow is given by the manufacturer as about 2 percent of the air
flow through the engine at an engine speed of 11,500 rpm.

TUNNEL INSTALLATION AND INSTRUMENTATION OF ENGINE

An I-40-3 engine was installed in an airplane fuselage mounted
in the 20-foot-diameter test section of the altitude wind tunnel as
shown in figure 2. Air entered the airplane through inlets on both
sides of the fuselage near the wing fillets (fig. 3) and flowed

through ducts into a plenum chamber surrounding the engine. The air then entered the engine through openings on both sides of the double-entry compressor. (See fig. 1.)

Two inlet configurations were used for these runs. In the first configuration, air was taken from the tunnel test section through the normal airplane intake ducts for "static tests" (fig. 3). In the second configuration, air from the tunnel make-up air system was introduced into the airplane's two inlet ducts through a Y-shaped ram pipe (fig. 4). This air was throttled from approximately sea-level pressure to the pressure corresponding to the desired ram pressure ratio at a given altitude.

This airplane installation included a tail pipe 93.3 inches in length. The tail pipe had a straight taper from a 21-inch diameter at the exhaust-cone discharge to a 19-inch diameter at the tail-pipe-nozzle outlet.

The engine was extensively instrumented. (See fig. 5.) The location of the nine stations used in making the engine analysis is shown in figure 1. The data presented were obtained by means of the instrumentation identified by slant type in figure 5. Thermocouples of the type used at stations 4 and 8 were calibrated for impact temperature rise over a range of Mach numbers from 0 to 0.75. The impact recovery factors thus obtained were used to correct the indicated thermocouple temperatures.


PROCEDURE

Investigations were conducted over a range of altitudes from 10,000 to 40,000 feet and ram pressure ratios from 0.98 to 1.76. At each altitude and ram pressure ratio, the engine speed was varied from approximately minimum operable speed to 11,500 rpm. During ram tests, the pressure in the ram pipe was adjusted to give a total pressure at the compressor inlet that corresponded to the desired ram pressure ratio at the desired altitude; the pressure in the tunnel was adjusted to the static pressure at that altitude. The air temperatures in the ram pipe and in the tunnel were maintained as close to the desired values as the tunnel refrigeration system and running time would allow.

When the ram pipe was installed, measurements of engine thrust and installation drag with the tunnel balance scale were made possible by the slip joint in the ram pipe about 36 feet upstream of the inlets. (See fig. 4.)

In order to determine the external drag of the installation, power-off drag tests were conducted with the inlets and the tail-pipe-nozzle outlet covered with streamlined fairings. Power-off drag tests were also run with the Y-shaped ram pipe installed and with a blind flange in the ram pipe just upstream of the slip joint.

During static tests, speeds of 76 to 127 feet per second were induced in the air of the tunnel test section by the ejector effect of the jet and by the tunnel exhaust scoop, which was located in the air stream immediately downstream of the test section.

## SYMBOLS

The symbols and necessary numerical values used in this report are as follows:

$A_4$      compressor outlet area at station 4, (1.621 sq ft)

$A_8$      tail-pipe-nozzle outlet area at station 8 (hot), (sq ft)

$A_8'$      tail-pipe-nozzle outlet area at station 8 at 520° R, (1.973 sq ft)

$A_x$      annular increment of area of tail-pipe-nozzle outlet, (sq ft)

C        jet-thrust calibration factor for tail-pipe-nozzle outlet rake, (0.968)

$c_p$      specific heat of air at constant pressure, (0.241 Btu/(lb)(°R))

$D_w$      windmilling drag, (lb)

$F_j$      jet thrust, (lb)

$F_n$      net thrust, (lb)

g        acceleration due to gravity, (ft/sec$^2$)

H        enthalpy of exhaust gas as obtained from figure 1 of reference 3, (Btu/lb)

J        mechanical equivalent of heat, (778 ft-lb/Btu)

K        gas-flow calibration factor for tail-pipe-nozzle outlet rake, (0.964)

M          mass flow, (slugs/sec)

N          engine speed, (rpm)

P          total pressure, (lb/sq ft absolute)

p          static pressure, (lb/sq ft absolute)

$P_2/p_0$  ram pressure ratio

q          dynamic pressure, (lb/sq ft)

R          gas constant, (ft-lb/(lb)($^\circ$R)); (for air = 53.30, for exhaust gas = 53.86)

T          total temperature, ($^\circ$R)

$T_i$      indicated temperature, ($^\circ$R)

t          static temperature, ($^\circ$R)

thp        net-thrust horsepower

V          velocity, (ft/sec)

v          airspeed, (mph)

W          weight flow

$W_f/F_j$  specific fuel consumption based on jet thrust, (lb/(hr)(lb thrust))

$W_f/F_n$  specific fuel consumption based on net thrust, (lb/(hr)(lb thrust))

$W_f/thp$  specific fuel consumption based on net-thrust horsepower, (lb/(hr)(net-thrust hp)) (Same as corrected specific fuel consumption based on net-thrust horsepower.)

$W_f/W_a$  fuel-air ratio

$\alpha$   thermocouple impact recovery factor (0.86 at stations 4 and 8)

$\gamma$   ratio of specific heats, (1.4 for air and variable for exhaust gas)

$\eta_b$   combustion efficiency, (percent)

$\eta_c$          compressor adiabatic efficiency, (percent)

$\eta_t$          turbine adiabatic efficiency, (percent)

$\rho$            density, (slugs/cu ft)

$\delta$          ratio of the average total pressure at front and near
                  compressor inlets to absolute static pressure of NACA
                  standard atmosphere at sea level

$\theta$          ratio of the average total temperature at front and
                  rear compressor inlets to absolute static tempera-
                  ture of NACA standard atmosphere at sea level

Subscripts:

0                 effective free-stream ambient conditions

2                 compressor inlet, (average of front and rear inlets)

4                 compressor outlet

5                 turbine-nozzle inlet

8                 tail-pipe-nozzle outlet

a                 air

f                 fuel

g                 exhaust gas

j                 vena contracta of exhaust jet

s                 tail-pipe-nozzle outlet shell

x                 annular increment of area in tail-pipe-nozzle outlet

The following parameters are generalized to NACA standard atmos-
pheric conditions at sea level:

$F_j/\delta$      corrected jet thrust, (lb)

$F_n/\delta$      corrected net thrust, (lb)

$N/\sqrt{\theta}$ corrected engine speed, (rpm)

$thp/(\delta\sqrt{\theta})$          corrected net-thrust horsepower

$v_O/\sqrt{\theta}$            corrected true airspeed, (mph)

$W_a\sqrt{\theta}/\delta$         corrected air flow, (lb/sec)

$W_f/(\delta\sqrt{\theta})$         corrected fuel flow, (lb/hr)

$W_f/(F_j\sqrt{\theta})$        corrected specific fuel consumption based on jet thrust,
                       (lb/(hr)(lb thrust))

$W_f/(F_n\sqrt{\theta})$        corrected specific fuel consumption based on net thrust,
                       (lb/(hr)(lb thrust))

$W_f/(W_a\theta)$           corrected fuel-air ratio

## METHOD OF CALCULATION

### Temperature

The effective free-stream ambient temperature with the ram pipe installed is calculated from the ram pressure ratio:

$$t_0 = T_2 \left(\frac{p_0}{P_2}\right)^{\frac{\gamma-1}{\gamma}} \tag{1}$$

The average total temperature at the compressor inlets was assumed to be equal to the average indicated temperature at the compressor inlets; this assumption resulted in an error of less than 0.2 percent.

Total temperature at the outlet of the compressor was calculated from the equation

$$T_4 = T_{i,4} + \left(\frac{1-\alpha}{2gJc_p}\right)\left(\frac{W_a R_a t_4}{p_4 A_4}\right)^2 \tag{2}$$

but with the indicated temperature $T_{i,4}$ and total pressure $P_4$ at the compressor outlet instead of static temperature $t_4$ and static pressure $p_4$, respectively. This procedure introduced a negligible error in the impact-recovery corrections.

The static temperature at the tail-pipe-nozzle outlet was calculated from

$$t_8 = \cfrac{T_{i,8}}{1 + \alpha\left[\left(\cfrac{P_8}{p_8}\right)^{\frac{\gamma-1}{\gamma}} - 1\right]} \tag{3}$$

and the total temperature is

$$T_8 = \cfrac{T_{i,8}\left(\cfrac{P_8}{p_8}\right)^{\frac{\gamma-1}{\gamma}}}{1 + \alpha\left[\left(\cfrac{P_8}{p_8}\right)^{\frac{\gamma-1}{\gamma}} - 1\right]} \tag{4}$$

The thermocouples in the turbine-nozzle inlet (fig. 5) did not accurately measure the temperature of the gas because of the proximity of the flame and the high turbulence of the flow. As a result the enthalpy $H_5$ at the turbine-nozzle inlet was calculated from the temperature at the tail-pipe-nozzle outlet by use of

$$H_5 = c_p (T_4 - T_2) + H_8 \tag{5}$$

Equation (5) is based on two assumptions: (a) The bearing friction losses and power to accessories are small, and (b) the total heat loss between the turbine outlet and the tail-pipe-nozzle outlet is small. The temperature at the inlet to the turbine nozzles $T_5$, corresponding to the total enthalpy $H_5$, was obtained from figure 1 of reference 3.

All data have been corrected for small variations in the temperature of the air at the compressor inlets from the temperature at the given altitude and ram pressure ratio by means of the usual altitude generalizing factors.

## Effective Airspeed

Inasmuch as all calculations are based on 100-percent ram effi-
ciency, the ram pressure ratio is used to determine the effective
free-stream velocity.  The effective free-stream velocity was cal-
culated from

$$V_0 = \sqrt{\frac{2\gamma g R_a}{\gamma-1} t_0 \left[ \left(\frac{P_2}{P_0}\right)^{\frac{\gamma-1}{\gamma}} - 1 \right]} \qquad (6)$$

Owing to the losses in the intake ducts during static tests,
the total pressure at the compressor inlets was slightly less than
the free-stream static pressure and the resulting ram pressure
ratio was less than 1.0.  Because effective free-stream velocity
becomes mathematically imaginary, quantities involving initial
momentum at a ram pressure ratio of 0.98 have been omitted from this
report.

## Gas Flow

Gas flow was calculated from temperature and pressure measure-
ments obtained with a survey rake located at the tail-pipe-nozzle
outlet.  The equation for calculating gas flow was derived from the
definition of weight flow:

$$W_g = g\rho_8 A_8 V_8 \qquad (7)$$

When Bernoulli's compressible-flow equation for velocity is applied,
the velocity of the jet at the nozzle outlet is

$$V_8 = \sqrt{\frac{2\gamma g R_8 t_8}{\gamma-1} \left[ \left(\frac{P_8}{p_8}\right)^{\frac{\gamma-1}{\gamma}} - 1 \right]} \qquad (8)$$

The expression for mass density is

$$\rho_8 = \frac{p_8}{g R_g t_8} \qquad (9)$$

and, when equations (8) and (9) are substituted into equation (7),
the equation for gas flow is

$$W_g = p_8 A_8 \sqrt{\frac{2\gamma g}{(\gamma-1)R_g t_8}} \sqrt{\left(\frac{P_8}{p_8}\right)^{\frac{\gamma-1}{\gamma}} - 1} \tag{10}$$

Inasmuch as the total and static pressures and temperatures vary appreciably across the tail pipe, the gas flow is the summation of the gas flow through each annular element of the tail-pipe-nozzle outlet area. Substitution of equation (3) and application of the gas-flow calibration factor in equation (10) gives

$$W_g = Kp_8 \sqrt{\frac{2\gamma g}{(\gamma-1)R_g}} \sum A_x \sqrt{\frac{\left[\left(\frac{P_x}{p_x}\right)^{\frac{\gamma-1}{\gamma}} - 1\right] + \alpha\left[\left(\frac{P_x}{p_x}\right)^{\frac{\gamma-1}{\gamma}} - 1\right]^2}{T_{i,x}}} \tag{11}$$

The values of $\gamma$ used in equation (11) correspond to the static temperatures at the tail-pipe-nozzle area and were obtained from a curve for a fuel-air ratio of 0.02 and a combustion efficiency of 70 percent.

In order to correct for the thermal expansion of the area of tail-pipe-nozzle outlet, the coefficient of expansion of area is taken as twice the linear coefficient of expansion times the temperature rise. Because the coefficient of linear expansion for Inconel is approximately $9 \times 10^{-6}$ inches per inch per $^\circ$F for a range of temperatures from $100^\circ$ to $1400^\circ$ F, the equation for the hot area becomes

$$A_8 = A_8' \left[1 + 1.8 \times 10^{-5} (T_s - 520)\right] \tag{12}$$

When modified to include the correction for the hot tail-pipe-nozzle outlet area, equation (11) becomes

$$W_g = \left\{Kp_8 \sqrt{\frac{2\gamma g}{(\gamma-1)R_g}} \sum A_x \sqrt{\frac{\left[\left(\frac{P_x}{p_x}\right)^{\frac{\gamma-1}{\gamma}} - 1\right] + \alpha\left[\left(\frac{P_x}{p_x}\right)^{\frac{\gamma-1}{\gamma}} - 1\right]^2}{T_{i,x}}}\right\} Y \tag{13}$$

where

$$Y = 1 + 1.8 \times 10^{-5} (T_s - 520)$$

Air flow is then found by subtracting the fuel flow

$$W_a = W_g - W_f \tag{14}$$

### Thrust

The thrust was calculated from the temperature and pressure measurements used in calculating the gas flow. Calculation of jet thrust was accomplished by the use of an equation derived from the general formula

$$F_j = M_g V_j = M_g V_8 + A_8 (p_8 - p_0) \tag{15}$$

where

$$M_g V_8 = \rho_8 A_8 V_8^2 \tag{16}$$

Substitution of equations (8) and (9) into equation (16) and summation of the forces from each incremental annular area gives

$$M_g V_8 = \frac{2\gamma}{\gamma - 1} p_8 \sum A_x \left[ \left( \frac{P_x}{p_x} \right)^{\frac{\gamma - 1}{\gamma}} - 1 \right] \tag{17}$$

Substituting equation (17) into equation (15) and applying the calibration factor C and the correction for the hot tail-pipe-nozzle outlet area gives the final equation for jet thrust

$$F_j = C \left\{ \frac{2\gamma}{\gamma - 1} p_8 \sum A_x \left[ \left( \frac{P_x}{p_x} \right)^{\frac{\gamma - 1}{\gamma}} - 1 \right] + A_8 (p_8 - p_0) \right\} Y \tag{18}$$

where

$$Y = 1 + 1.8 \times 10^{-5} (T_s - 520)$$

and $\gamma$ varies with the tail-pipe temperature.

The jet-thrust and the gas-flow calibration factors, which are defined as the ratio of the measured to the calculated values, are

0.968 and 0.964, respectively, for the tail-pipe-nozzle outlet rake.
These factors were determined from sea-level, static test-stand
data. Altitude-wind-tunnel investigations indicated that these
factors were unaffected by altitude and engine speed.

Subtracting the initial free-stream momentum of the inlet air
from the jet thrust gives the following equation for net thrust:

$$F_n = F_j - M_a V_0 \tag{19}$$

Windmilling drag was calculated from the expression

$$D_w = M_a (V_0 - V_j) \tag{20}$$

which was in agreement with drag measured with the wind-tunnel
balance.

## Horsepower

Net-thrust horsepower may be calculated from the product of
airspeed in feet per second and net thrust by the relation

$$thp = \frac{F_n V_0}{550} \tag{21}$$

## Compressor Efficiency

Compressor adiabatic efficiency is defined as the ratio of the
adiabatic temperature rise to the actual temperature rise through
the compressor

$$\eta_c = \frac{\left(\dfrac{P_4}{P_2}\right)^{\frac{\gamma-1}{\gamma}} - 1}{\dfrac{T_4}{T_2} - 1} \tag{22}$$

## Combustion Efficiency

Combustion efficiency may be defined as the ratio of the "ideal"
fuel-air ratio required for the production of the measured combustion
temperature to the fuel-air ratio actually measured

$$\eta_b = \frac{\text{ideal fuel-air ratio}}{\text{actual fuel-air ratio}} \tag{23}$$

The ideal fuel-air ratio is obtained by use of an alinement chart (fig. 1 of reference 2). The initial air temperature is taken as the average compressor-inlet temperature $T_2$ and the final combustion temperature is taken as the tail-pipe-nozzle outlet total temperature $T_8$. The engine burned kerosene with a hydrogen-carbon ratio of 0.175 and a lower heating value of 18,600 Btu per pound.

## Turbine Efficiency

Turbine efficiency as used herein is the ratio of the actual temperature drop to the adiabatic temperature drop from the turbine-nozzle inlet pressure to the tail-pipe-nozzle outlet pressure

$$\eta_t = \frac{1 - \dfrac{T_8}{T_5}}{1 - \left(\dfrac{P_8}{P_5}\right)^{\frac{\gamma-1}{\gamma}}} \tag{24}$$

Turbine efficiency is uncorrected for losses in the tail pipe because the instrumentation gave inaccurate temperatures at the turbine outlet. Equation (24) probably gives values close to the actual turbine efficiency because the losses in the tail pipe are small.

## RESULTS AND DISCUSSION

### Component Efficiencies

The performance of a jet-propulsion engine is determined to a large extent by the efficiencies of its components. Knowledge of the effects of altitude and ram pressure ratio on the component efficiencies is of assistance in analyzing the over-all performance of a jet engine. Figures 6 to 8 present the variation of compressor adiabatic efficiency, combustion efficiency, and turbine adiabatic efficiency, respectively, of the I-40 engine with engine speed, altitude, and ram pressure ratio.

Compressor efficiency. - Compressor adiabatic efficiency at a ram pressure ratio of approximately 1.2 reached a maximum of 69.5 percent at an engine speed of 10,000 rpm and fell off to 68 percent at

11,500 rpm (fig. 6(a)). Altitude had no significant effect on compressor efficiency at any engine speed. Figure 6(b) shows that the compressor efficiency decreased rapidly with increasing ram pressure ratio at low engine speeds. At engine speeds above 10,000 rpm, however, ram pressure ratio had little effect.

Combustion efficiency. - The combustion efficiency decreased rapidly with increasing altitude at low engine speeds, as shown in figure 7(a). At 11,500 rpm the combustion efficiency varied from approximately 96 to 94 percent with a change in altitude from 10,000 to 40,000 feet. Combustion efficiency was unaffected by ram pressure ratio (fig. 7(b)).

Turbine efficiency. - Turbine adiabatic efficiency at a ram pressure ratio of approximately 1.2 reached a maximum of nearly 84 percent at an engine speed of 7000 rpm and decreased to 80 percent at 11,500 rpm (fig. 8(a)). Altitude had no discernible effect on turbine efficiency at any engine speed. The data in figure 8(b) indicate that turbine efficiency is at a maximum at a ram pressure ratio of approximately 1.08 at all engine speeds and decreases with both increasing and decreasing ram pressure ratio. At engine speeds above approximately 8000 rpm, the effect of ram pressure ratio on the turbine efficiency was small. No data points are shown in figure 8(b) because the great number of points would obscure the effect of ram pressure ratio.

## Engine Performance

Altitude effect on performance. - Comparison of engine performance at altitudes of 10,000, 20,000, 30,000, and 40,000 feet at a ram pressure ratio of approximately 1.2 shows that air flow, jet thrust, net thrust, and net-thrust horsepower (figs. 9 to 12) decreased with altitude as a result of decreased air density and decreased mass air flow at high altitudes.

Altitude had no effect on the specific fuel consumption based on net-thrust horsepower as shown in figure 13. Inasmuch as the compressor-inlet air temperature decreased with increasing altitude and the compressor operated at a higher effective corrected engine speed and a higher compressor pressure ratio, the cycle efficiency was increased. This increase in cycle efficiency was apparently balanced by the loss in combustion efficiency (fig. 7). Increased specific fuel consumption in the low engine-speed range was caused by the low component and cycle efficiencies. Similarly, the specific fuel consumption based on net thrust (fig. 14) showed no altitude effect. At an engine speed of 11,500 rpm and a ram pressure ratio

of approximately 1.2, the specific fuel consumption was 1.40 pounds of fuel per horsepower-hour and 1.35 pounds of fuel per hour per pound of net thrust.

Specific fuel consumption based on jet thrust (fig. 15) decreased with increasing engine speed and decreasing altitude.

The fuel consumption of the I-40 engine (fig. 16) decreased with increasing altitude at constant engine speed because the net thrust horsepower (fig. 12) decreased with increasing altitude and the specific fuel consumption based on net thrust horsepower (fig. 13) was unaffected by altitude.

The fuel-air ratio (fig. 17) increased with altitude throughout the entire range of engine speeds. The increase in fuel-air ratio at a given altitude as idling speed is approached is caused by the rapid decrease in combustion efficiency.

Ram-pressure-ratio effect on performance. - Performance results showing the effects of ram pressure ratio at an altitude of 30,000 feet are shown in figures 18 to 26. The increase in air flow with increasing ram pressure ratio over the entire range of engine speeds is shown in figure 18. The jet thrust (fig. 19) was greater at high ram pressure ratios as a result of the increasing mass air flow and jet velocity.

The curves of net thrust at an altitude of 30,000 feet plotted against engine speed for several ram pressure ratios cross as shown in figure 20. A similar effect of ram pressure ratio and engine speed on net thrust horsepower is shown in figure 21.

At engine speeds greater than 8500 rpm, the specific fuel consumption based on net thrust horsepower (fig. 22) decreased with increasing ram pressure ratio because the cycle efficiency improved. In the range of low engine speeds the specific fuel consumption increased with ram pressure ratio because the compressor efficiency (fig. 6(b)) and the turbine efficiency (fig. 8(b)) decreased rapidly with an increase in ram pressure ratio from 1.08 to 1.76, even though cycle efficiency improved with ram pressure ratio.

Specific fuel consumption based on net thrust (fig. 23) increased with increasing ram pressure ratio at all engine speeds; whereas specific fuel consumption based on jet thrust decreased (fig. 24). The increase in specific fuel consumption based on net thrust with increasing ram pressure ratio results from the omission of airspeed in the determination of the net thrust specific fuel consumption.

The extended portions of the curves in figures 22 and 23 were determined from the faired curves of fuel flow, net thrust, and net thrust horsepower plotted against engine speed.

Fuel consumption was increased by increased ram pressure ratio (fig. 25) at engine speeds greater than 9000 rpm and was decreased at lower speeds. Fuel-air ratio (fig. 26) decreased with increased ram pressure ratio at all engine speeds.

The specific fuel-consumption data in figures 22 and 23 are replotted in figures 27 and 28 against net thrust horsepower and net thrust, respectively. The power specific fuel consumption of the I-40 engine is a minimum at maximum power output.

As an aid in estimating the performance of an airplane-engine combination, net thrust, net thrust horsepower, and specific fuel consumption based on net thrust horsepower are plotted against air-speed at several altitudes (fig. 29 to 31).

At an engine speed of 11,500 at all altitudes, the minimum net thrust (fig. 29) was at approximately 275 miles per hour. The decrease in net thrust at an engine speed of 11,500 rpm was approximately 25 percent per 10,000-foot increase in altitude at any air-speed. At 30,000 feet and 11,500 rpm, an increase in airspeed from 235 miles per hour to 640 miles per hour resulted in an increase in net thrust from 1525 pounds to 1890 pounds (fig. 29) and an increase in net thrust horsepower from 955 to 3200 (fig. 30).

At an engine speed of 11,500 rpm the specific fuel consumption based on net thrust horsepower (fig. 31) decreased from 2.10 pounds to 0.80 pound of fuel per horsepower-hour as airspeed increased from 235 to 640 miles per hour. Specific fuel consumption based on net thrust horsepower showed no altitude effect.

## Generalizing Factors

Performance testing of jet-propulsion engines would be greatly facilitated if data obtained at a given altitude and ram pressure ratio could be used to estimate engine performance at any altitude condition. The generalizing factors $\theta$ and $\delta$ have been derived for the reduction of data obtained at altitude conditions to sea-level conditions by applying the methods of dimensional analysis (reference 3). The generalized parameters used to present engine performance are: engine speed, $N/\sqrt{\theta}$; jet thrust, $F_j/\delta$; net

thrust, $F_n/\delta$; net thrust horsepower, $thp/(\delta\sqrt{\theta})$; air flow, $W_a\sqrt{\theta}/\delta$; fuel flow, $W_f/(\delta\sqrt{\theta})$; jet thrust specific fuel consumption, $W_f/(F_j\sqrt{\theta})$; net thrust specific fuel consumption, $W_f/(F_n\sqrt{\theta})$; net thrust horsepower specific fuel consumption, $W_f/thp$; and fuel-air ratio, $W_f/(W_a\theta)$.

Altitude effect on generalized data. - Corrected air flow, corrected jet thrust, corrected net thrust, and corrected net thrust horsepower each reduced to a single curve at low engine speeds for all altitudes at a ram pressure ratio of approximately 1.2 are shown in figures 32 to 35. At 11,500 rpm, an increase in altitude from 20,000 to 40,000 feet decreased the corrected air flow about 5 percent and decreased the corrected jet thrust, corrected net thrust, and corrected net thrust horsepower about 9 percent each. The failure of the data to generalize to one curve in figures 32 to 35 is attributed to Reynolds number effect.

The specific fuel consumption based on net thrust horsepower and net thrust, which coincidently fall on single curves in figures 13 and 14, failed to reduce to single curves in figures 36 and 37 because the combustion efficiency was omitted from the generalizing factors. Corrected specific fuel consumption based on jet thrust (fig. 38) was higher at high altitudes throughout the entire range of engine speeds. The corrected fuel consumption plotted against corrected engine speed (fig. 39) reduced to a single curve only at corrected engine speeds greater than 11,000 rpm.

Corrected fuel-air ratio (fig. 40) came within about 10 percent or less of being a single curve at corrected engine speeds greater than 11,000 rpm and a ram pressure ratio of approximately 1.2.

Inasmuch as quantities involving air flow generalized to one curve only at low engine speeds and quantities involving fuel flow generalized to one curve only at high engine speeds, the use of generalizing factors for the I-40 engine gives only fair results.

Corrected performance data over a range of ram pressure ratios at 30,000 feet are presented in figures 41 to 49. Performance at a particular ram pressure ratio at any altitude can be estimated from these curves with the apparent accuracy indicated in the generalization of altitude data.

## Windmilling Drag Characteristics

A jet engine is said to be windmilling when it is driven solely
by air forced through the engine by the forward motion of the plane.
Values of the ratio of windmilling drag to net thrust developed with
the engine operating at 11,500 rpm for the I-40 engine are plotted
against true airspeed in figure 50. The net thrust used in this
ratio was obtained from figure 29 corresponding to the airspeed and
altitude at which the windmilling drag was measured. At an alti-
tude of 20,000 feet, when the engine was windmilling at airspeeds
of 235 and 550 miles per hour, the internal drag increased from 2.6
to 13.7 percent of the net thrust developed by the engine operating
at 11,500 rpm at the same respective airspeeds. At an airspeed of
400 miles per hour the windmilling drag decreased from 8.4 percent
at an altitude of 10,000 feet to 5.6 percent at 40,000 feet.

Altitude had no effect on the ratio of windmilling drag to
free-stream dynamic pressure, which varied from 0.67 to 0.74 with
airspeeds of 125 and 650 miles per hour, respectively. (See
fig. 51.) An induction-system efficiency of 100 percent was
assumed in computing the value of drag. In order to obtain the
total internal drag of the engine installation in a particular air-
plane, the addition of the drag induced by losses in the induction
system to the windmilling drag of the engine is necessary.

The origin of windmilling drag is shown in surveys of the
total and static pressures through the engine while windmilling.
(See fig. 52.)

## SUMMARY OF RESULTS

From performance investigations of the I-40 jet-propulsion
engine over a range of altitudes from 10,000 to 40,000 feet and ram
pressure ratios, based on compressor-inlet pressures, from approxi-
mately 0.98 to 1.76, the following results were obtained:

1. At an engine speed of 11,500 rpm, the net thrust and net
thrust horsepower decreased about 25 percent with each 10,000-foot
increase in altitude at any airspeed.

2. Specific fuel consumption based on net thrust horsepower
showed no effect of altitude. At an engine speed of 11,500 rpm
the specific fuel consumption based on net thrust horsepower
decreased from 2.10 pounds to 0.80 pound of fuel per horsepower-
hour as the ram pressure ratio increased from 1.08 to 1.76, which
corresponds to an increase in airspeed from 235 to 640 miles per
hour.

3. At an altitude of 30,000 feet and an engine speed of 11,500 rpm, an increase in airspeed from 235 to 640 miles per hour resulted in an increase in net thrust from 1525 to 1890 pounds and an increase in net thrust horsepower from 955 to 3200.

4. The use of generalizing factors for estimating altitude performance of the I-40 engine gave only fair results. Performance of the engine at an altitude of 40,000 feet may be calculated from wind-tunnel data obtained at 20,000 feet with an accuracy within about 9 percent at a corrected engine speed of 11,500 rpm.

5. At an altitude of 20,000 feet, the internal drag when the engine was windmilling at airspeeds of 235 and 550 miles per hour increased from 2.6 to 13.7 percent of the net thrust developed by the engine operating at 11,500 rpm at the same respective airspeeds. At an airspeed of 400 miles per hour the windmilling drag decreased from 8.4 percent at an altitude of 10,000 feet to 5.6 percent at 40,000 feet.

Flight Propulsion Research Laboratory,
       National Advisory Committee for Aeronautics,
              Cleveland, Ohio.

## REFERENCES

1. Silverstein, Abe:  Investigations of Jet-Propulsion Engines in the NACA Altitude Wind Tunnel.  NACA ACR No. E5H23, 1945.

2. Turner, L. Richard, and Lord, Albert M.:  Thermodynamic Charts for the Computation of Combustion and Mixture Temperatures at Constant Pressure.  NACA TN No. 1086, 1946.

3. Sanders, Newell D.:  Performance Parameters for Jet-Propulsion Engines.  NACA TN No. 1106, 1946.

Instrumentation station

| | | | |
|---|---|---|---|
| 0 | Free stream | 4 | Compressor outlet |
| 1 | Duct inlet | 5 | Turbine-nozzle inlet |
| 2 | Compressor inlets | 6 | Turbine outlet |
| 3 | Compressor face | 7 | Calibration ring |
| | | 8 | Tail-pipe-nozzle outlet |

⟵ Inlet air and exhaust gas

⟵ cooling air



Cooling-air passage

Tapered tail pipe

Cooling-air fan

Engine-nacelle baffle

Plenum chamber

Splitter vane

NACA
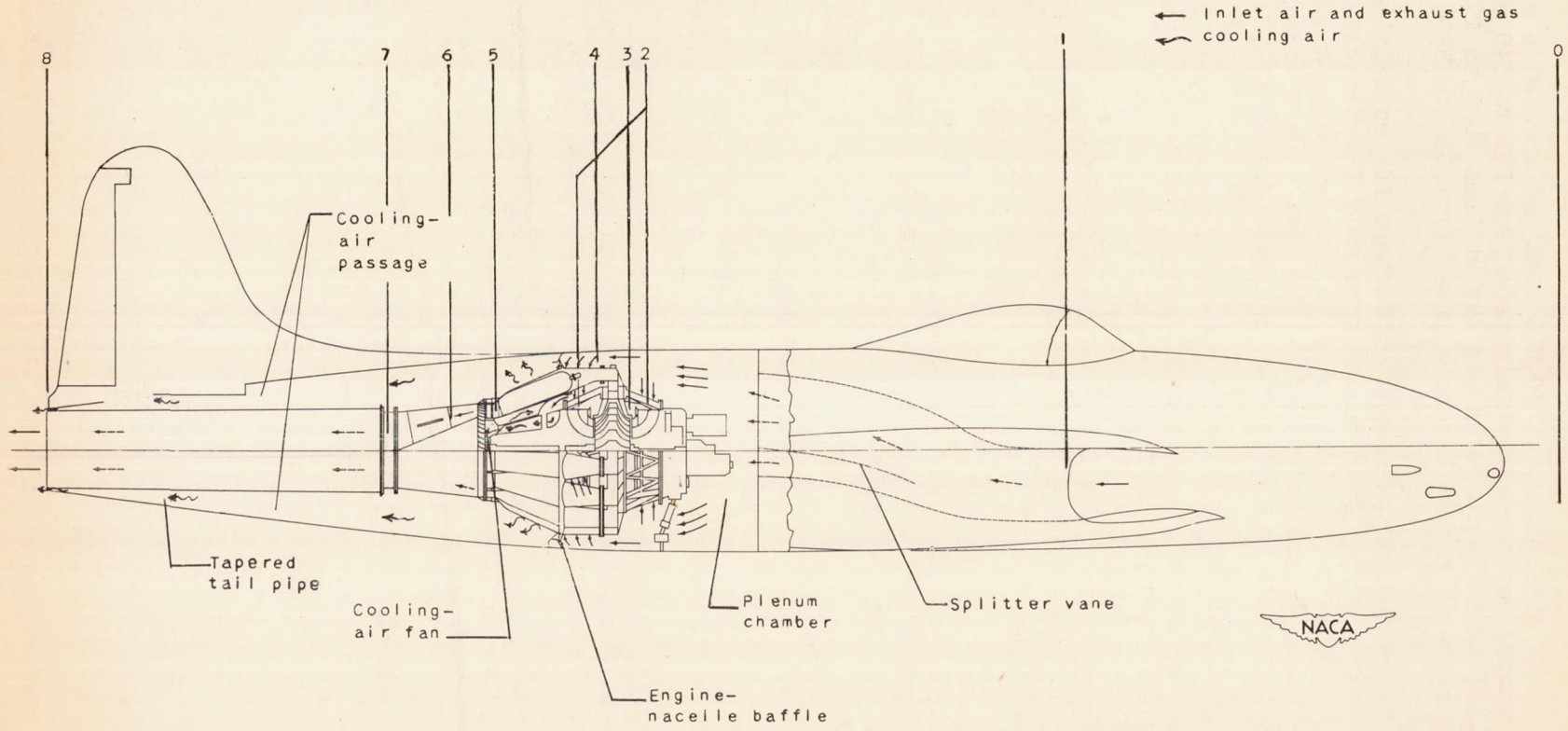
Figure 1. Installation of I-40 jet-propulsion engine.
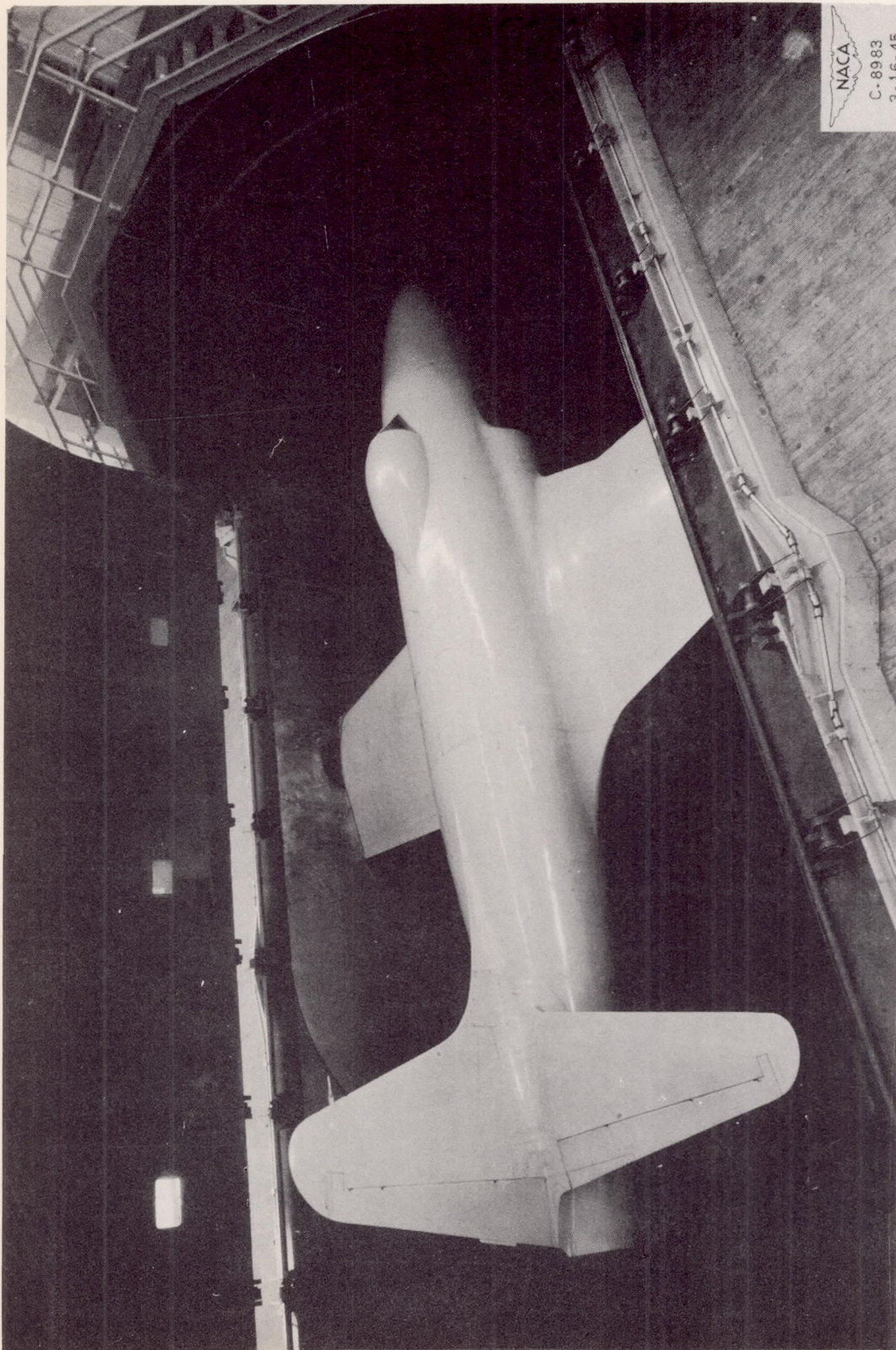
Figure 2. - Airplane fuselage installed in Cleveland altitude wind tunnel.
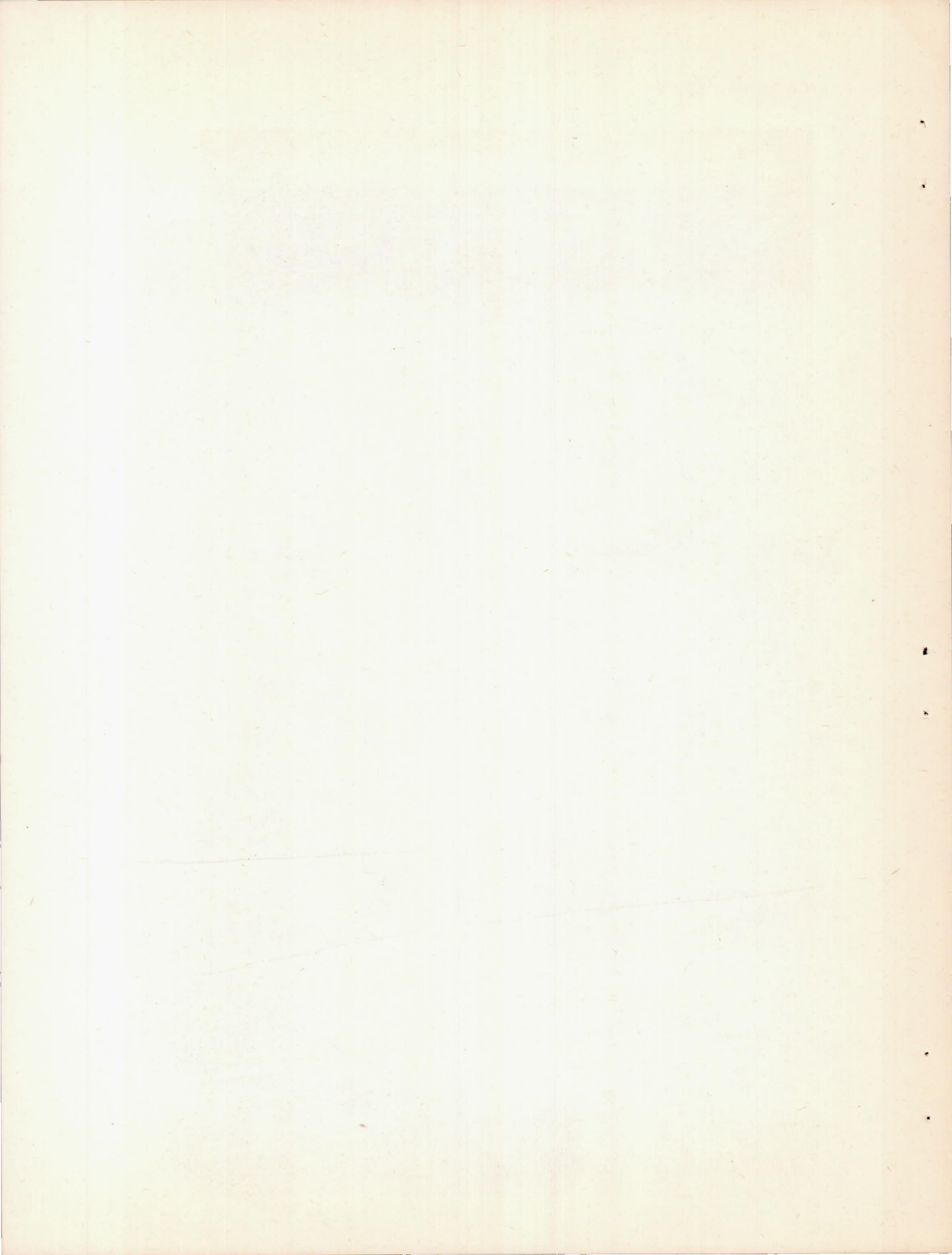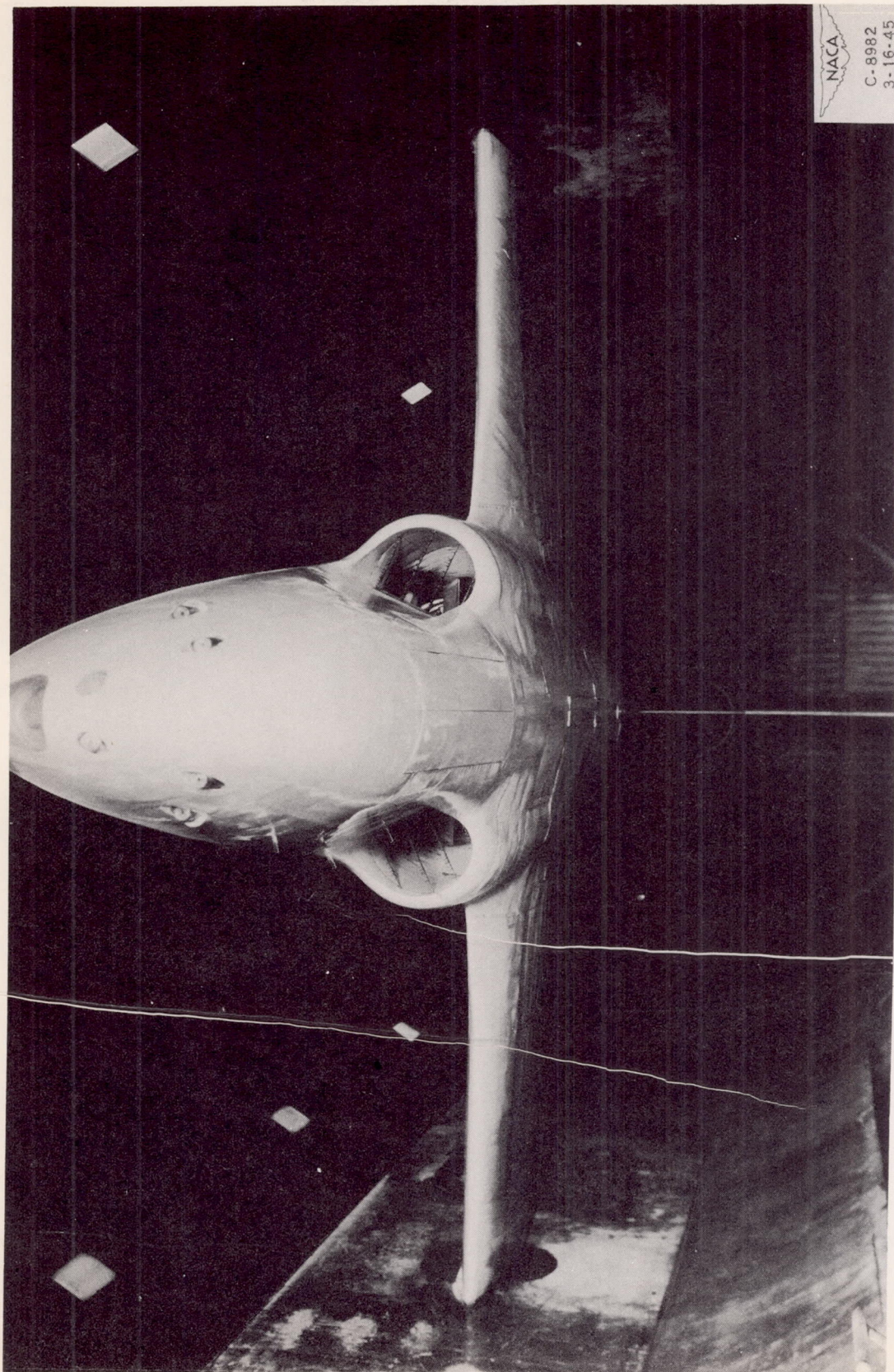
Figure 3. — View of airplane fuselage showing induction-system air inlets.
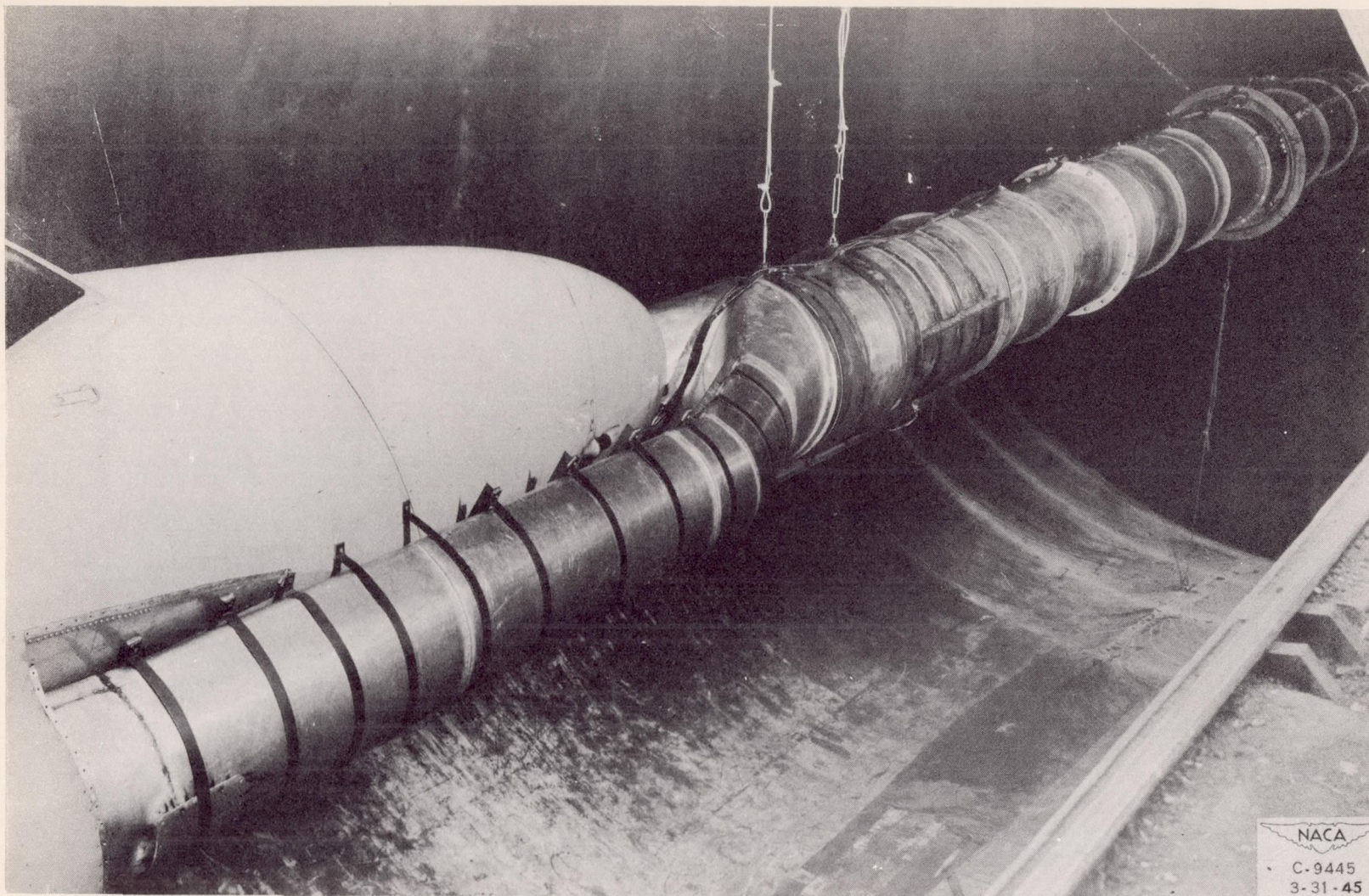
Figure 4. — Y-shaped ram pipe attached to nose of airplane.
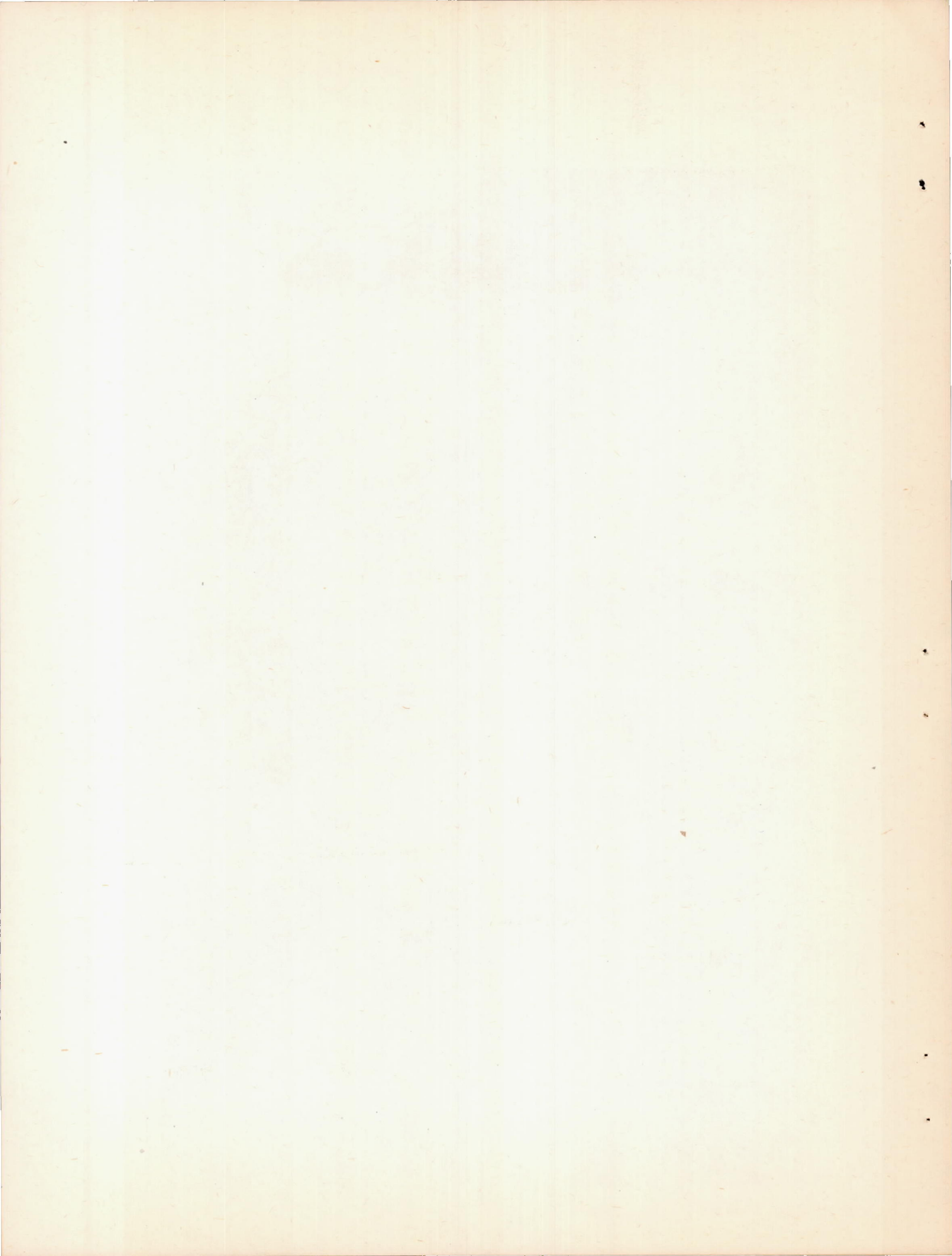
A    *Tail-pipe-nozzle outlet static pressure*
B    Calibration ring, total pressure and temperature
C    *Tail-pipe temperature*
D    *Turbine nozzle-inlet total pressure*
E    Turbine-nozzle-inlet temperature
F    Compressor outlet total pressure and temperature
G    *Compressor-outlet total pressure and temperature survey (NACA)*
H    Generator-pipe total and static pressures and temperatures
I    Front compressor-face static-pressure survey
J    Generator cooling-air outlet-manifold static-pressure orifice

K    Generator cooling-air inlet toal pressure and temperature
L    *Tail-pipe-nozzle outlet total and static pressure and temperature survey*
M    *Turbine-outlet total pressure and temperature*
N    Turbine cooling-air outlet temperature
P    Engine cooling-air outlet total pressure
Q    *Rear compressor total pressure*
R    *Rear compressor total pressure and temperature*
S    Front compressor-face total pressure survey
T    *Front compressor total pressure and temperature*
U    Gear-casing oil temperature
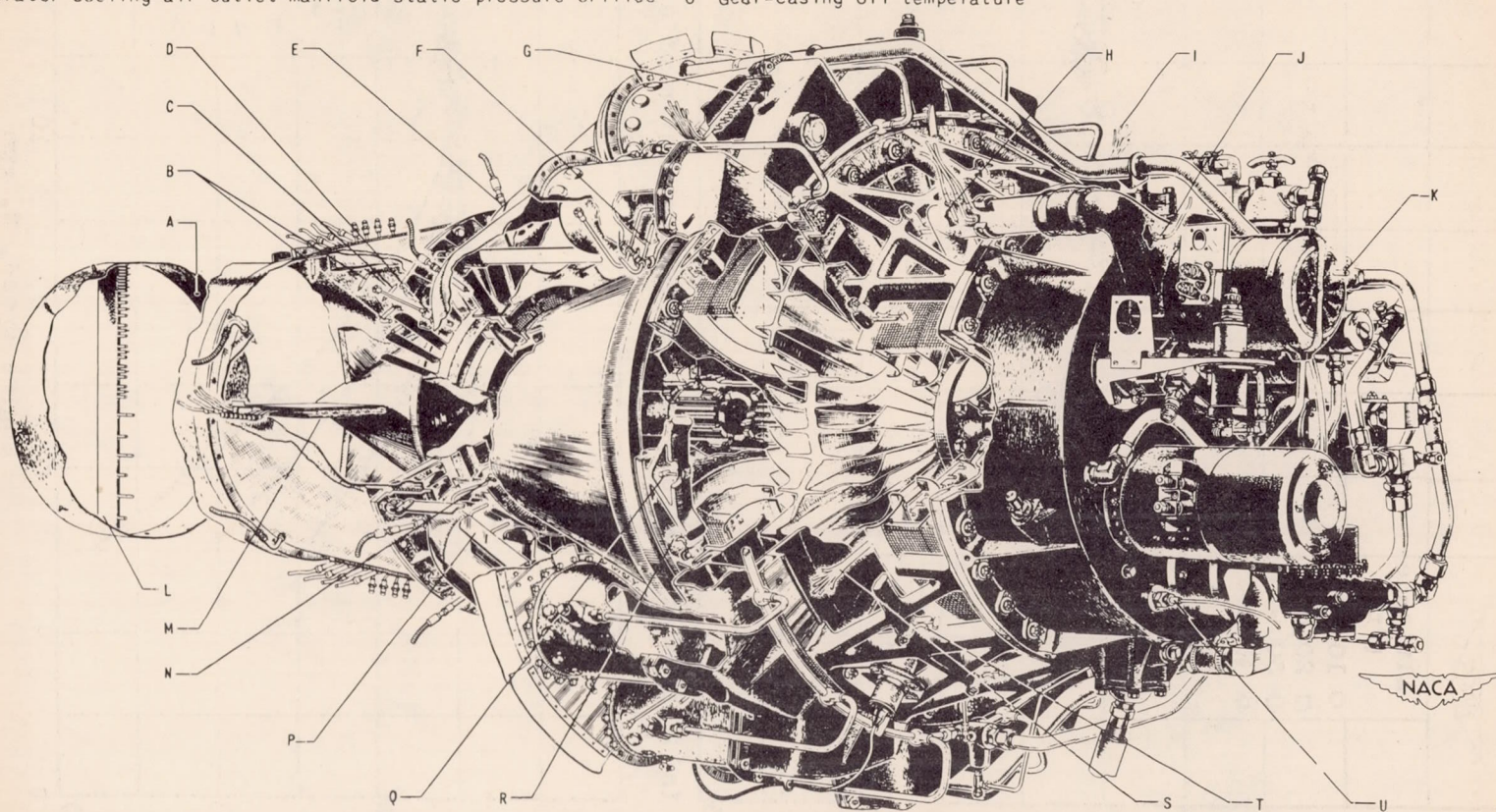


Figure 5. – Drawing of I-40 jet-propulsion engine showing location of instrumentation. (Slant type indicates instrumentation used to obtain data presented in this report.)
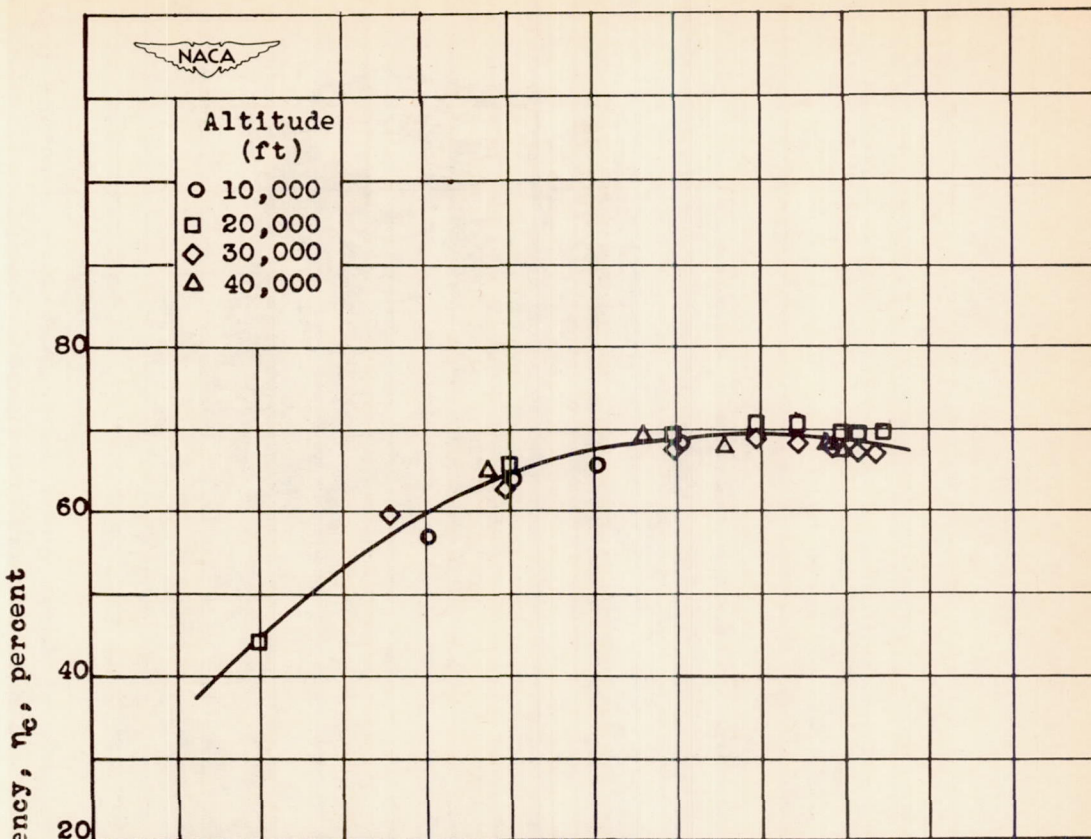
(a) Effect of altitude at ram-pressure ratio of approximately 1.2.
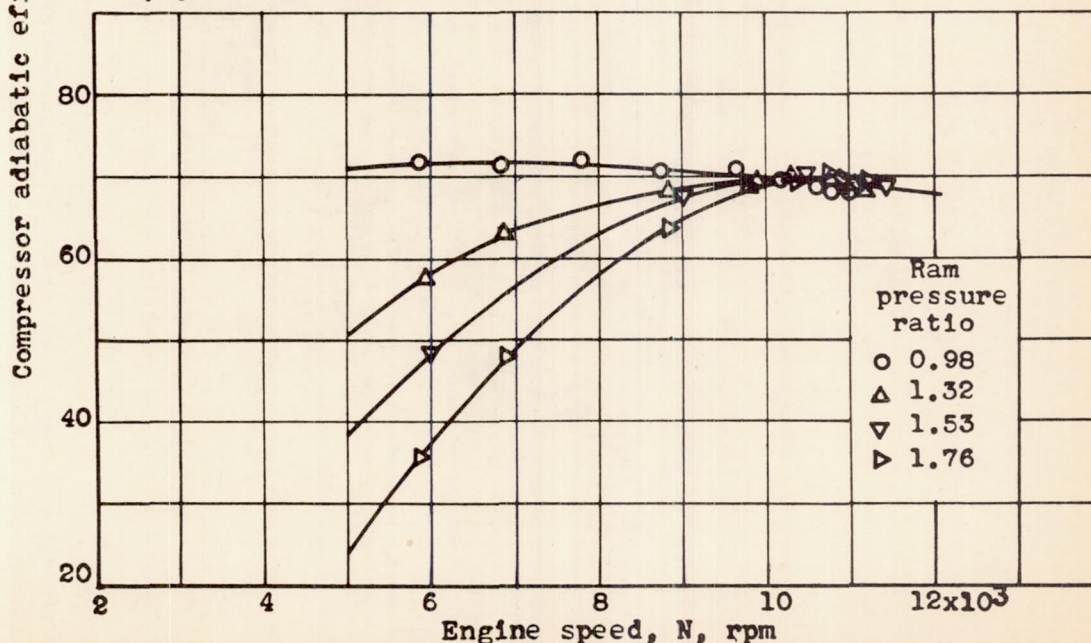
(b) Effect of ram pressure ratio at altitude of 30,000 feet.

Figure 6.- Effect of engine speed, altitude, and ram pressure ratio on compressor adiabatic efficiency.
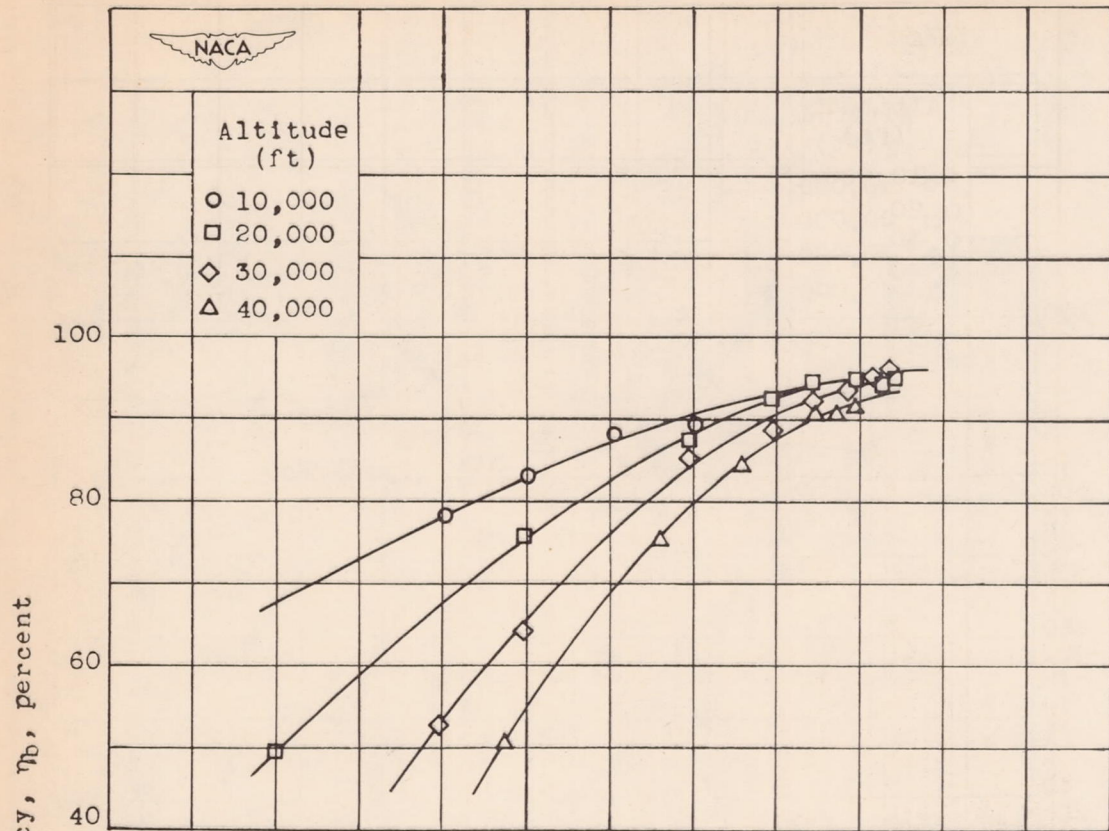
(a) Effect of altitude at ram pressure ratio of approximately 1.2.
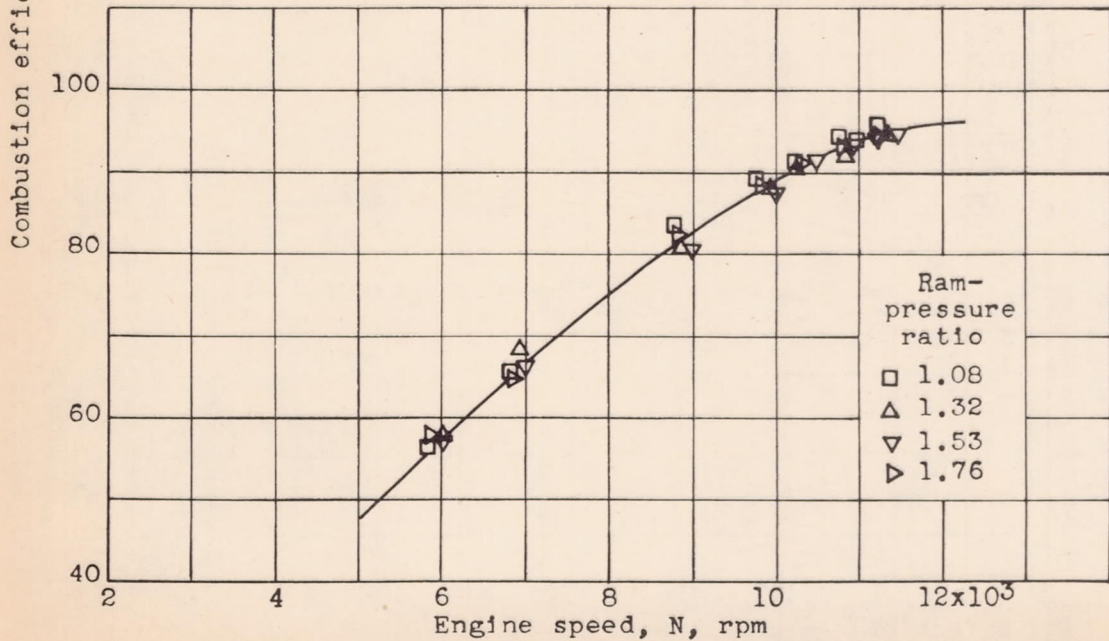
(b) Effect of ram pressure ratio at altitude of 30,000 feet.

Figure 7.- Effect of engine speed, altitude, and ram pressure ratio on combustion efficiency.
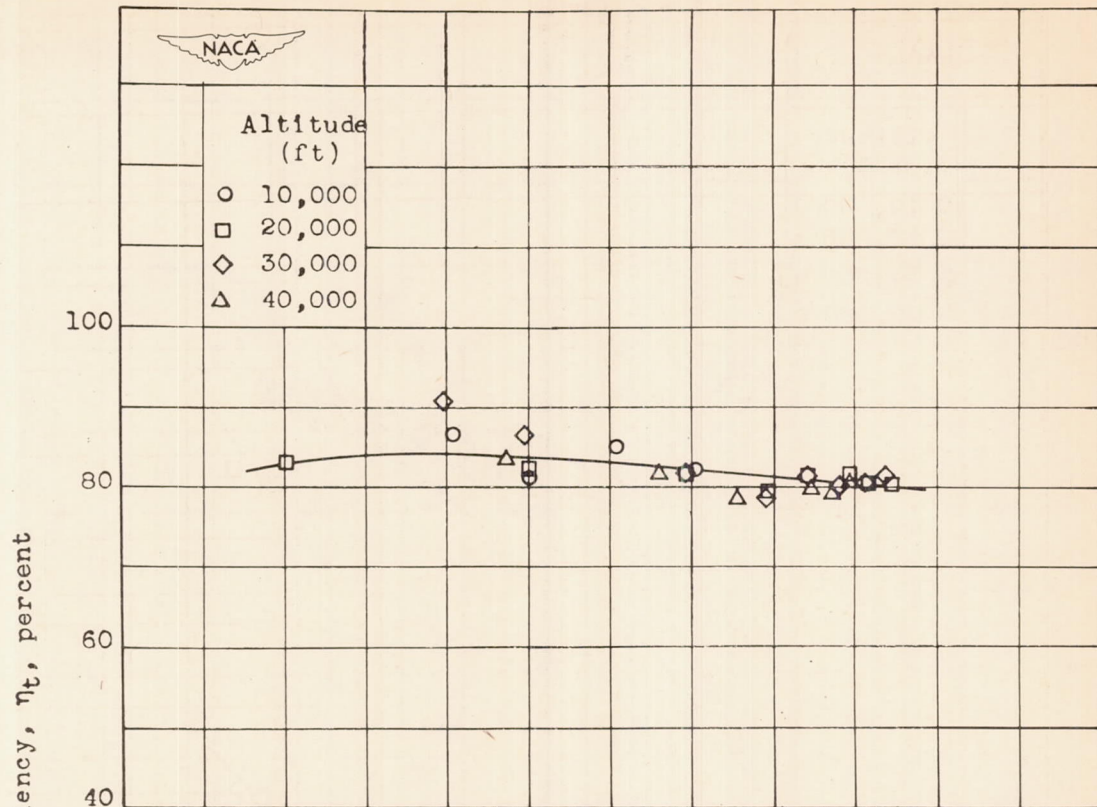
(a) Effect of altitude at ram pressure ratio of approxi-
    mately 1.2.
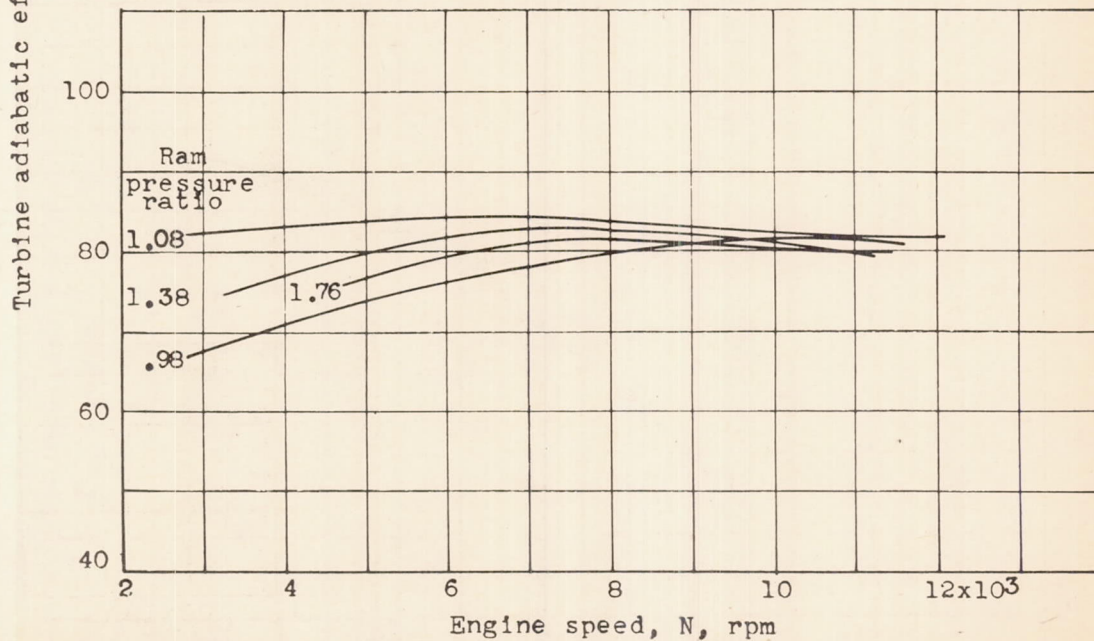
(b) Effect of ram pressure ratio at altitudes from 10,000 to
    40,000 feet.

Figure 8.- Effect of engine speed, altitude, and ram pressure
    ratio on turbine adiabatic efficiency.
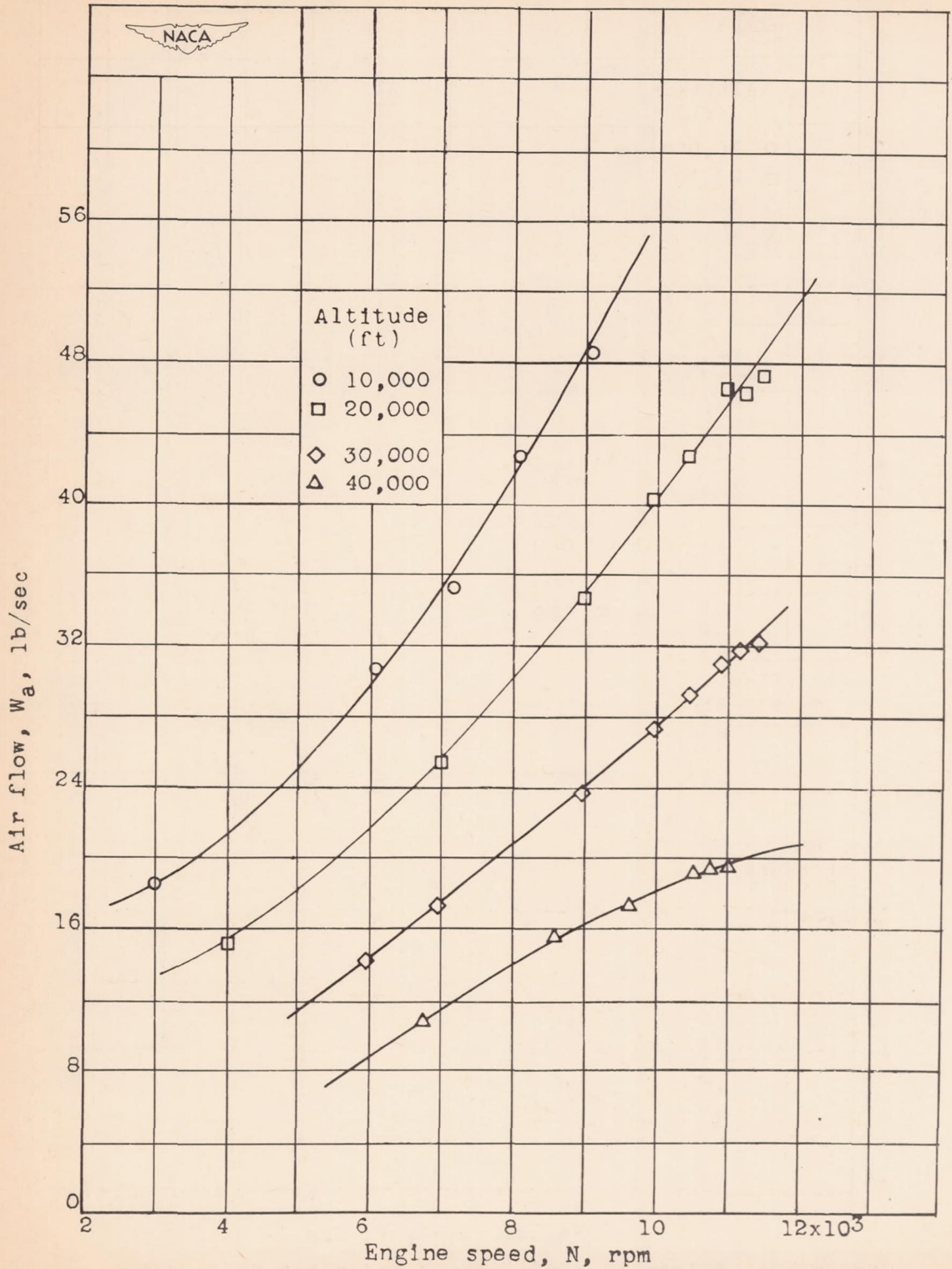
Figure 9.- Effect of engine speed and altitude on air flow
at ram pressure ratio of approximately 1.2.
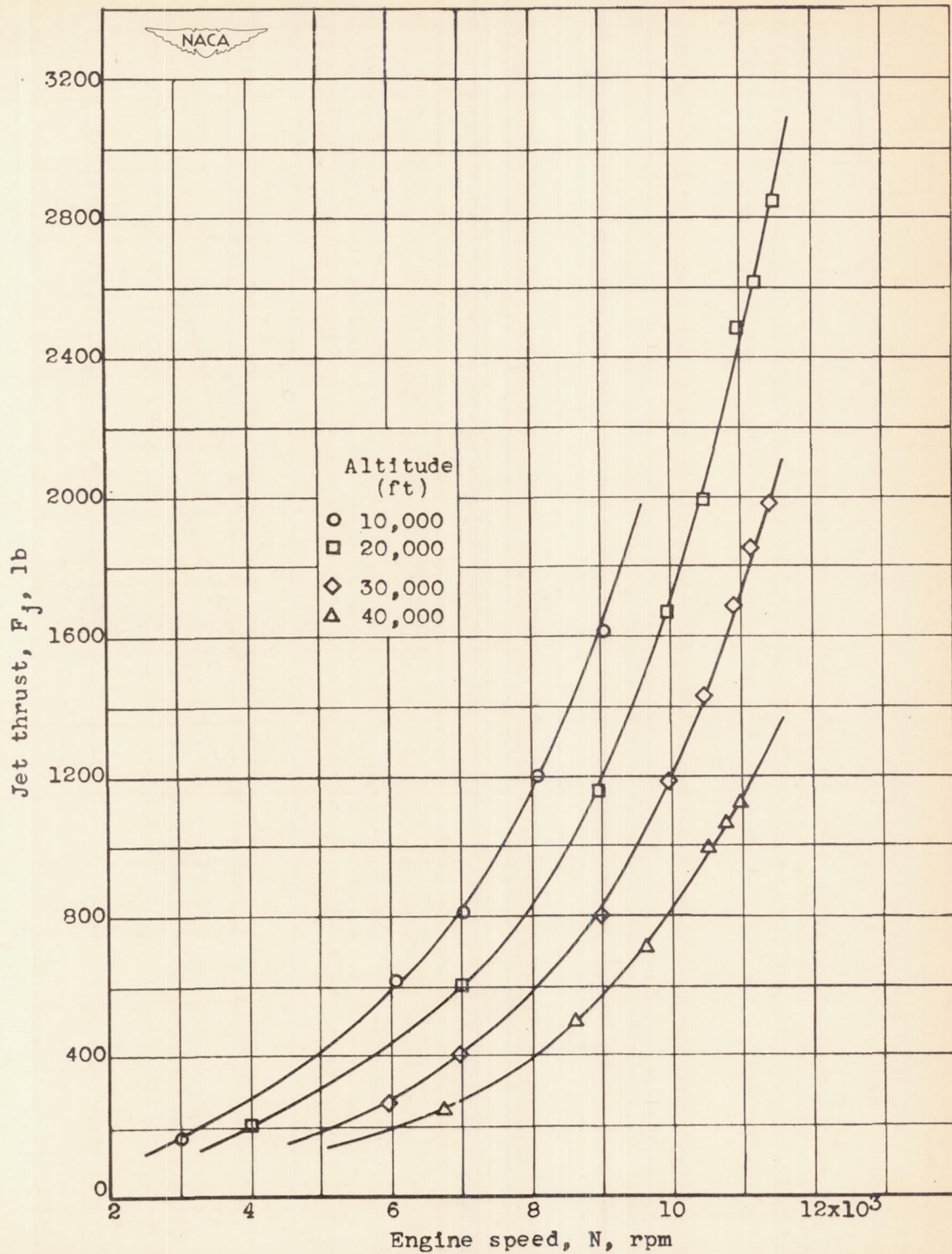
Figure 10.- Effect of engine speed and altitude on jet
thrust at ram pressure ratio of approximately 1.2.
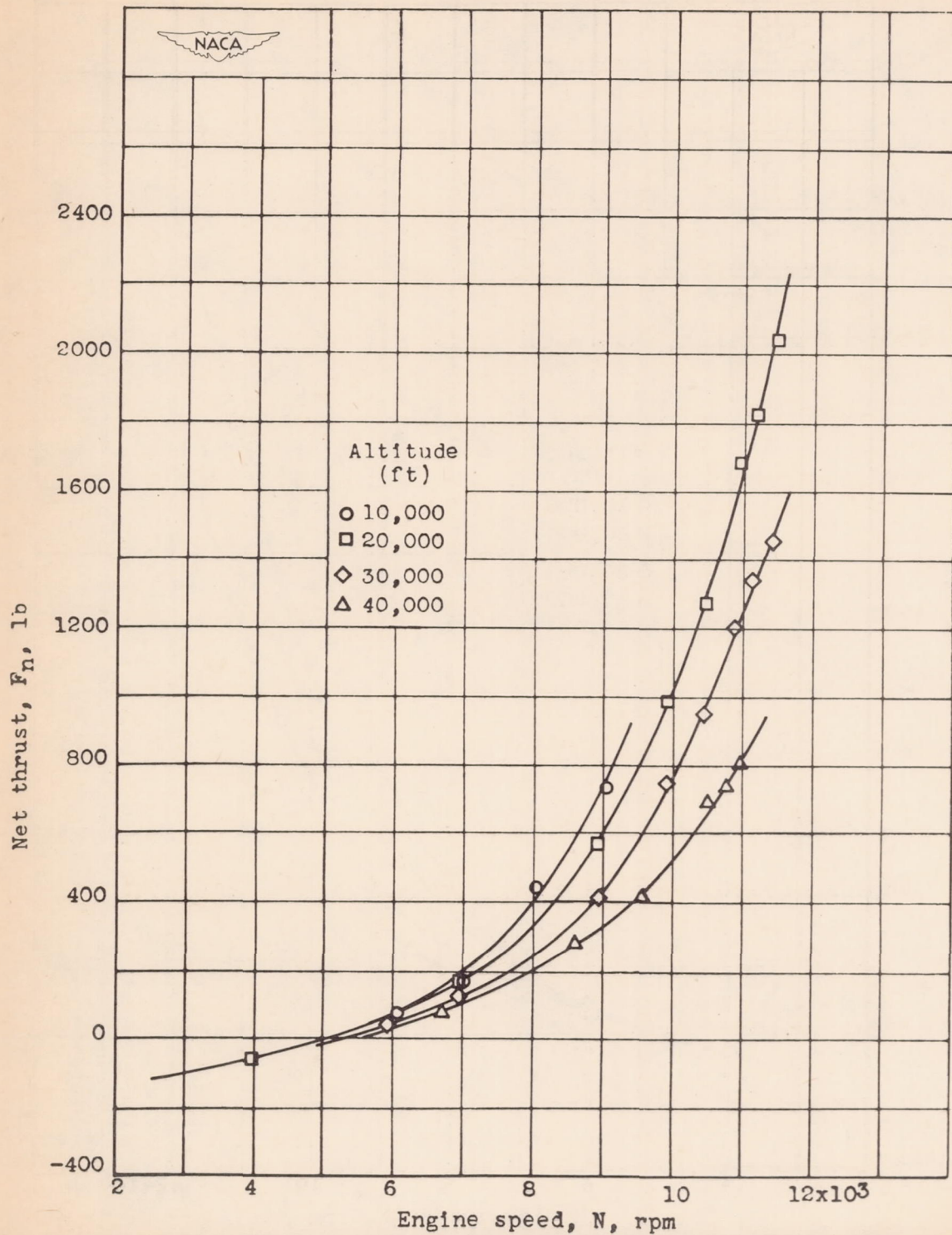
Figure 11.- Effect of engine speed and altitude on net thrust
at ram pressure ratio of approximately 1.2.
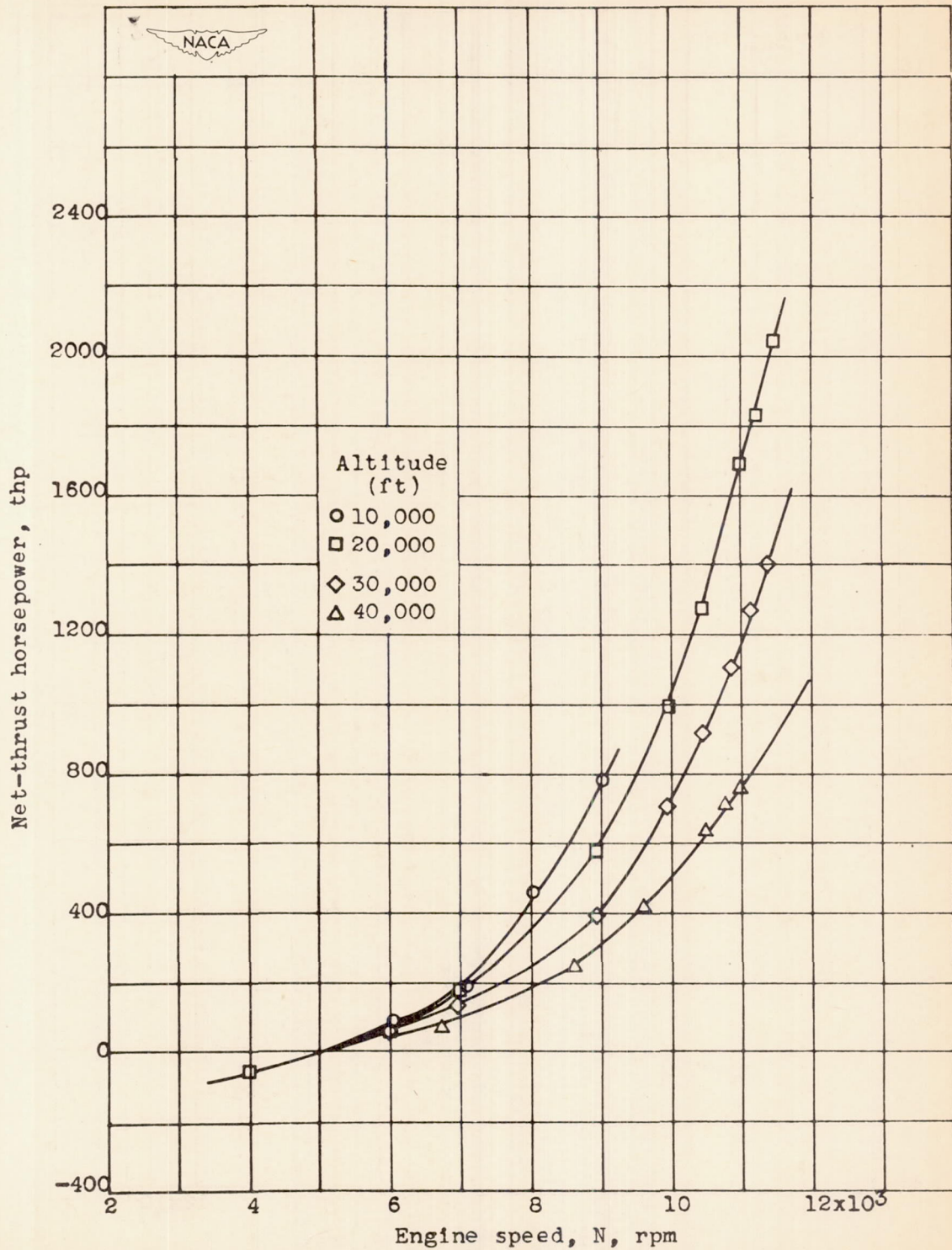
Figure 12.- Effect of engine speed and altitude on net-thrust horsepower at ram pressure ratio of approximately 1.2.
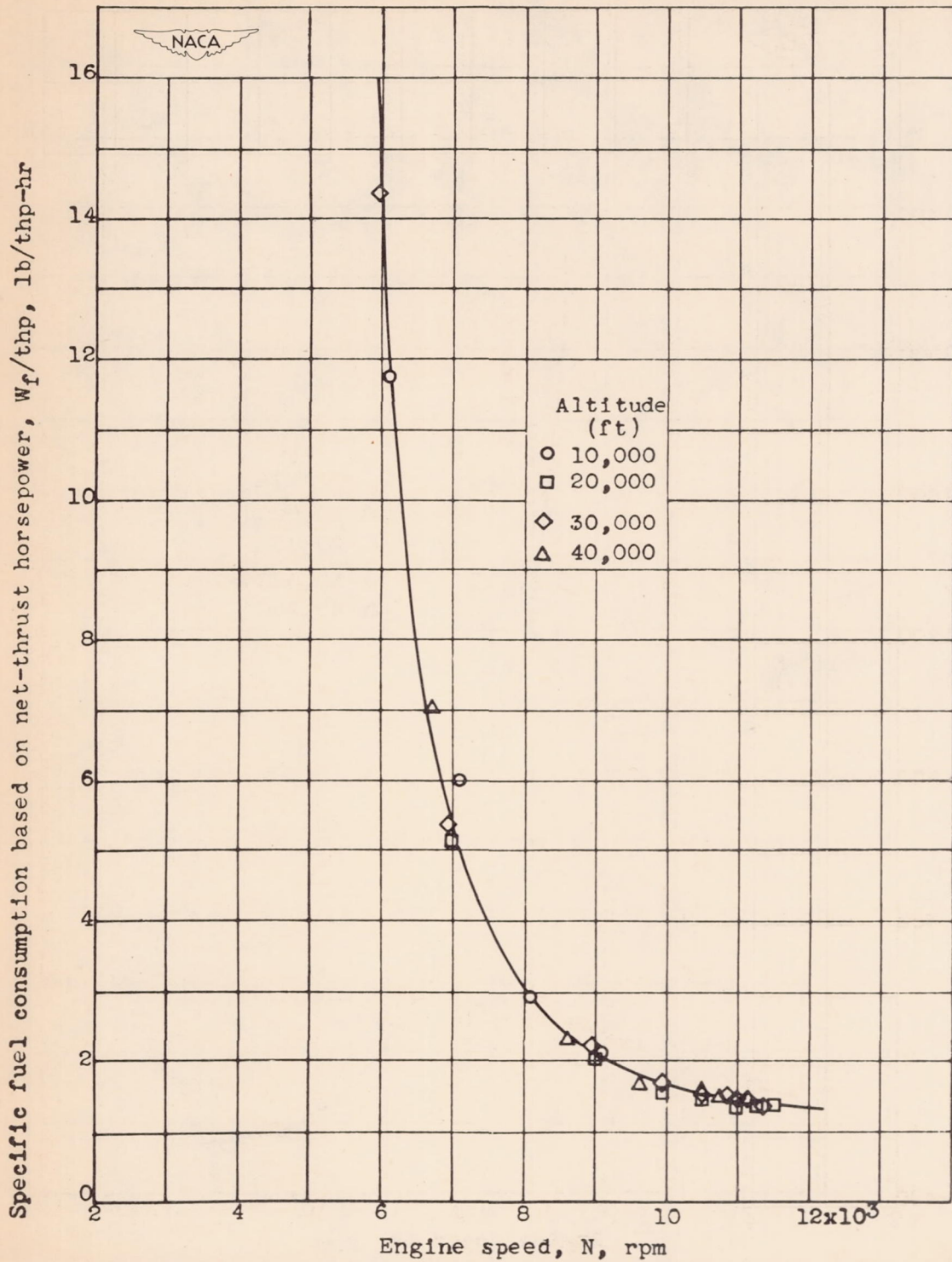
Figure 13.- Effect of engine speed and altitude on specific
fuel consumption based on net-thrust horsepower at ram
pressure ratio of approximately 1.2.
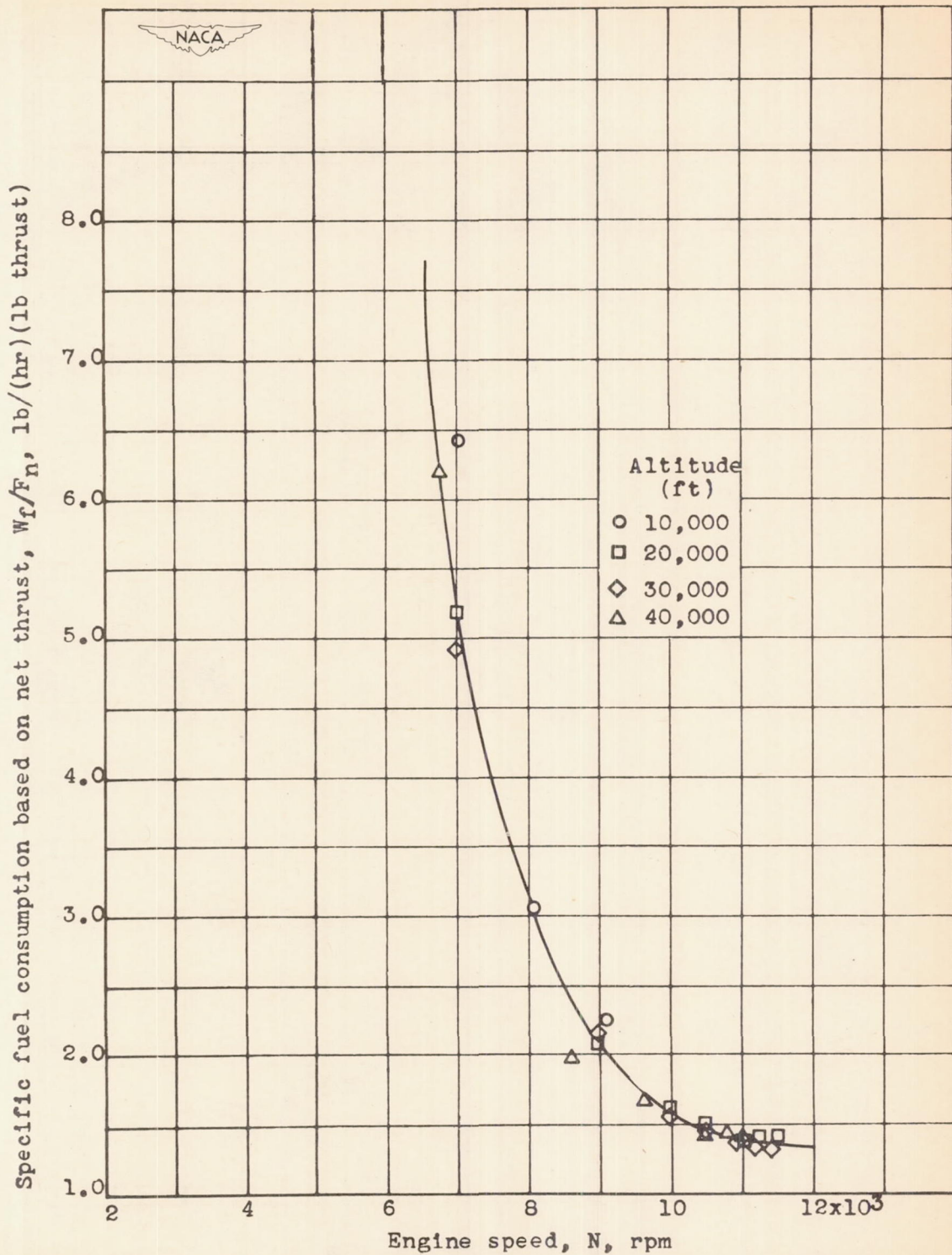
Figure 14.- Effect of engine speed and altitude on specific
fuel consumption based on net thrust at ram pressure ratio
of approximately 1.2.
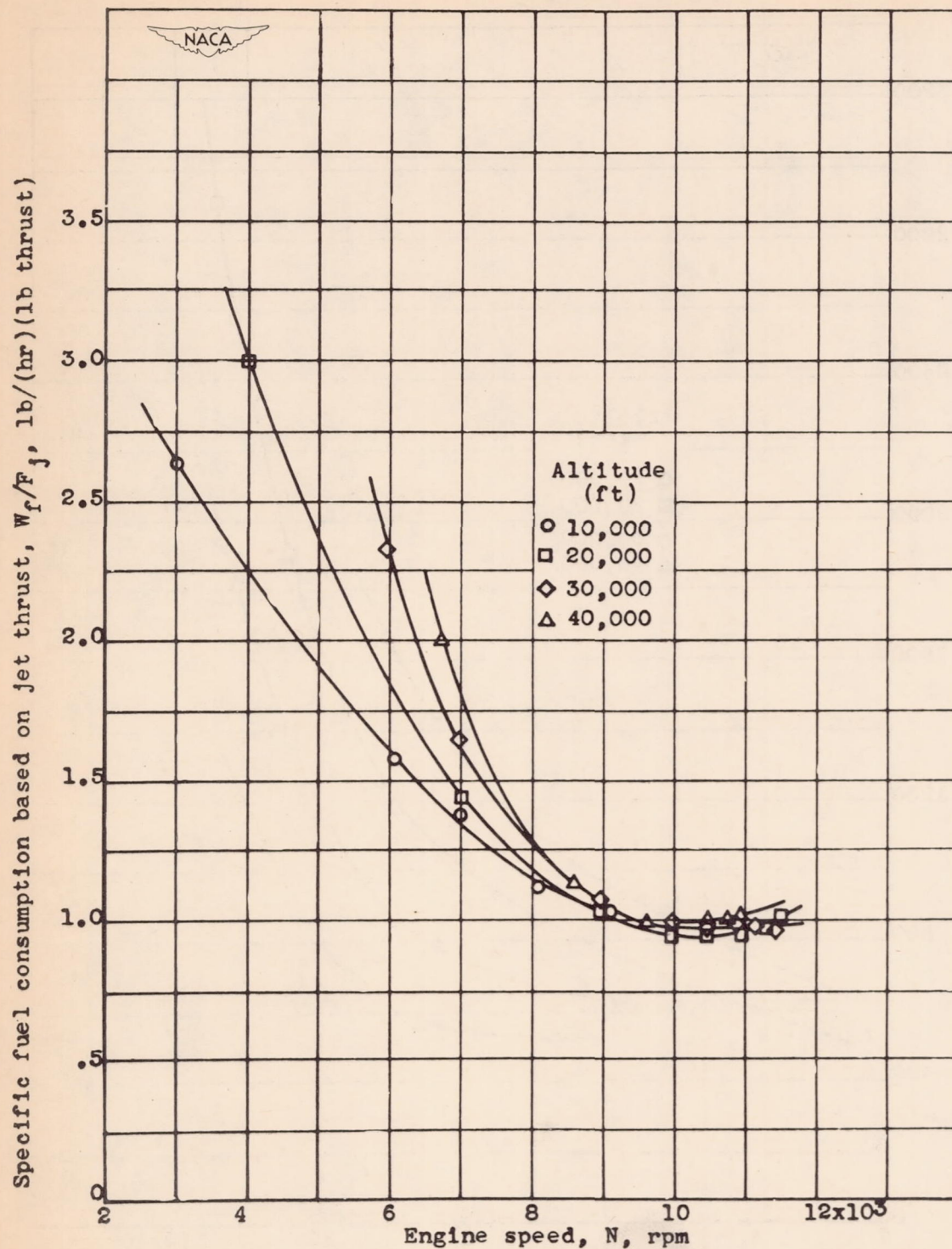
Figure 15.- Effect of engine speed and altitude on specific fuel consumption based on jet thrust at ram pressure ratio of approximately 1.2.
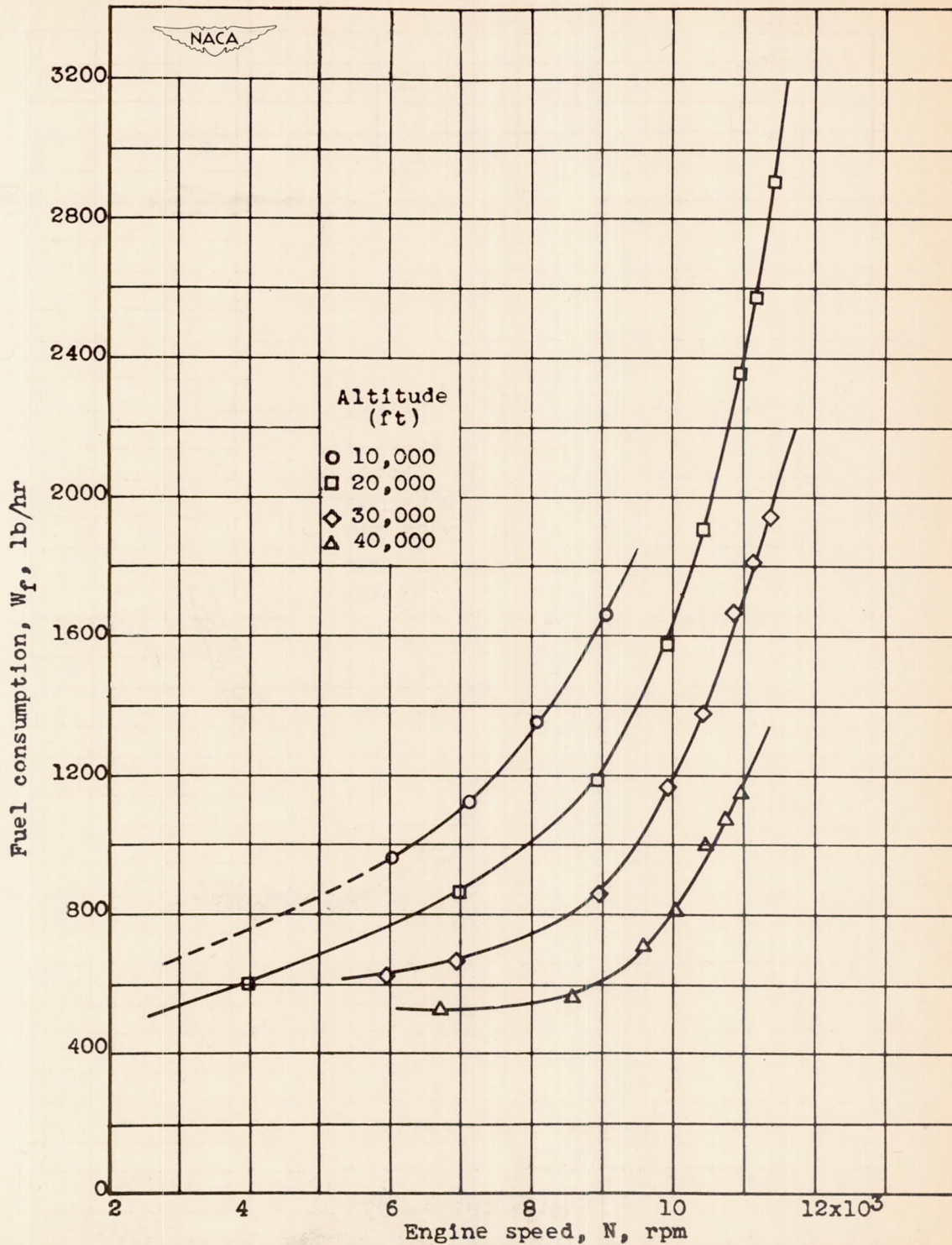
Figure 16.- Effect of engine speed and altitude on fuel consumption at ram pressure ratio of approximately 1.2.
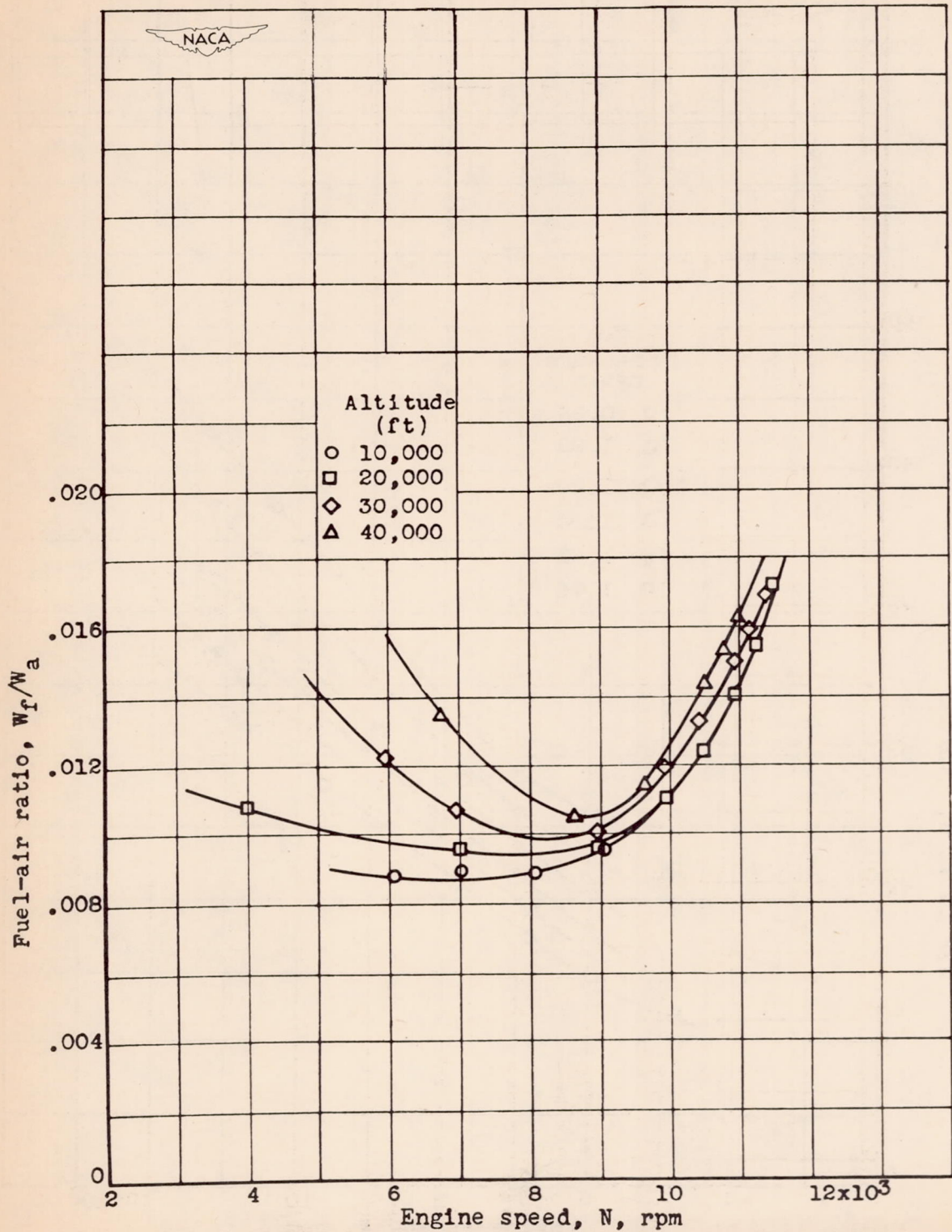
Figure 17.- Effect of engine speed and altitude on fuel-air
ratio at ram pressure ratio of approximately 1.2.
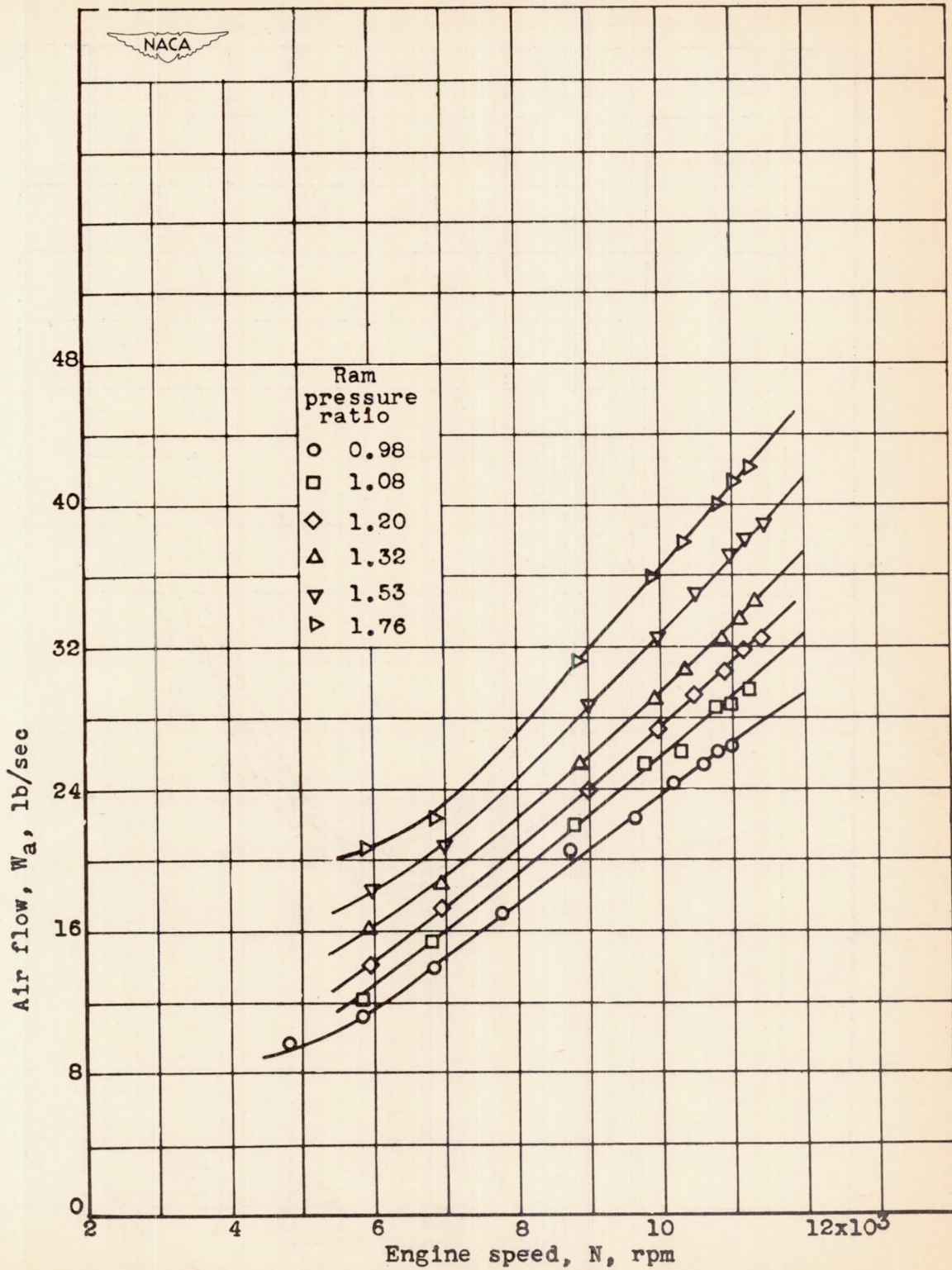
Figure 18.- Effect of engine speed and ram pressure ratio on
    air flow at altitude of 30,000 feet.
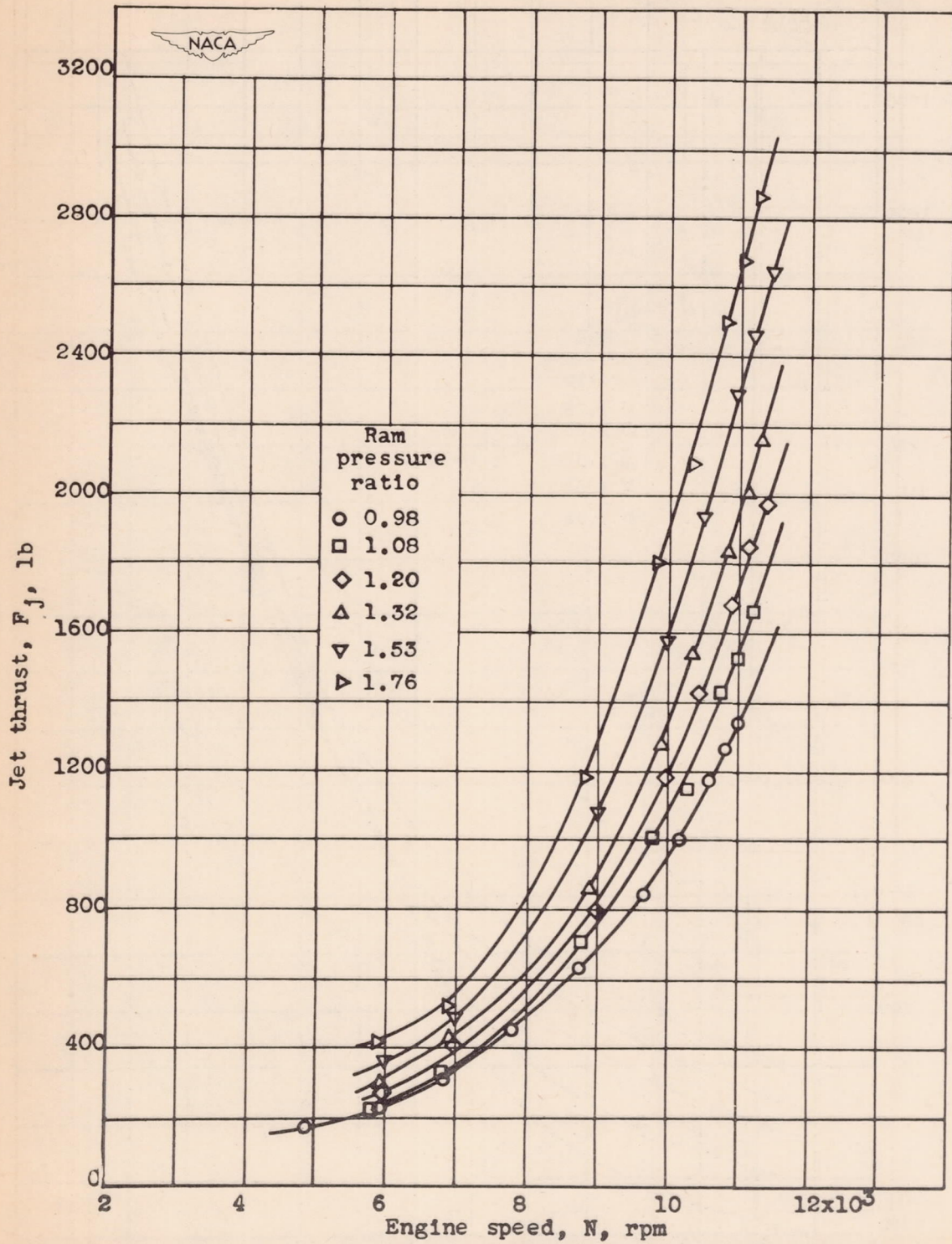
Figure 19.- Effect of engine speed and ram pressure ratio on jet thrust at altitude of 30,000 feet.
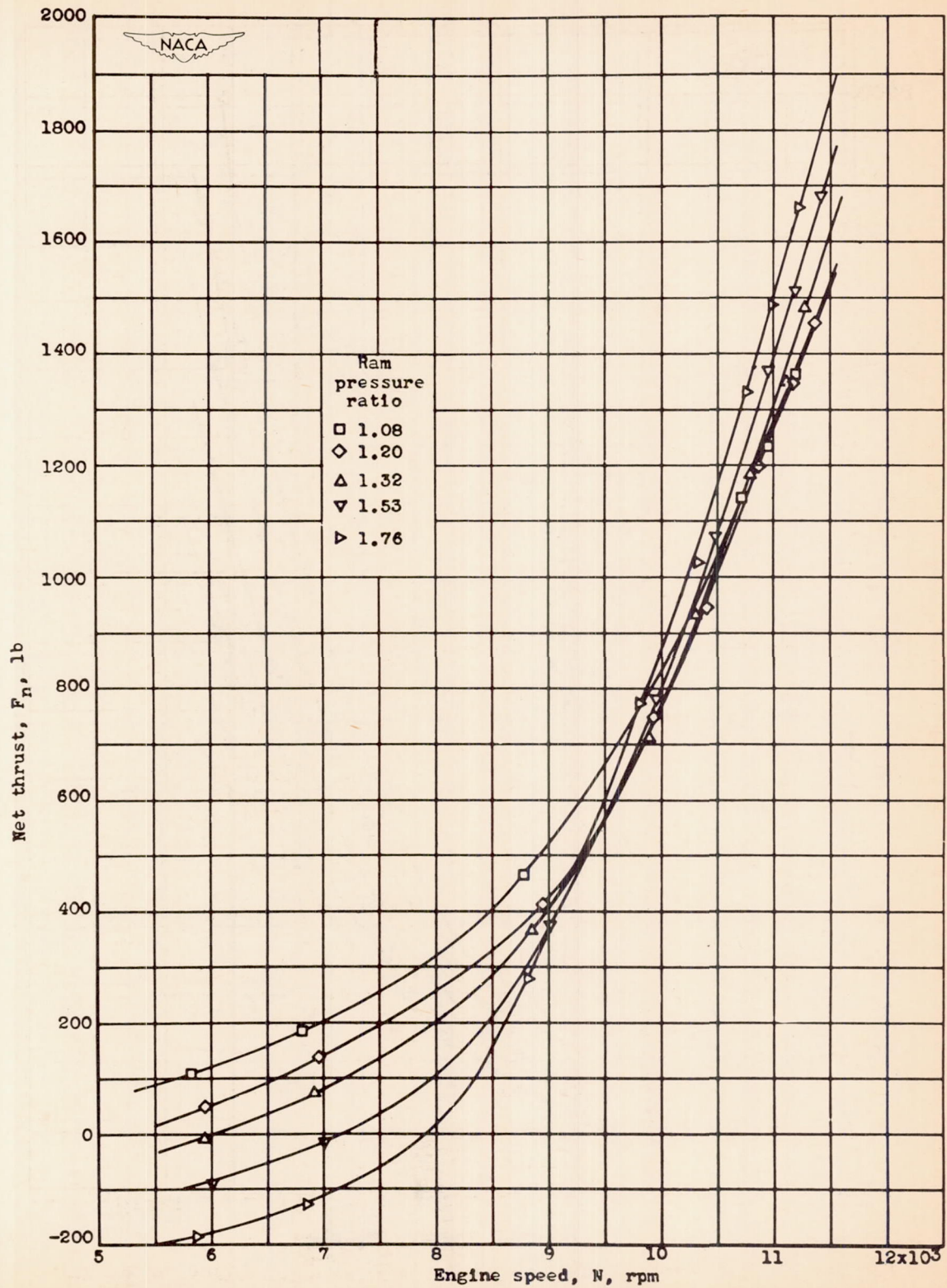
Figure 20.- Effect of engine speed and ram pressure ratio on net thrust at altitude of 30,000 feet.
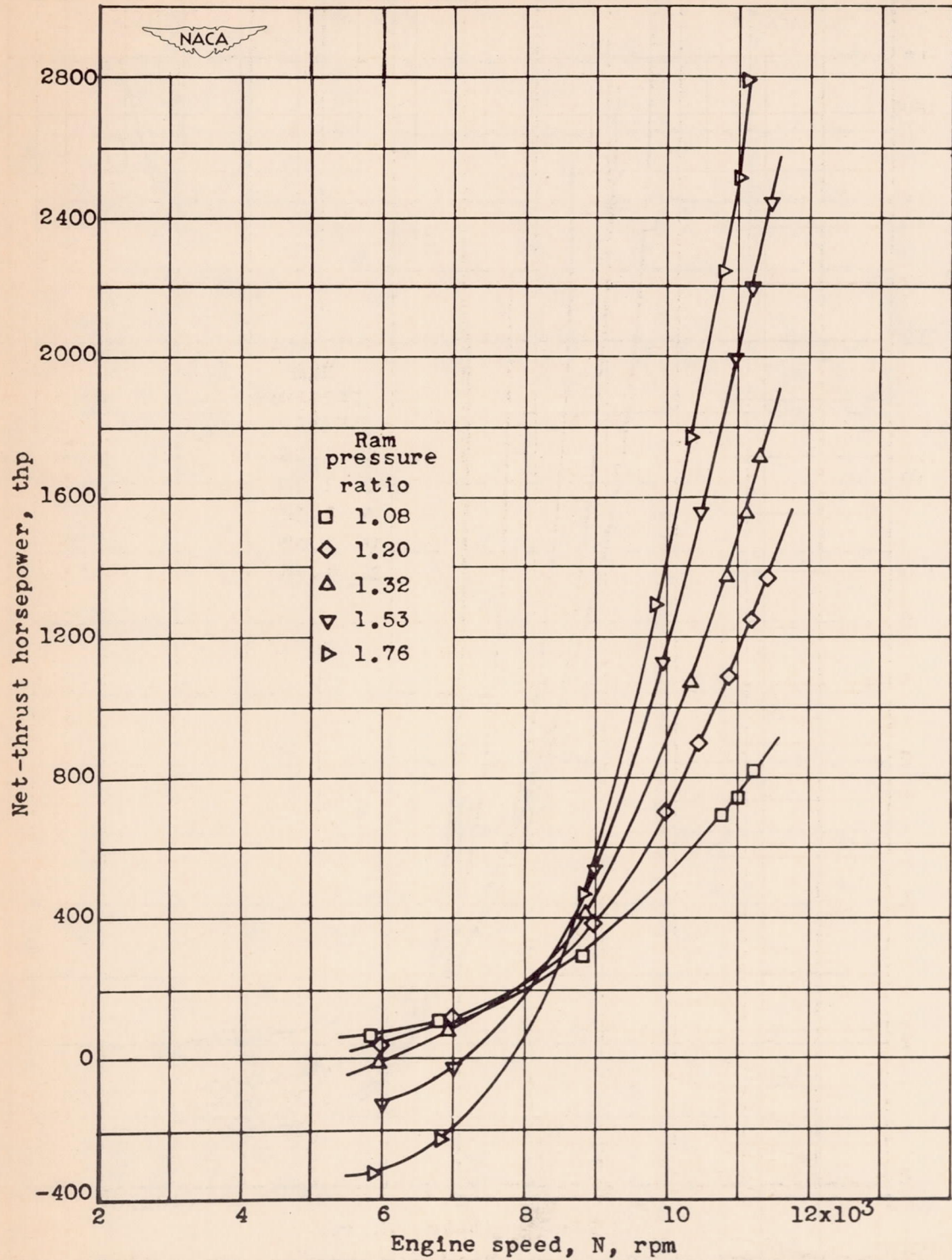
Figure 21.- Effect of engine speed and ram pressure ratio on net-thrust horsepower at altitude of 30,000 feet.
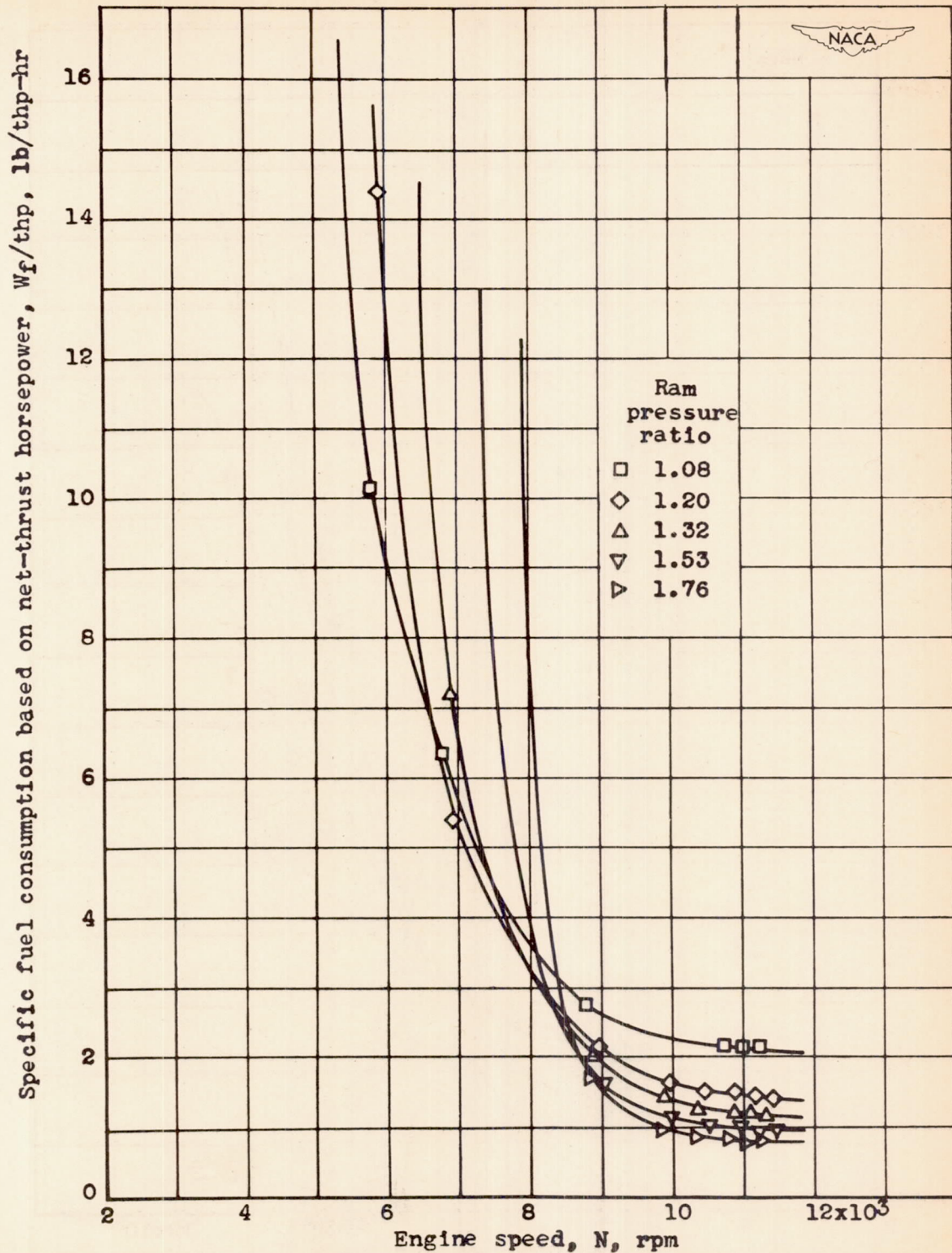
Figure 22.- Effect of engine speed and ram pressure ratio on
    specific fuel consumption based on net-thrust horsepower
    at altitude of 30,000 feet.
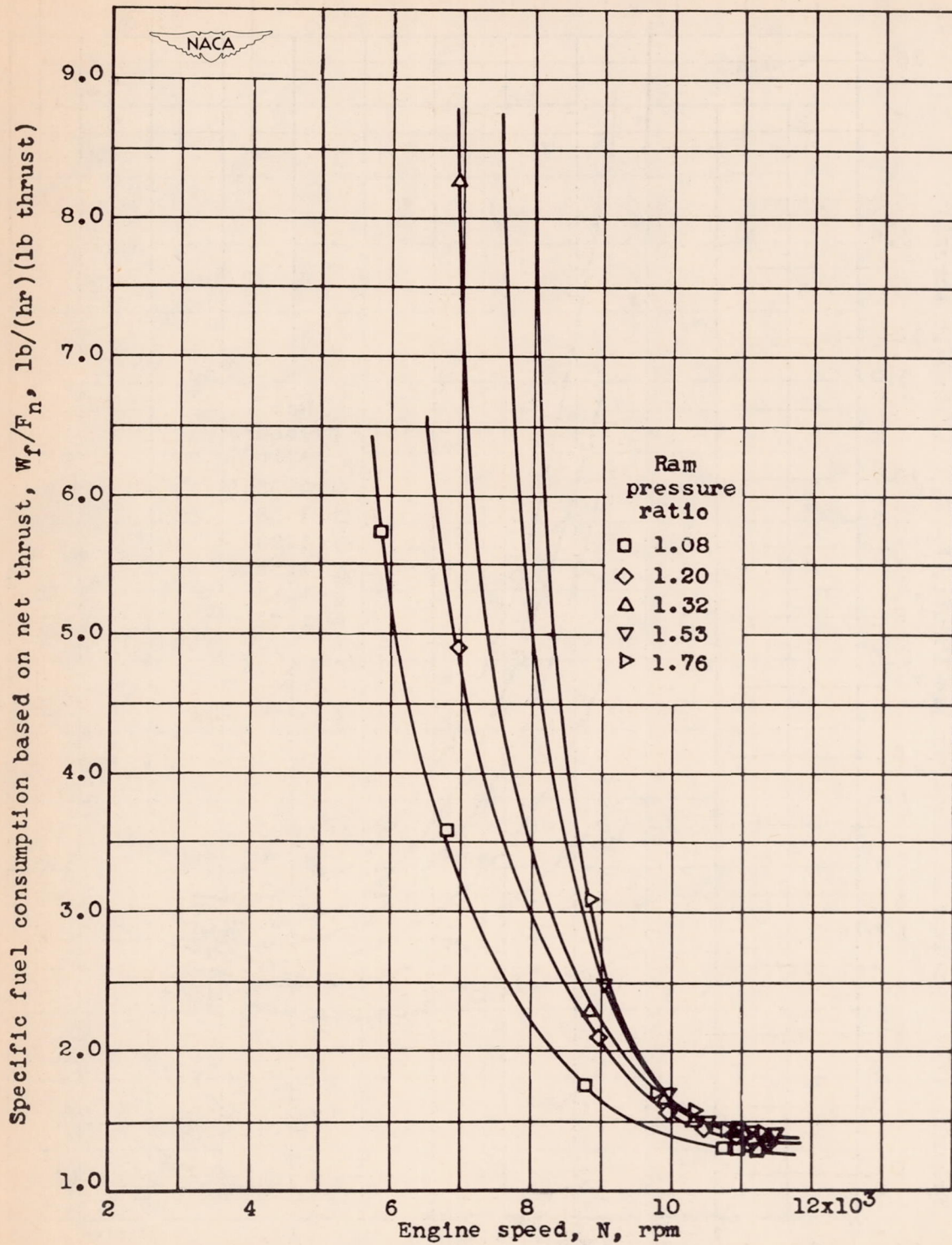
Figure 23.— Effect of engine speed and ram pressure ratio on specific fuel consumption based on net thrust at altitude of 30,000 feet.
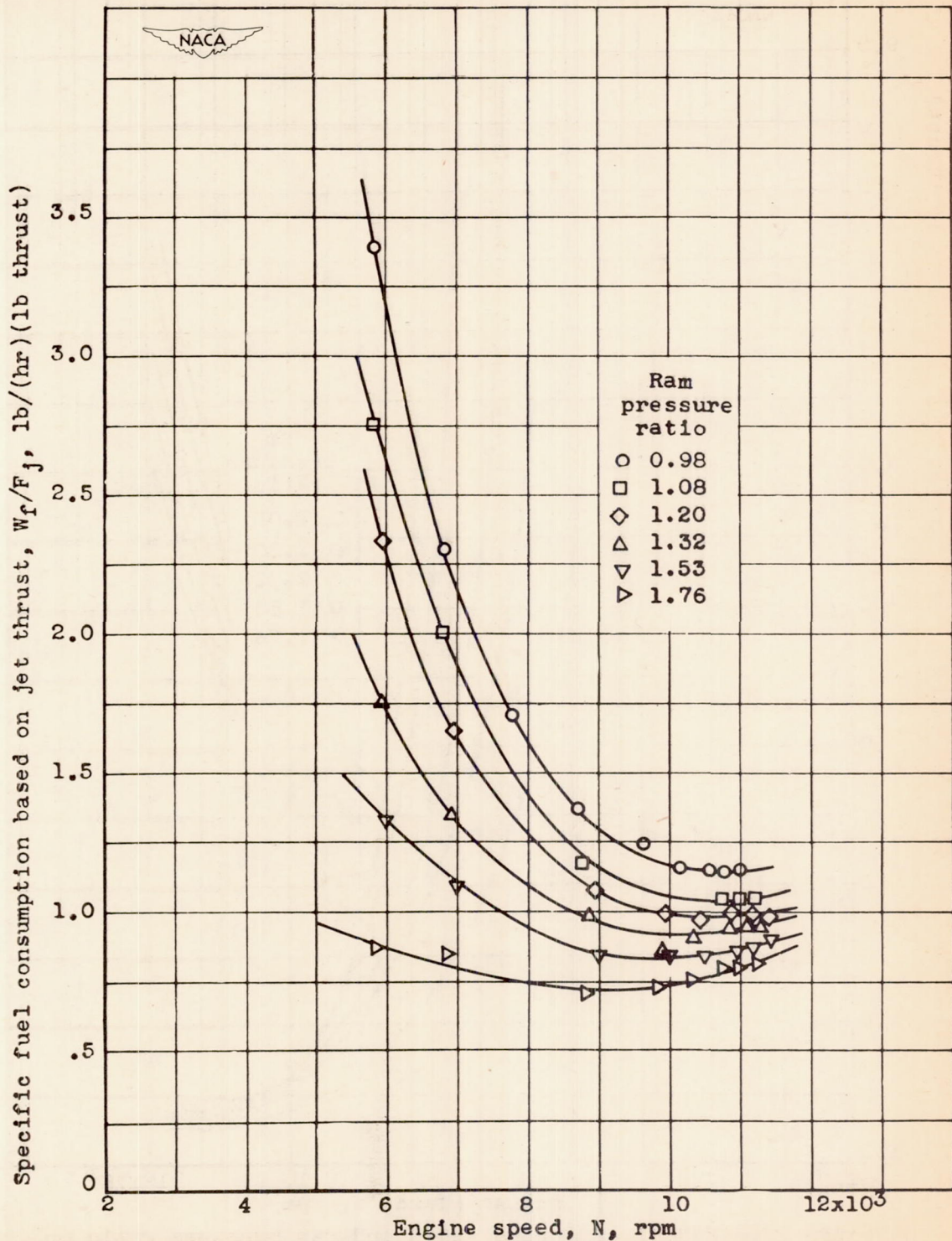
Figure 24.- Effect of engine speed and ram pressure ratio on specific fuel consumption based on jet thrust at altitude of 30,000 feet.
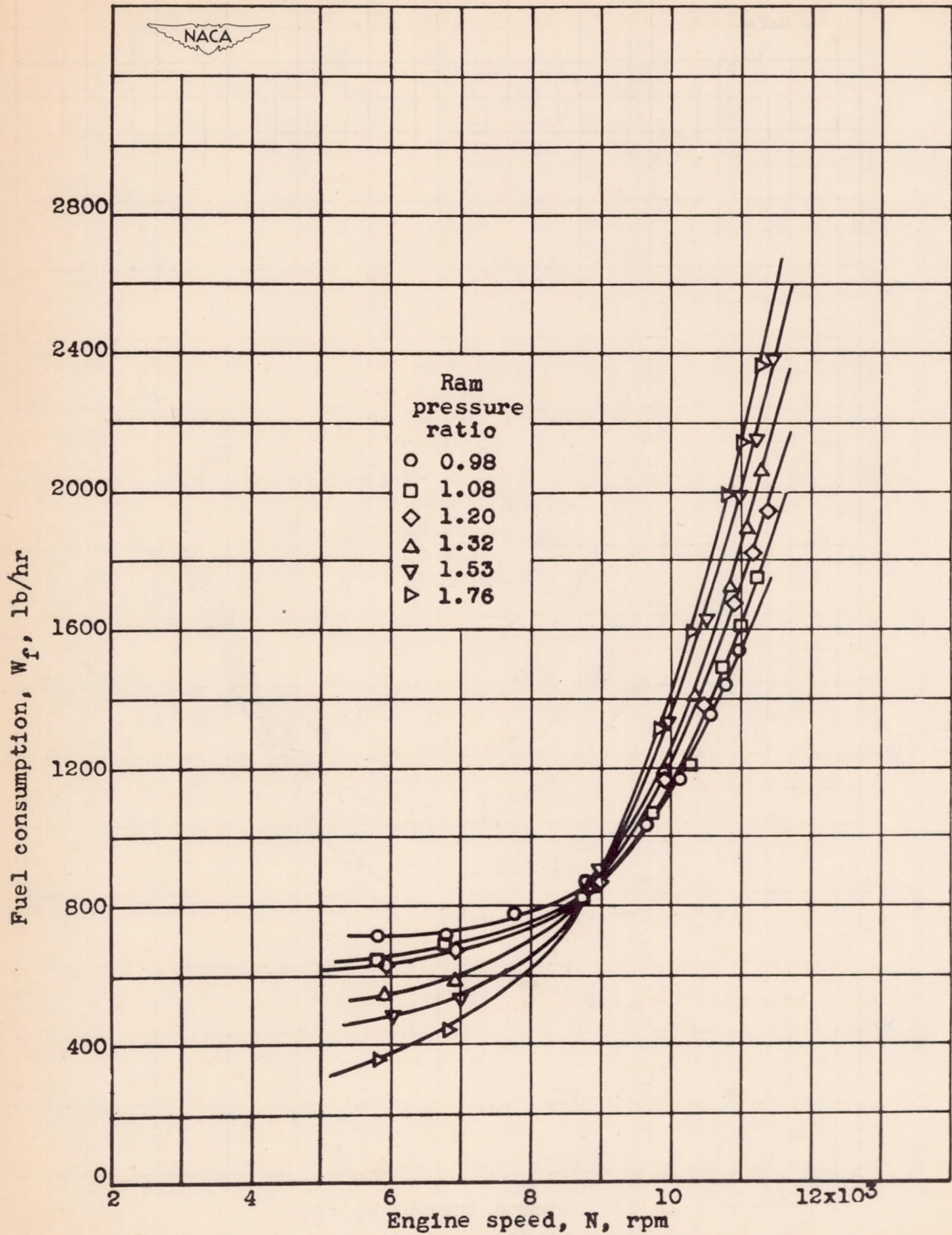
Figure 25.- Effect of engine speed and ram pressure ratio on fuel consumption at altitude of 30,000 feet.
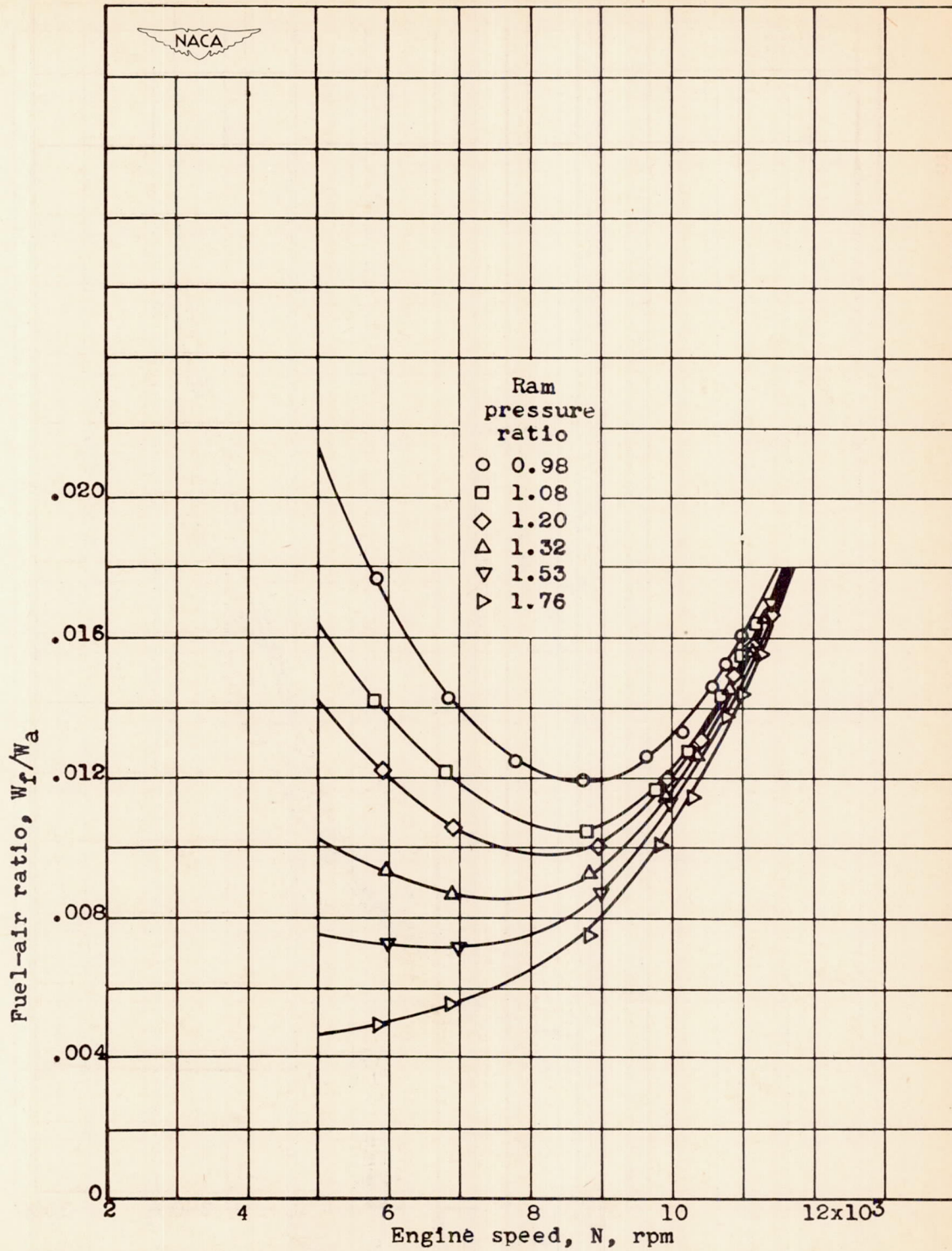
Figure 26.- Effect of engine speed and ram pressure ratio on
fuel-air ratio at altitude of 30,000 feet.
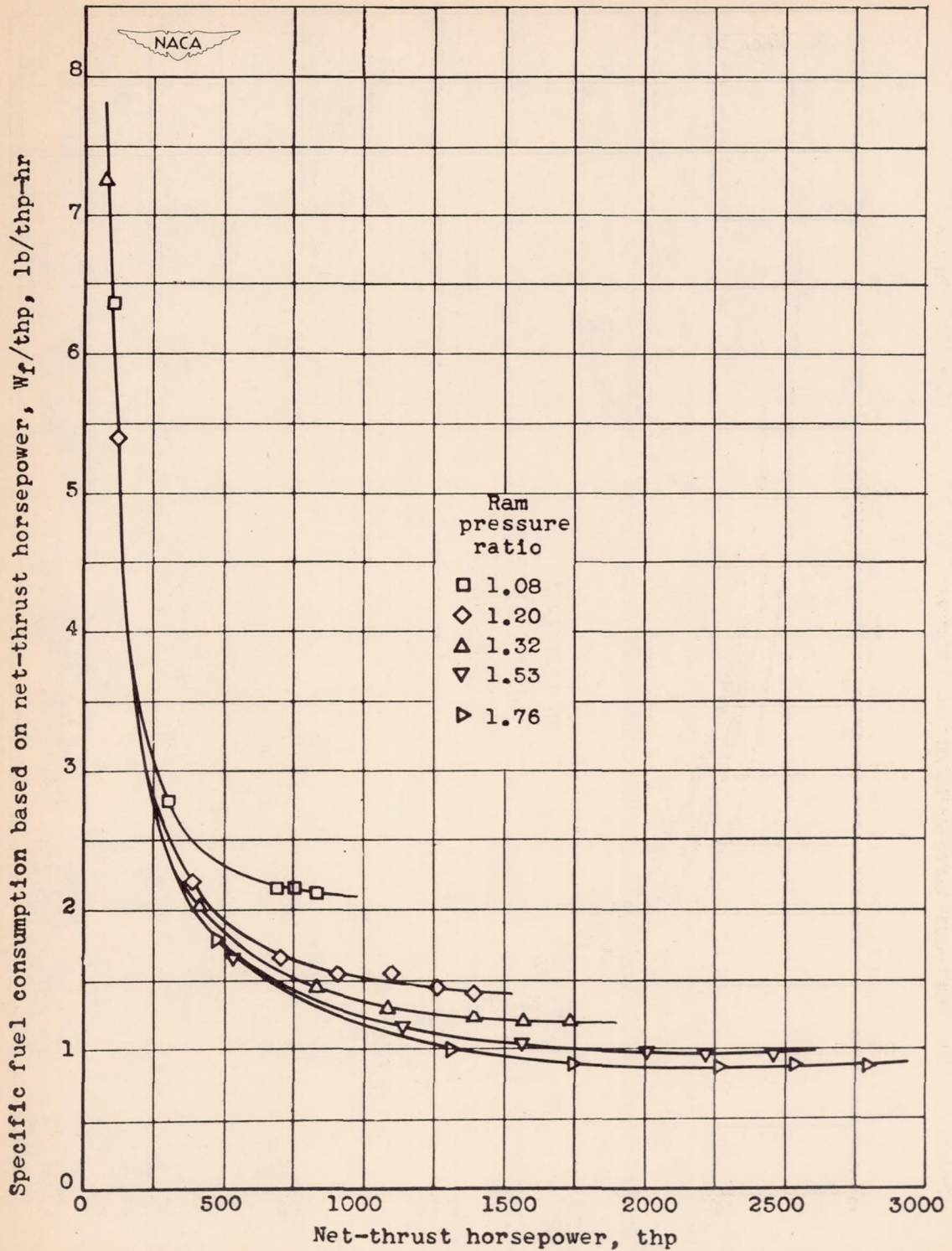
Figure 27.- Variation of specific fuel consumption based on
net-thrust horsepower with ram pressure ratio and net-thrust
horsepower at altitude of 30,000 feet.
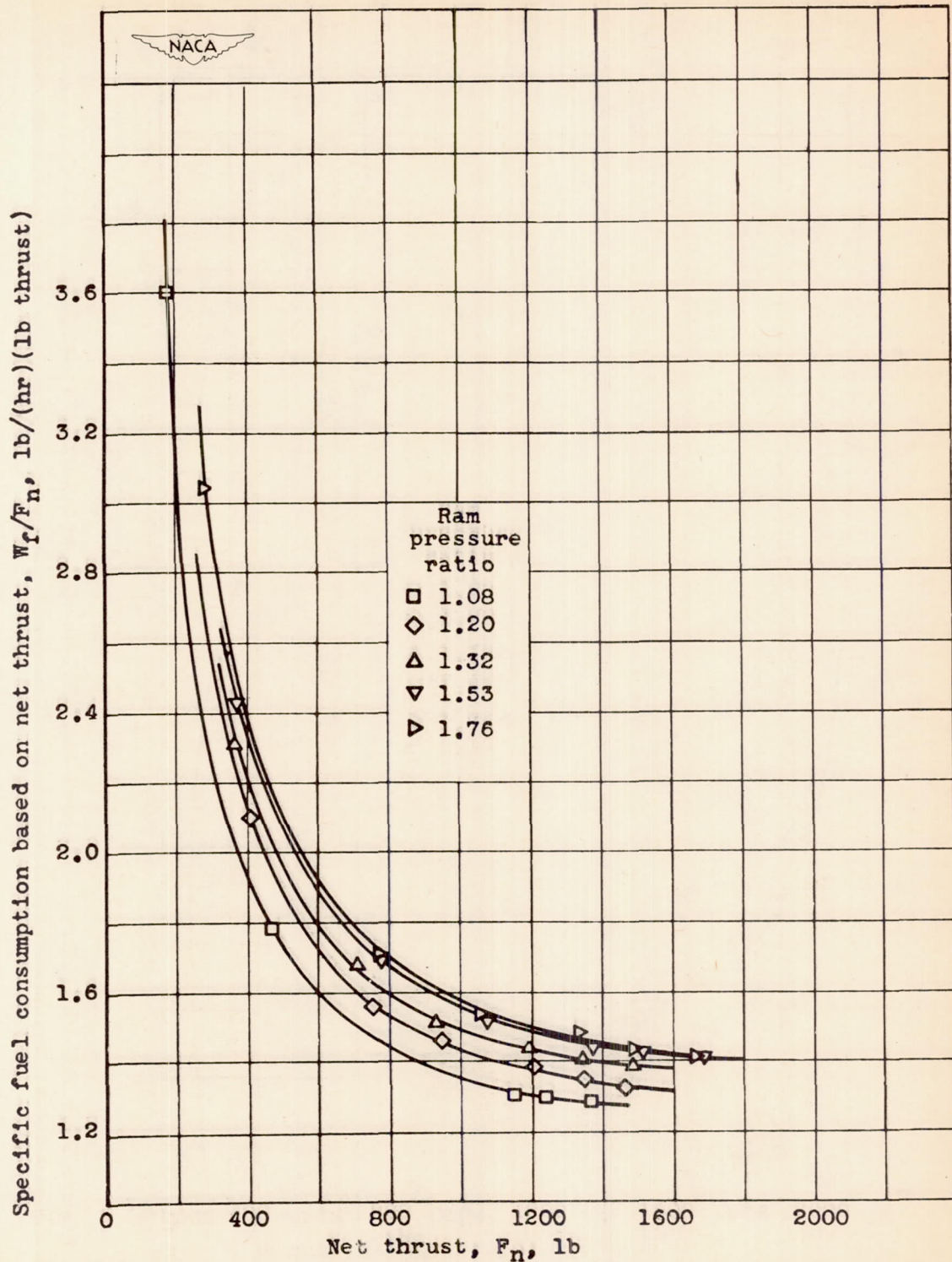
Figure 28.- Variation of specific fuel consumption based on net thrust with ram pressure ratio and net thrust at altitude of 30,000 feet.
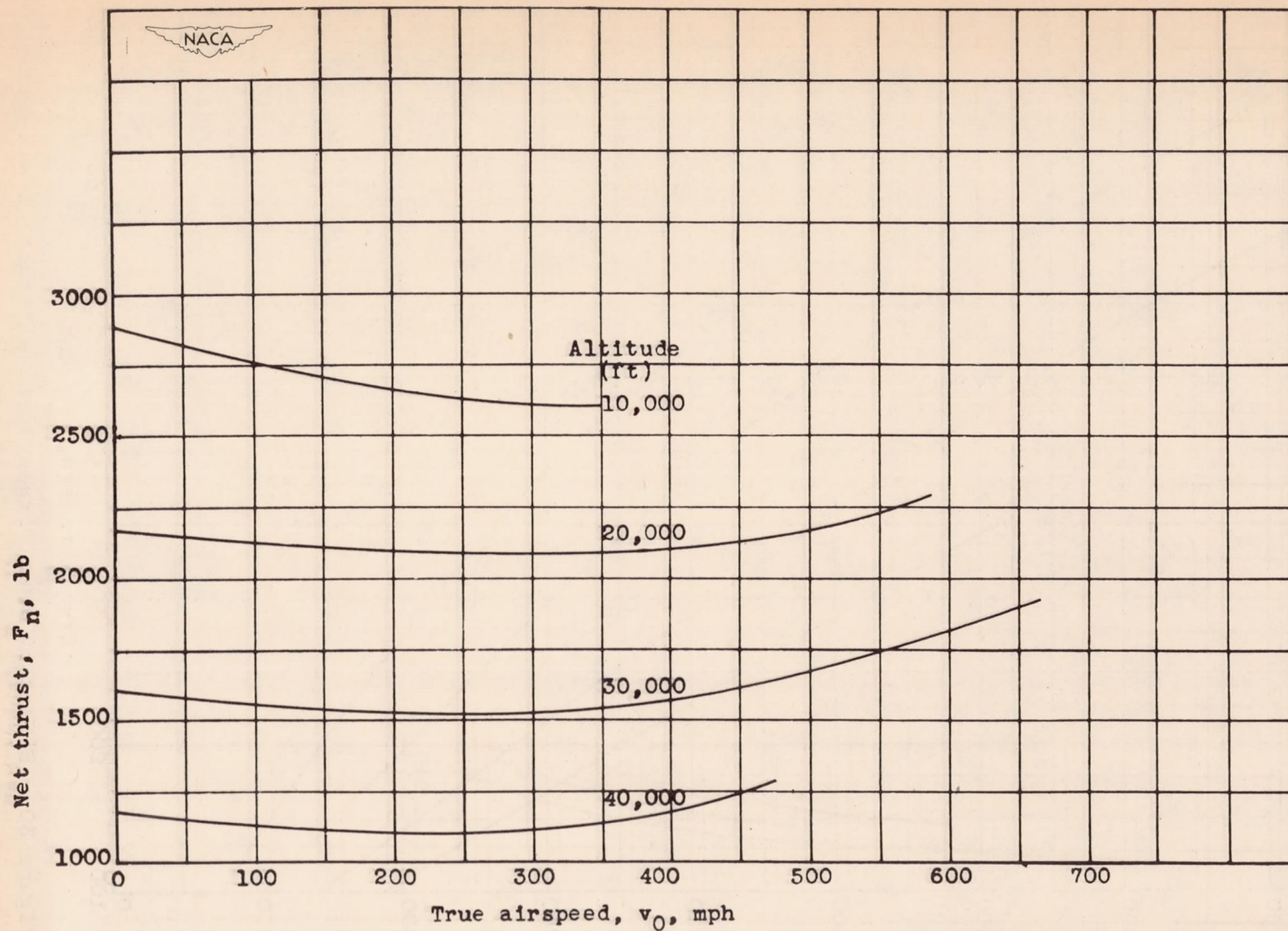
Figure 29.- Effect of true airspeed and altitude on net thrust at engine speed of 11,500 rpm.
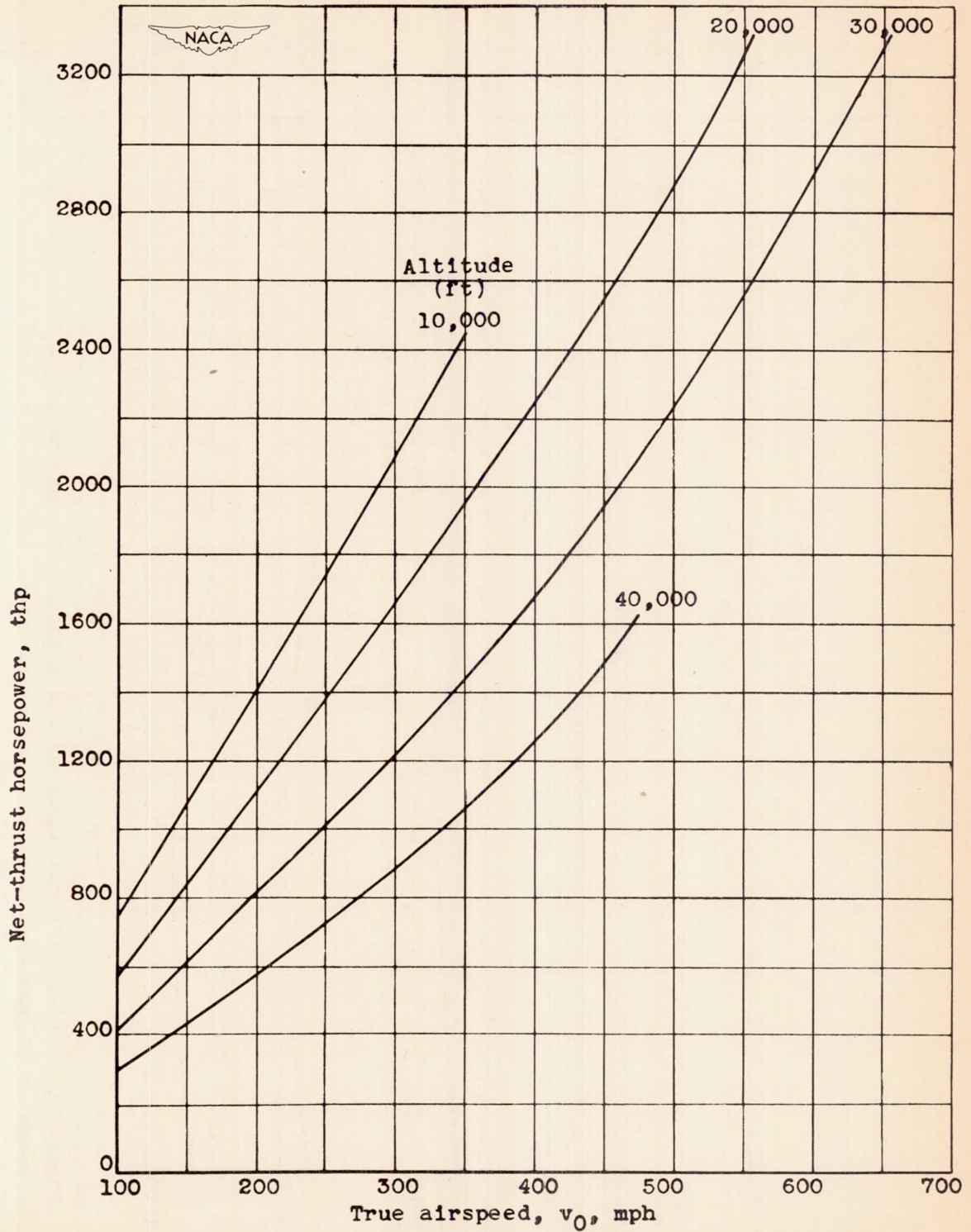
Figure 30.- Effect of true airspeed and altitude on net-thrust
horsepower at engine speed of 11,500 rpm.
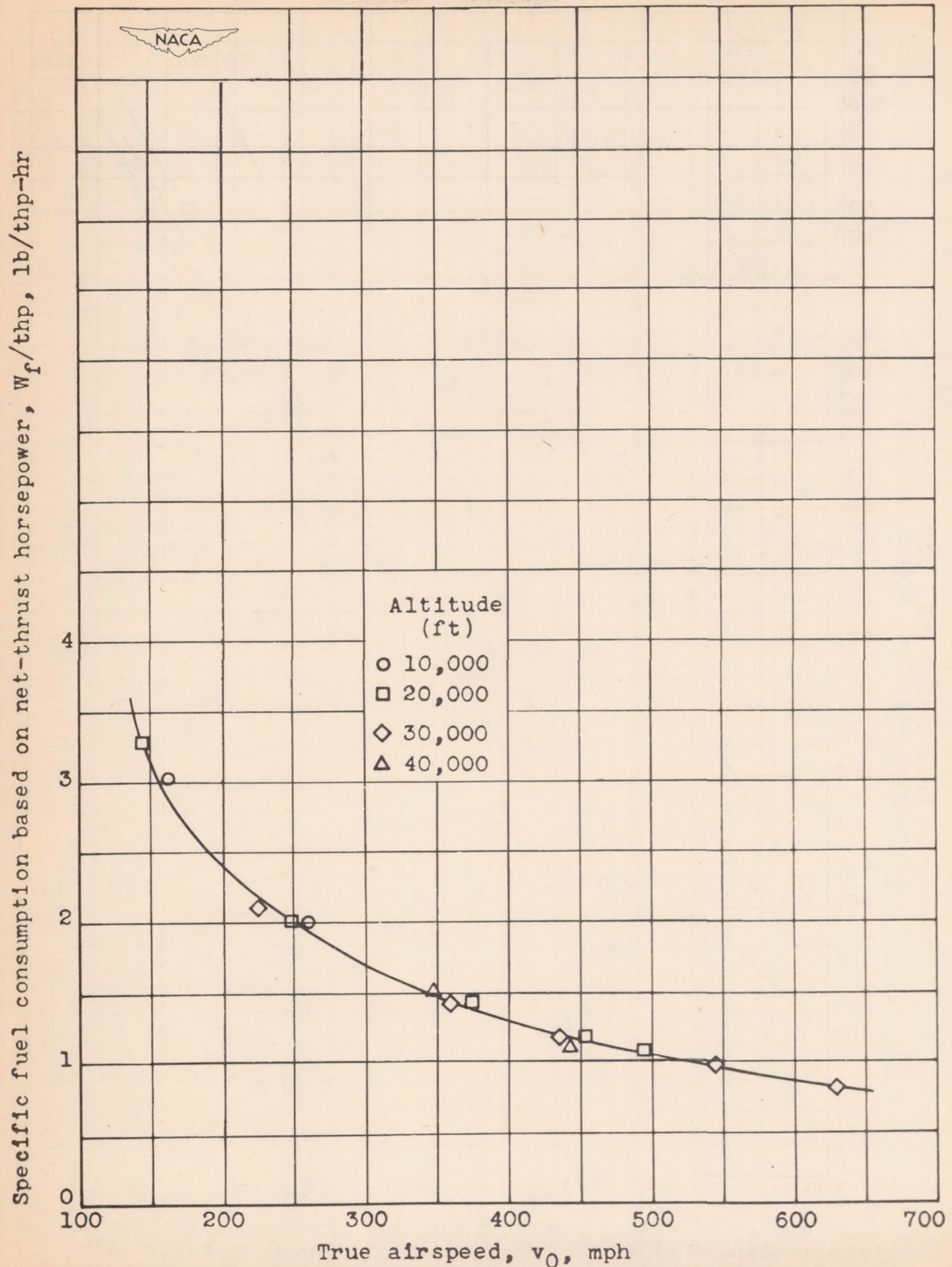
Figure 31.- Effect of true airspeed and altitude on specific
fuel consumption based on net-thrust horsepower at engine
speed of 11,500 rpm.
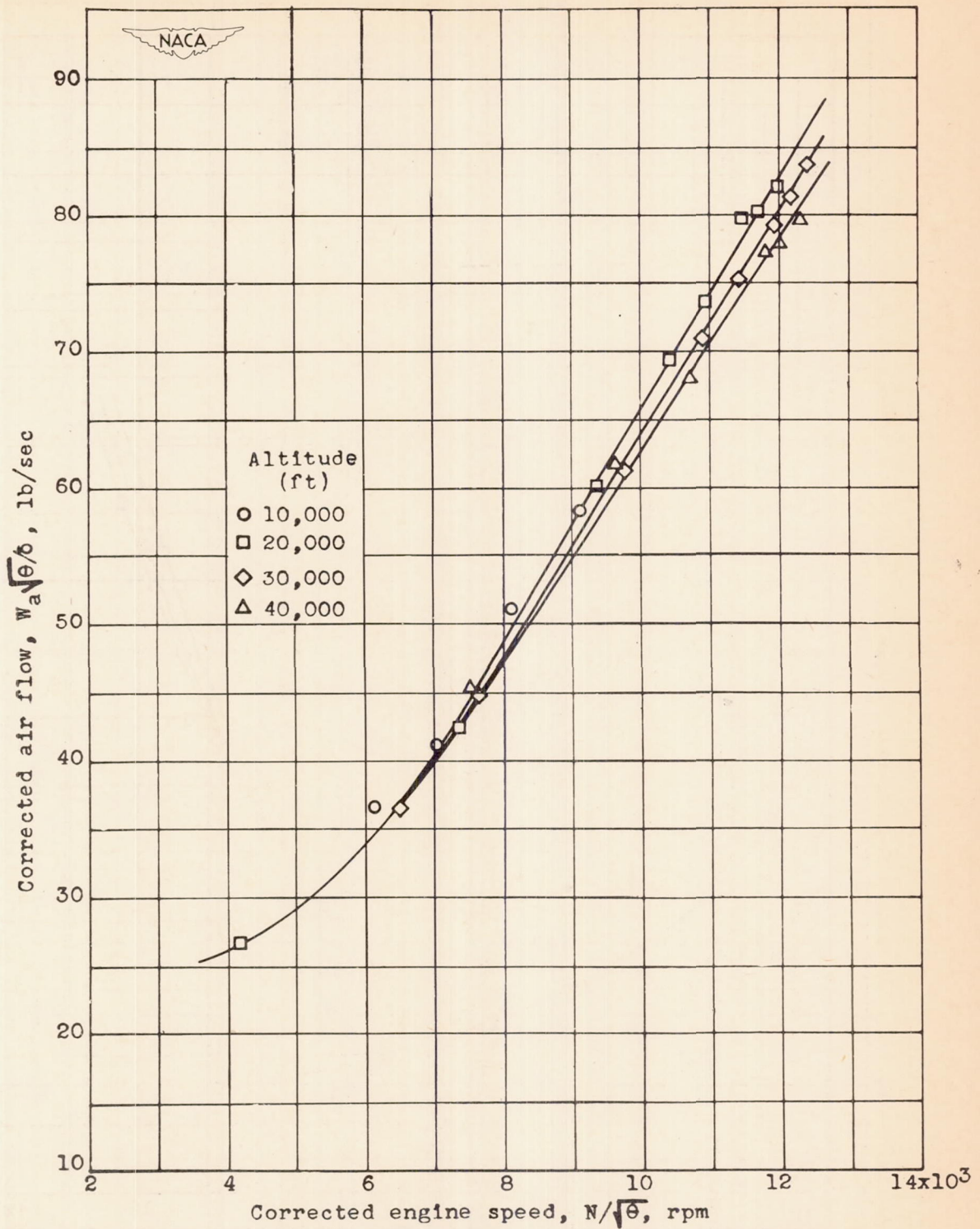
Figure 32.– Effect of corrected engine speed and altitude on corrected air flow at ram pressure ratio of approximately 1.2. Air flow and engine speed corrected to NACA standard atmospheric conditions at sea level.
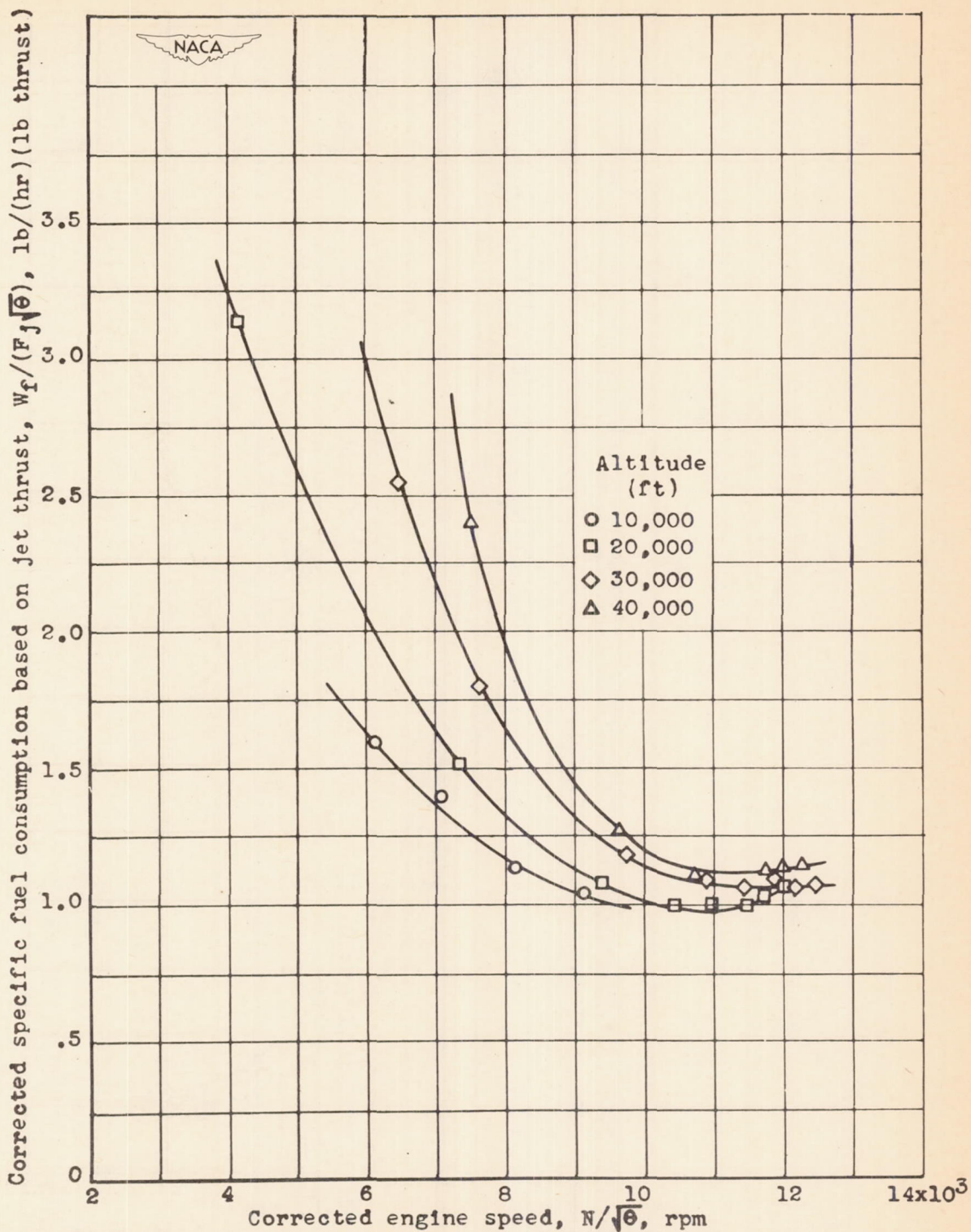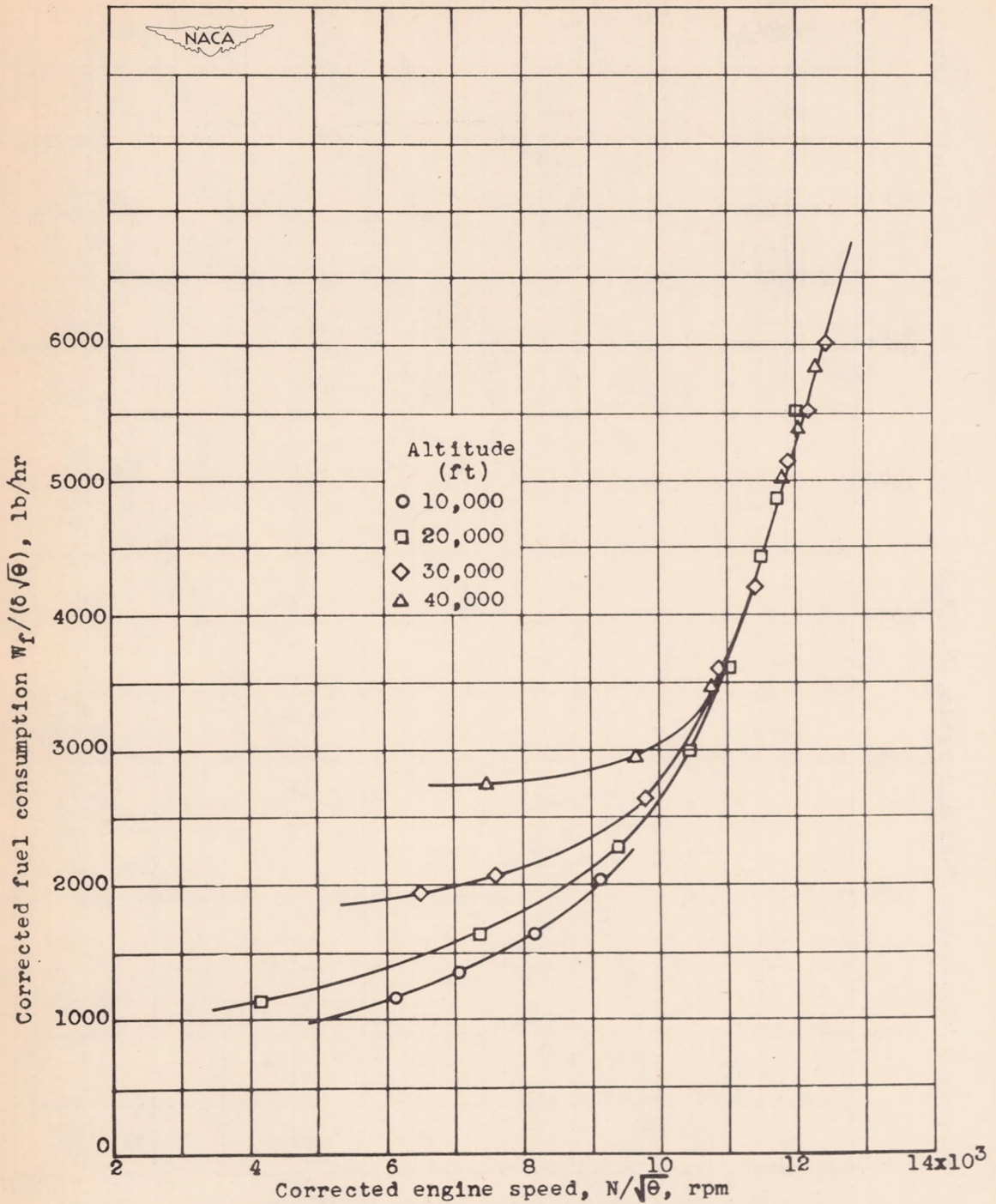
626
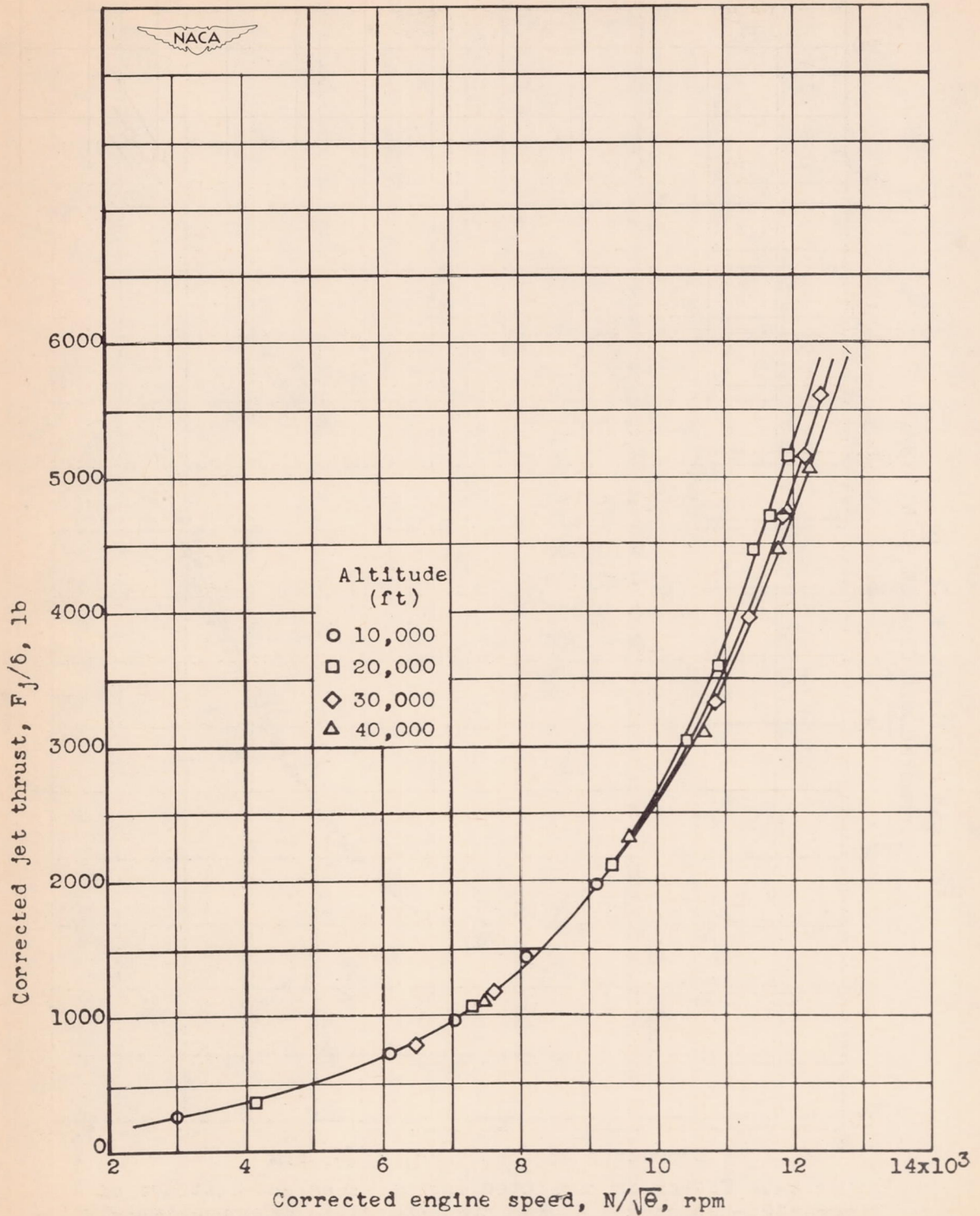


Figure 33.- Effect of corrected engine speed and altitude on corrected jet thrust at ram pressure ratio of approximately 1.2. Engine speed and jet thrust corrected to NACA standard atmospheric conditions at sea level.
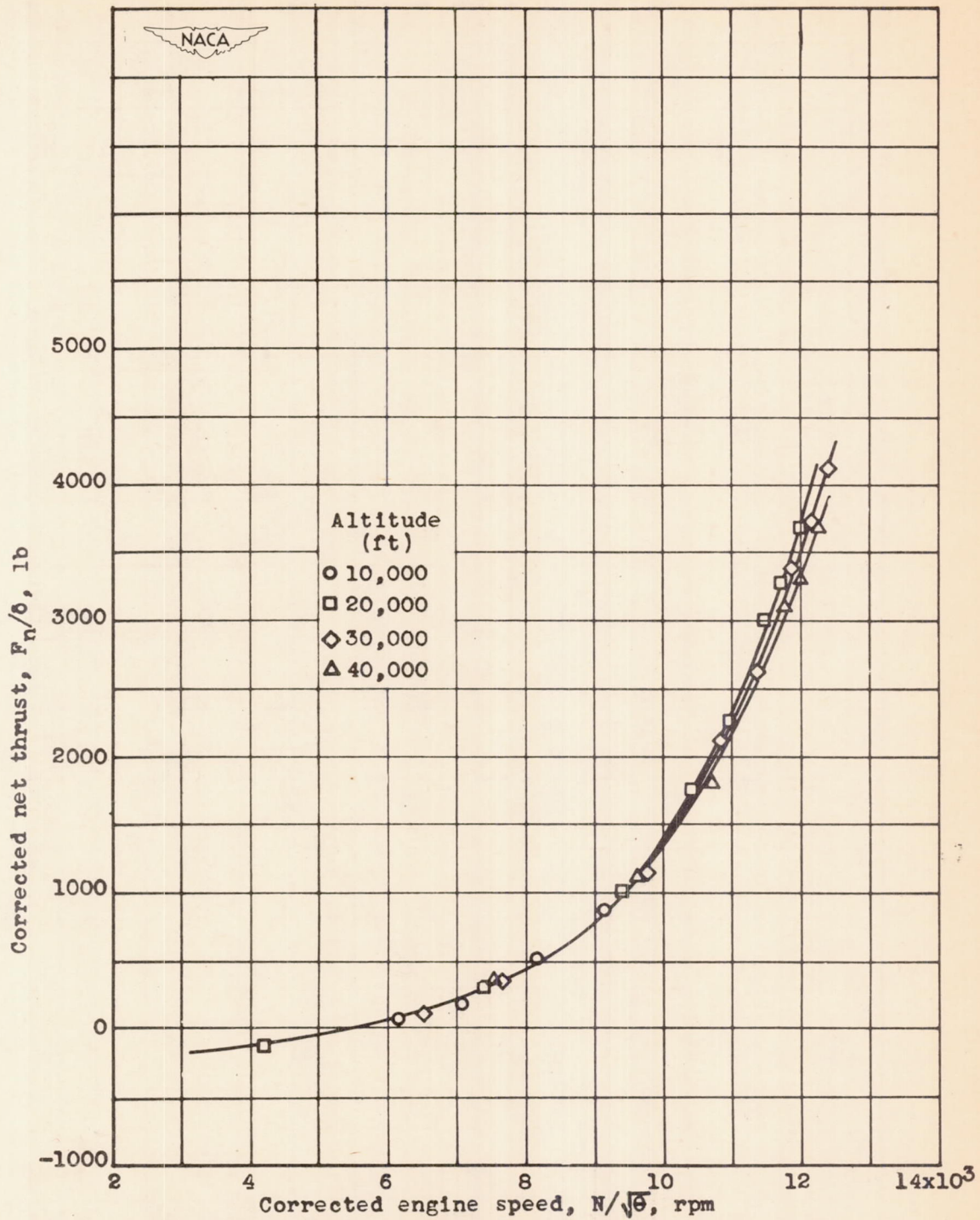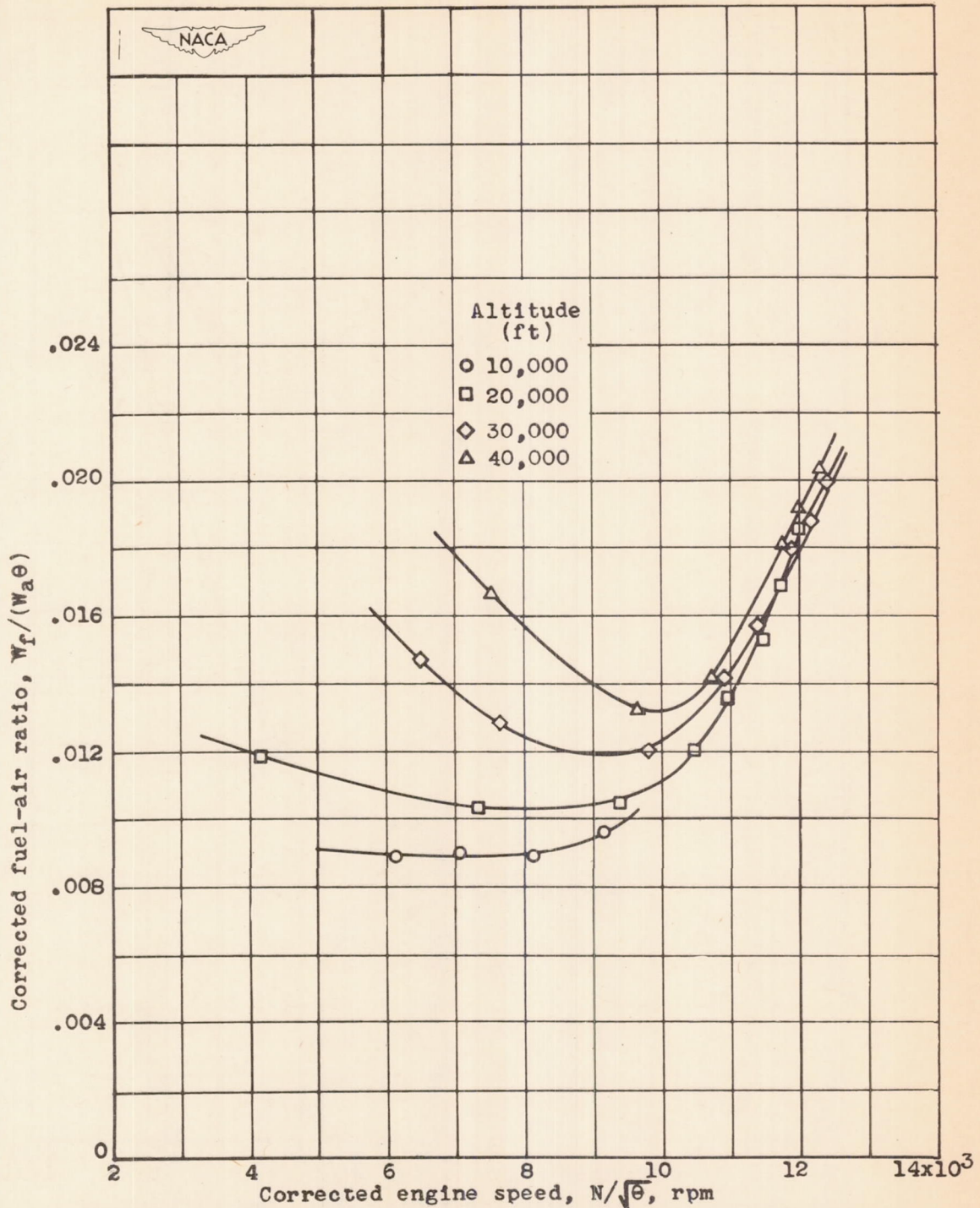
Figure 34.- Effect of corrected engine speed and altitude on corrected net thrust at ram pressure ratio of approximately 1.2. Engine speed and net thrust corrected to NACA standard atmospheric conditions at sea level.
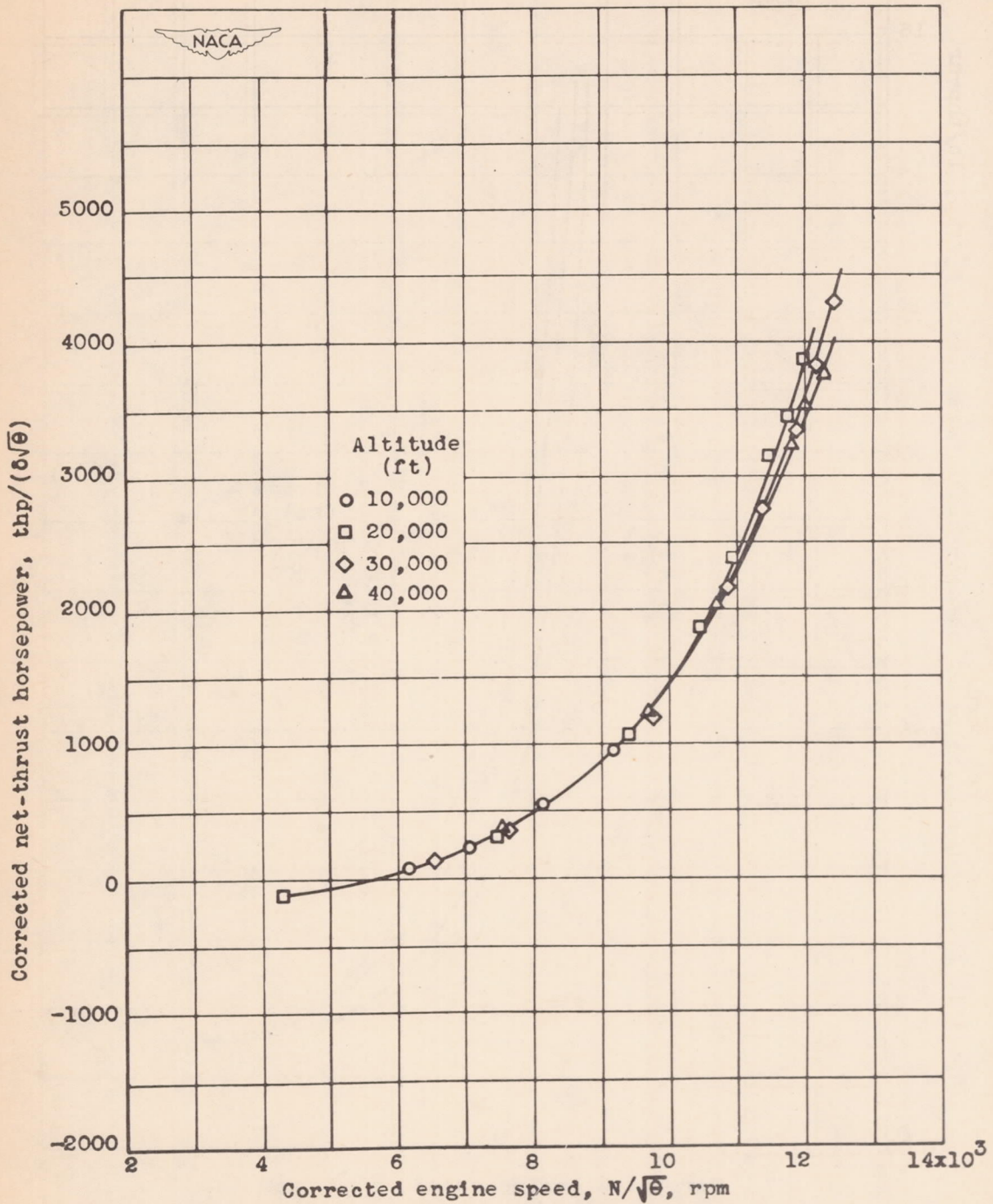
Figure 35.— Effect of corrected engine speed and altitude on
corrected net-thrust horsepower at ram pressure ratio of
approximately 1.2.  Engine speed and net-thrust horsepower
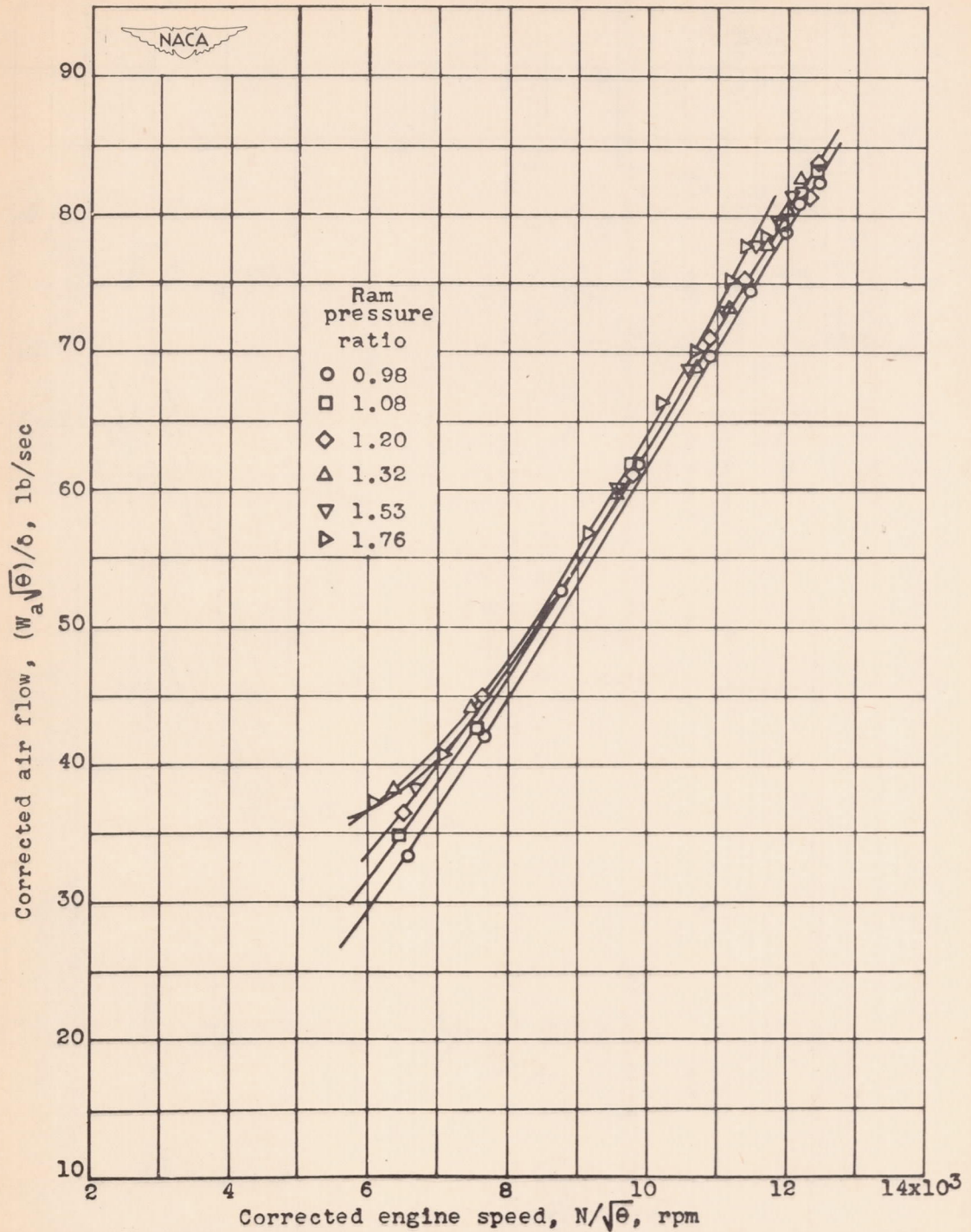corrected to NACA standard atmospheric conditions at sea
level.
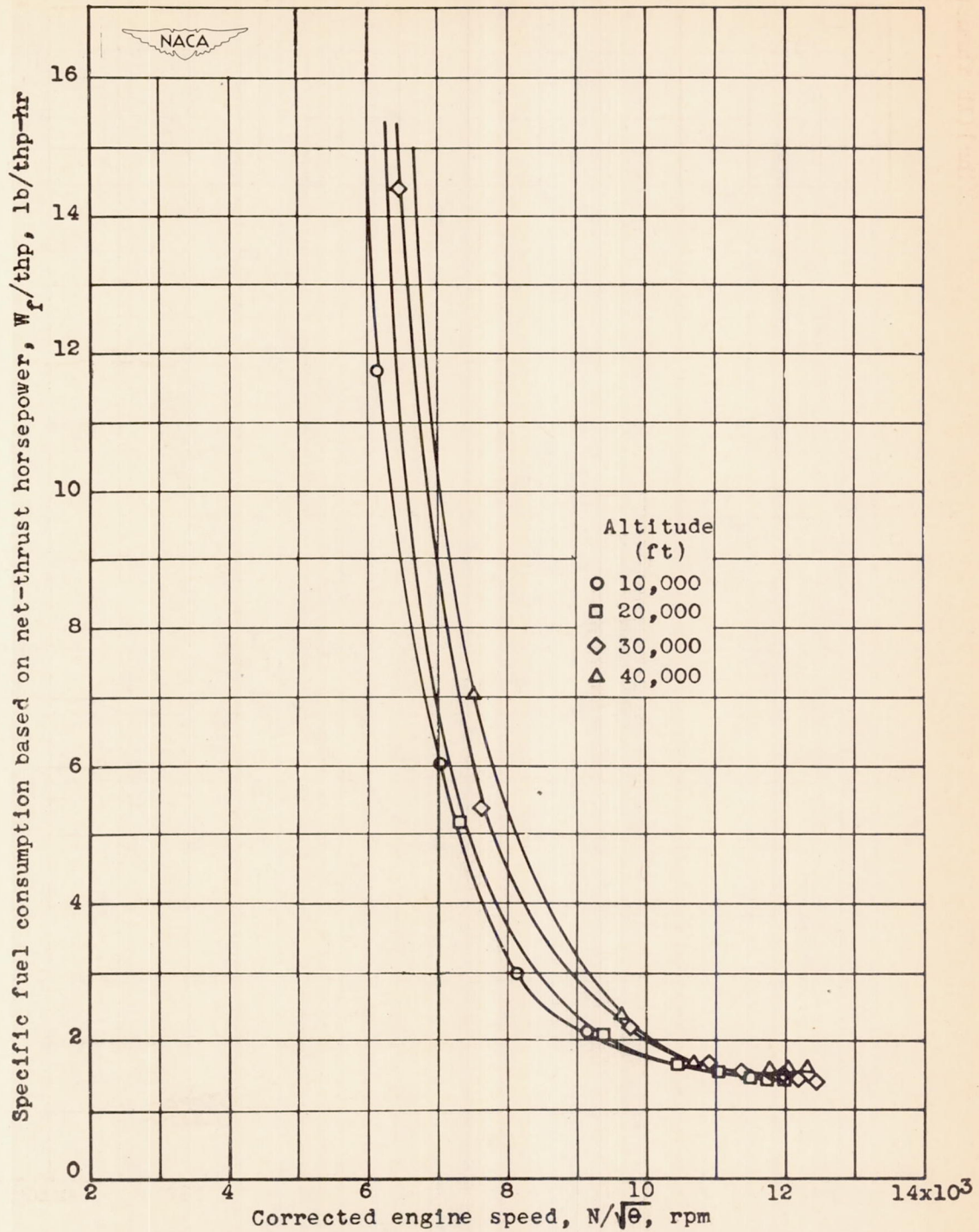
Figure 36.- Effect of corrected engine speed and altitude on specific fuel consumption based on net-thrust horsepower at ram pressure ratio of approximately 1.2. Engine speed corrected to NACA standard atmospheric conditions at sea level.
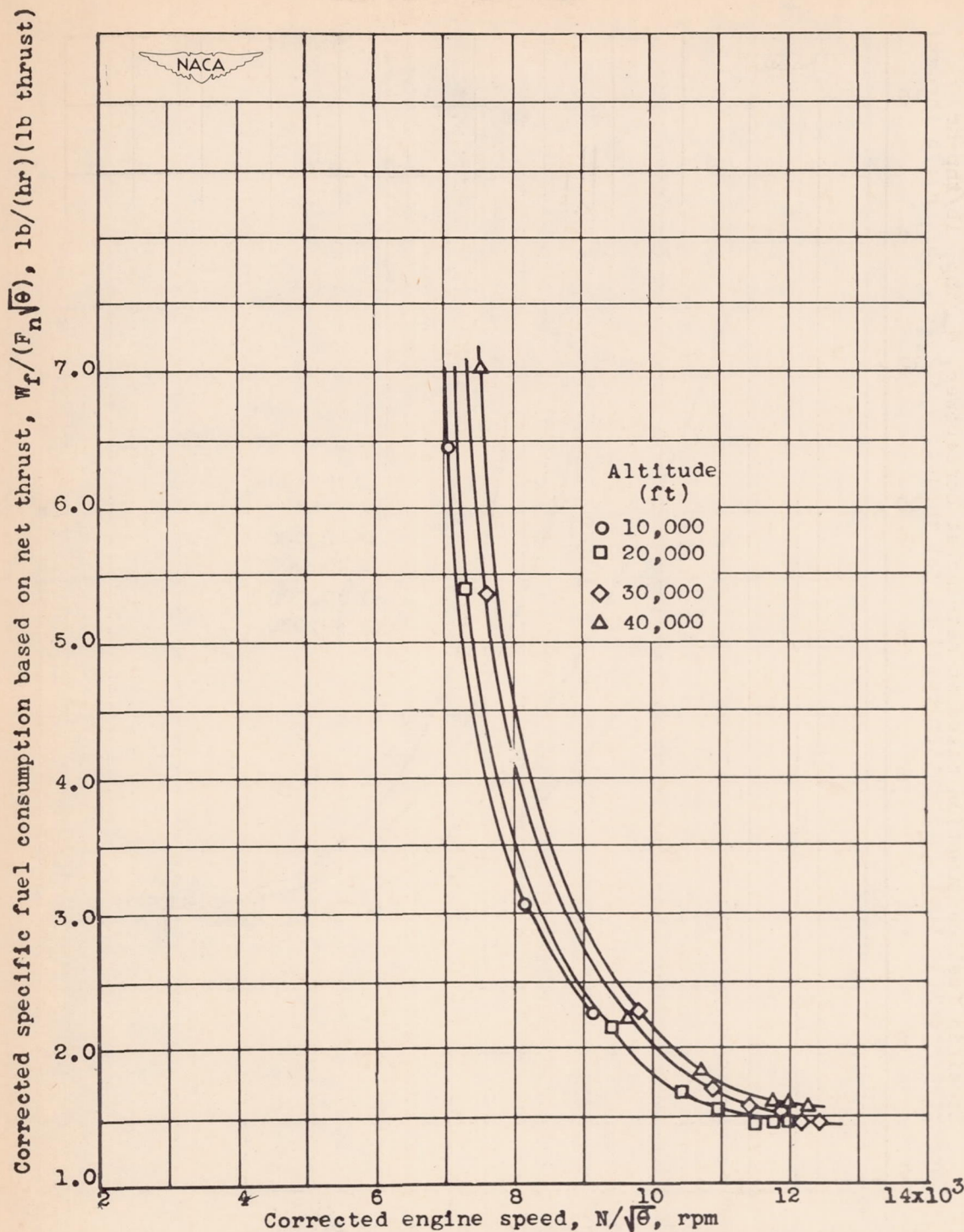
Figure 37.- Effect of corrected engine speed and altitude on corrected specific fuel consumption based on net thrust at ram pressure ratio of approximately 1.2. Engine speed and specific fuel consumption corrected to NACA standard atmospheric conditions at sea level.

Figure 38.- Effect of corrected engine speed and altitude on
corrected specific fuel consumption based on jet thrust at
ram pressure ratio of approximately 1.2.  Engine speed and
specific fuel consumption corrected to NACA standard atmos-
pheric conditions at sea level.

Figure 39.- Effect of corrected engine speed and altitude on
corrected fuel consumption at ram pressure ratio of approxi-
mately 1.2. Engine speed and fuel consumption corrected to
NACA standard atmospheric conditions at sea level.

Figure 40.- Effect of corrected engine speed and altitude on
corrected fuel-air ratio at ram pressure ratio of approxi-
mately 1.2.   Engine speed and fuel-air ratio corrected to
NACA standard atmospheric conditions at sea level.

Figure 41.- Effect of corrected engine speed and ram pressure
ratio on corrected air flow at altitude of 30,000 feet.
Engine speed and air flow corrected to NACA standard atmos-
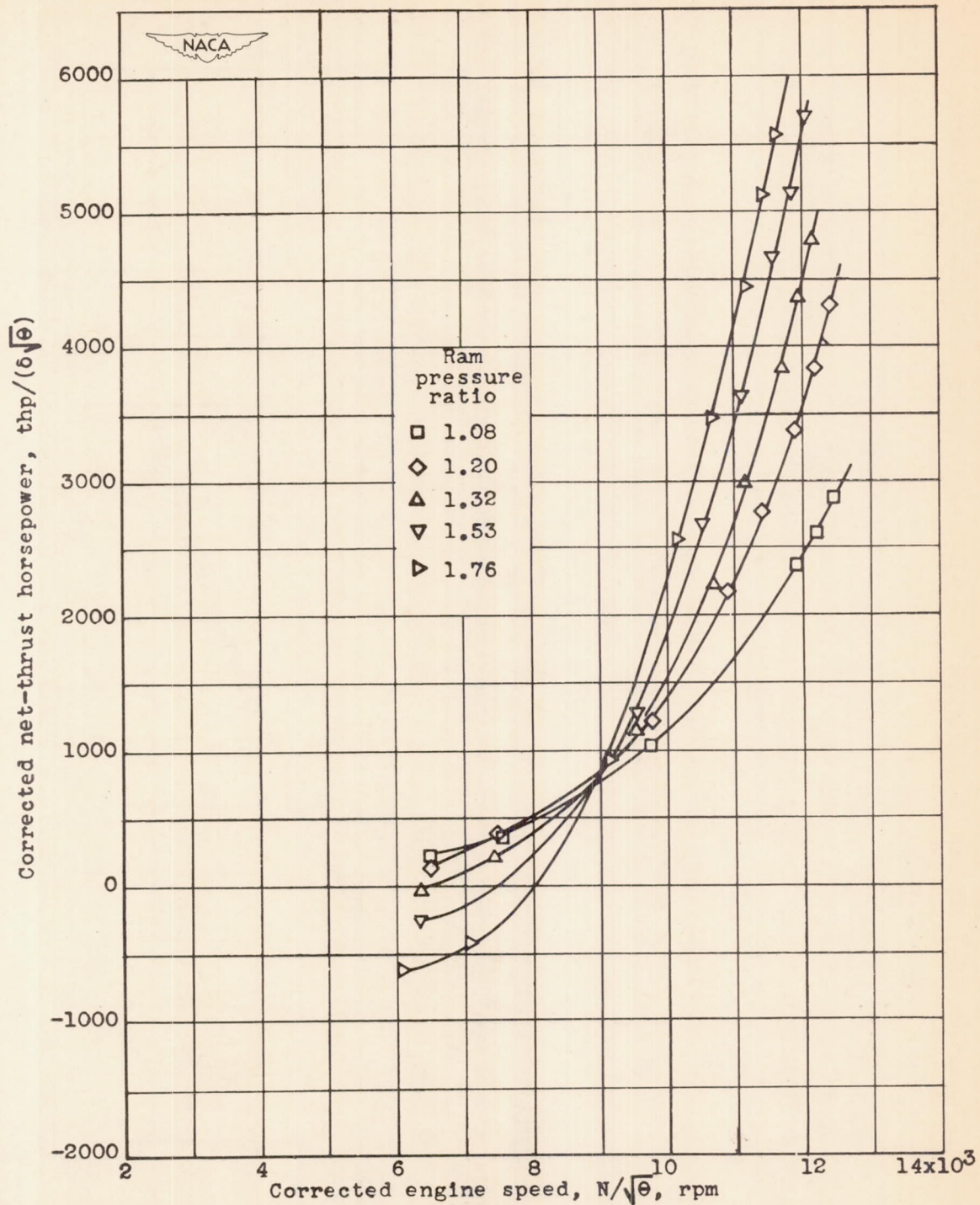pheric conditions at sea level.
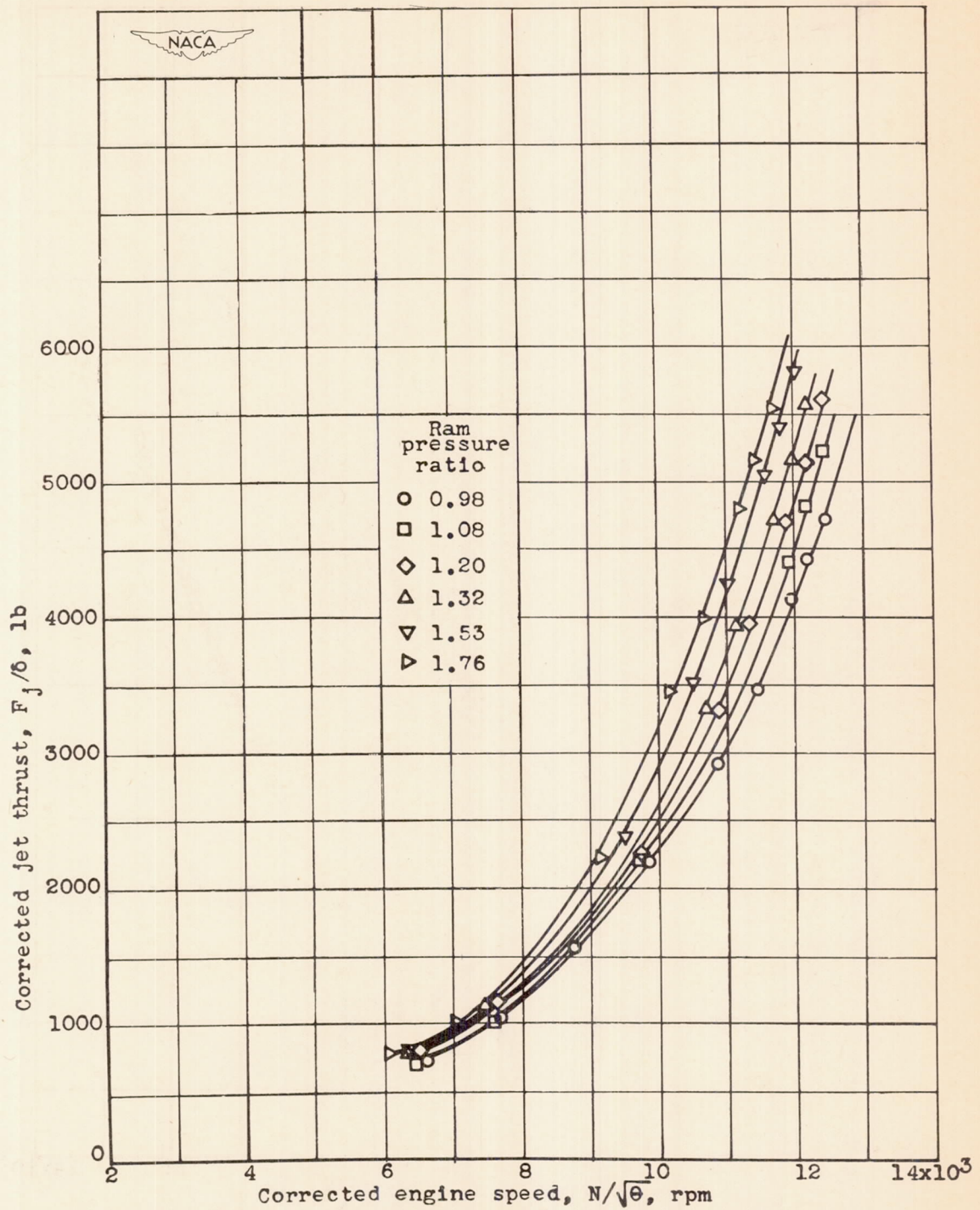
Figure 42.- Effect of corrected engine speed and ram pressure
ratio on corrected jet thrust at altitude of 30,000 feet.
Engine speed and jet thrust corrected to NACA standard atmos-
pheric conditions at sea level.
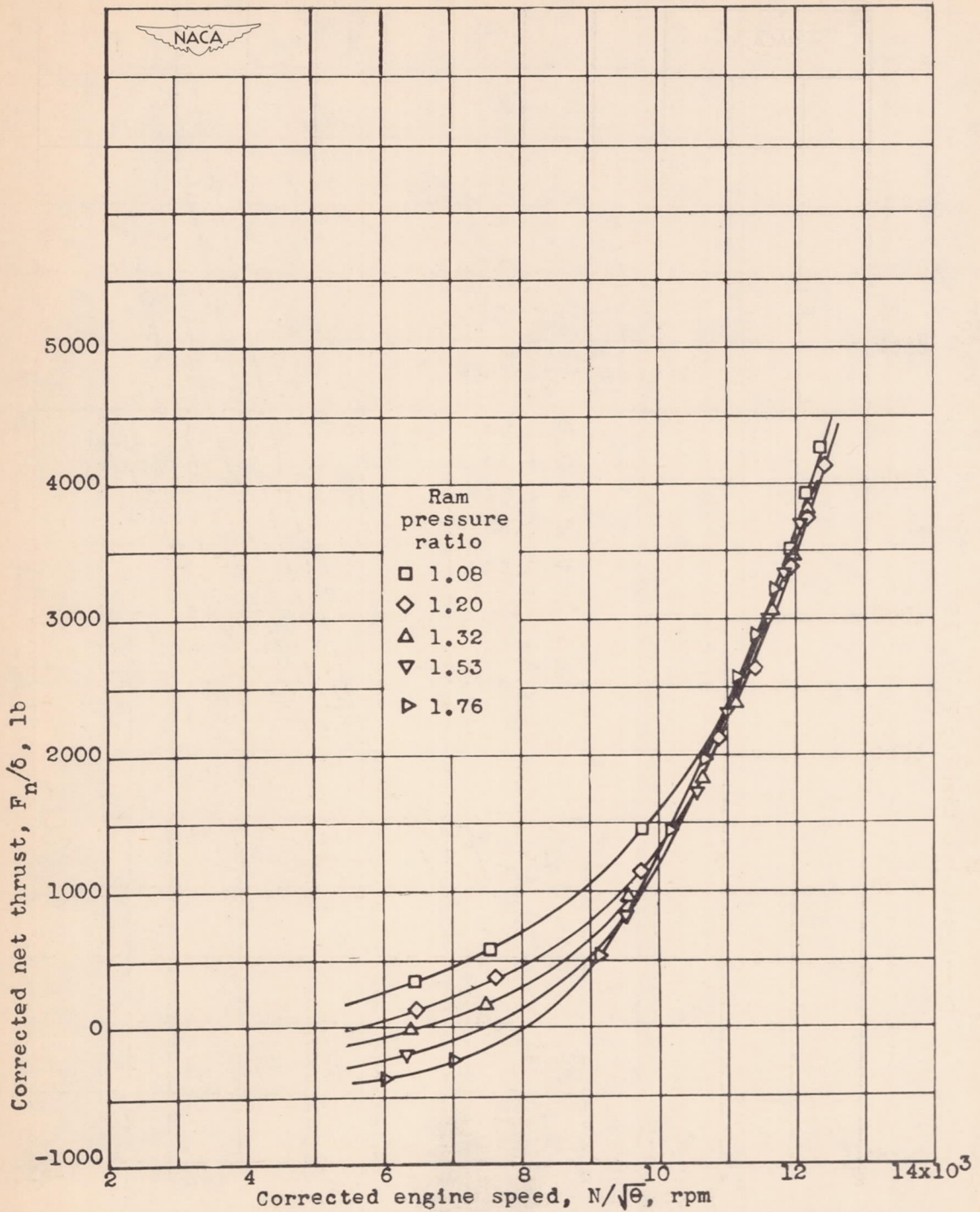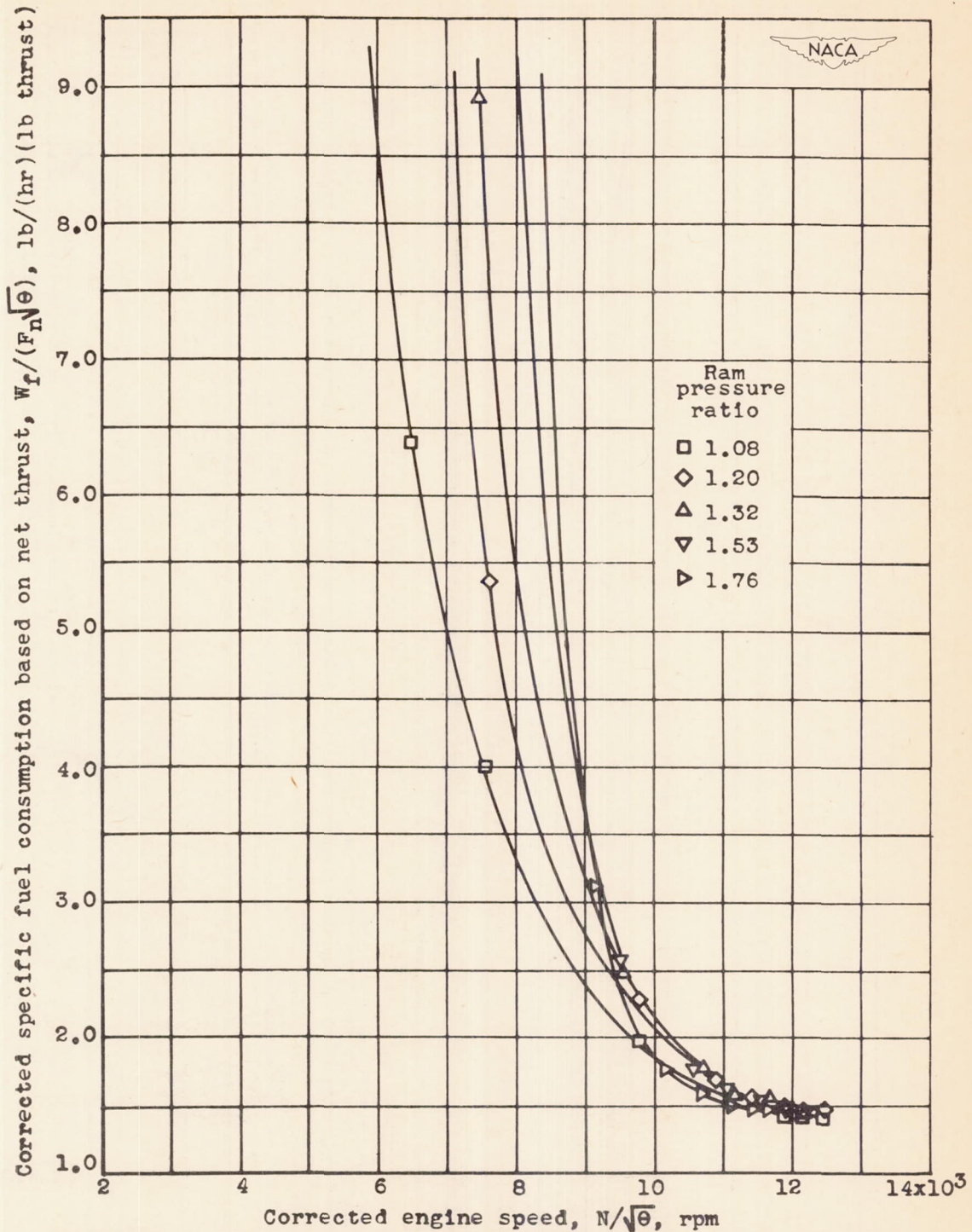
Figure 43.- Effect of corrected engine speed and ram pressure
ratio on corrected net thrust at altitude of 30,000 feet.
Engine speed and net thrust corrected to NACA standard atmos-
pheric conditions at sea level.

Figure 44.- Effect of corrected engine speed and ram pressure
ratio on corrected net-thrust horsepower. Engine speed and
net-thrust horsepower corrected to NACA standard atmospheric
conditions at sea level.
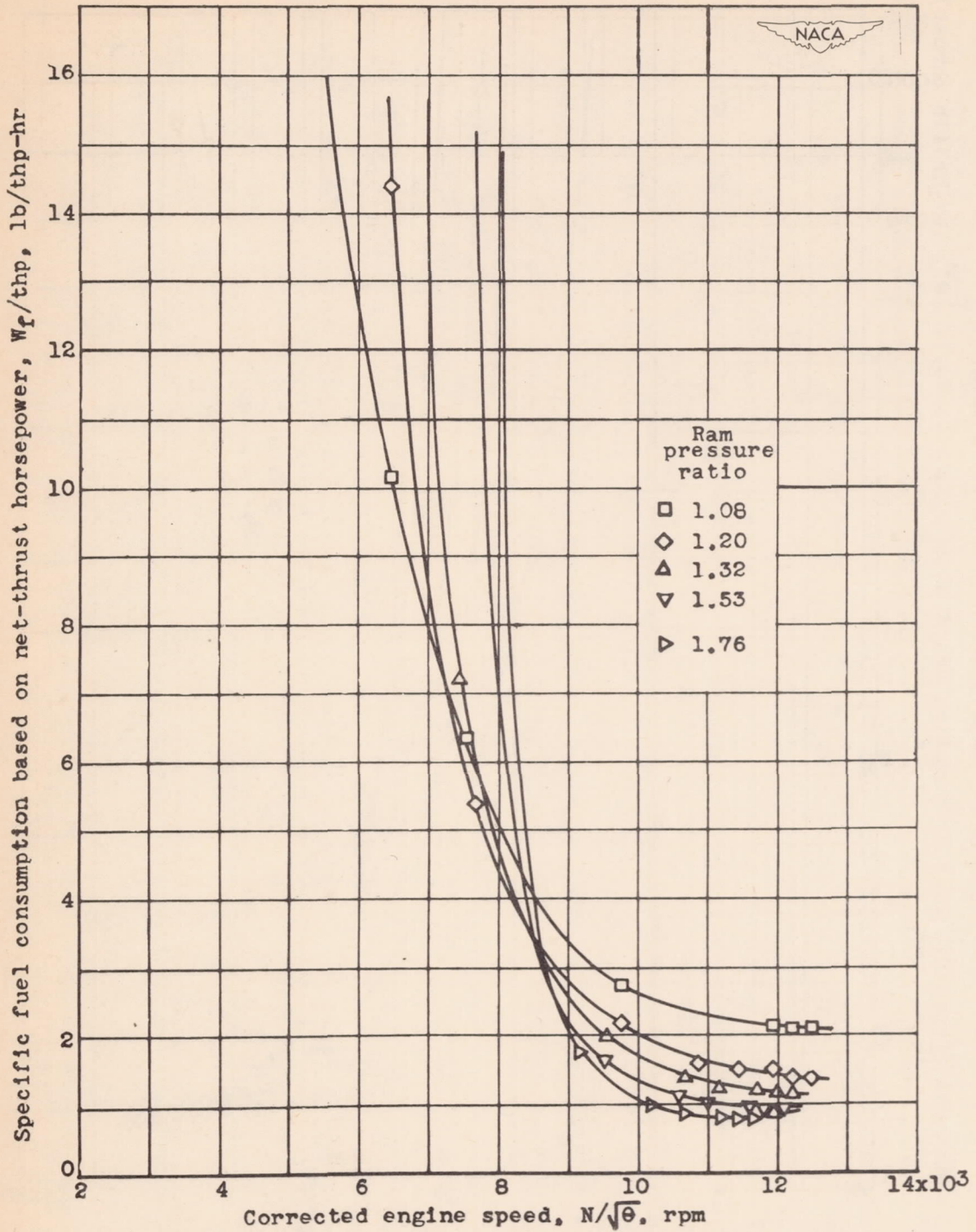
Figure 45.- Effect of corrected engine speed and ram pressure
ratio on specific fuel consumption based on net-thrust horse-
power at altitude of 30,000 feet. Engine speed corrected to
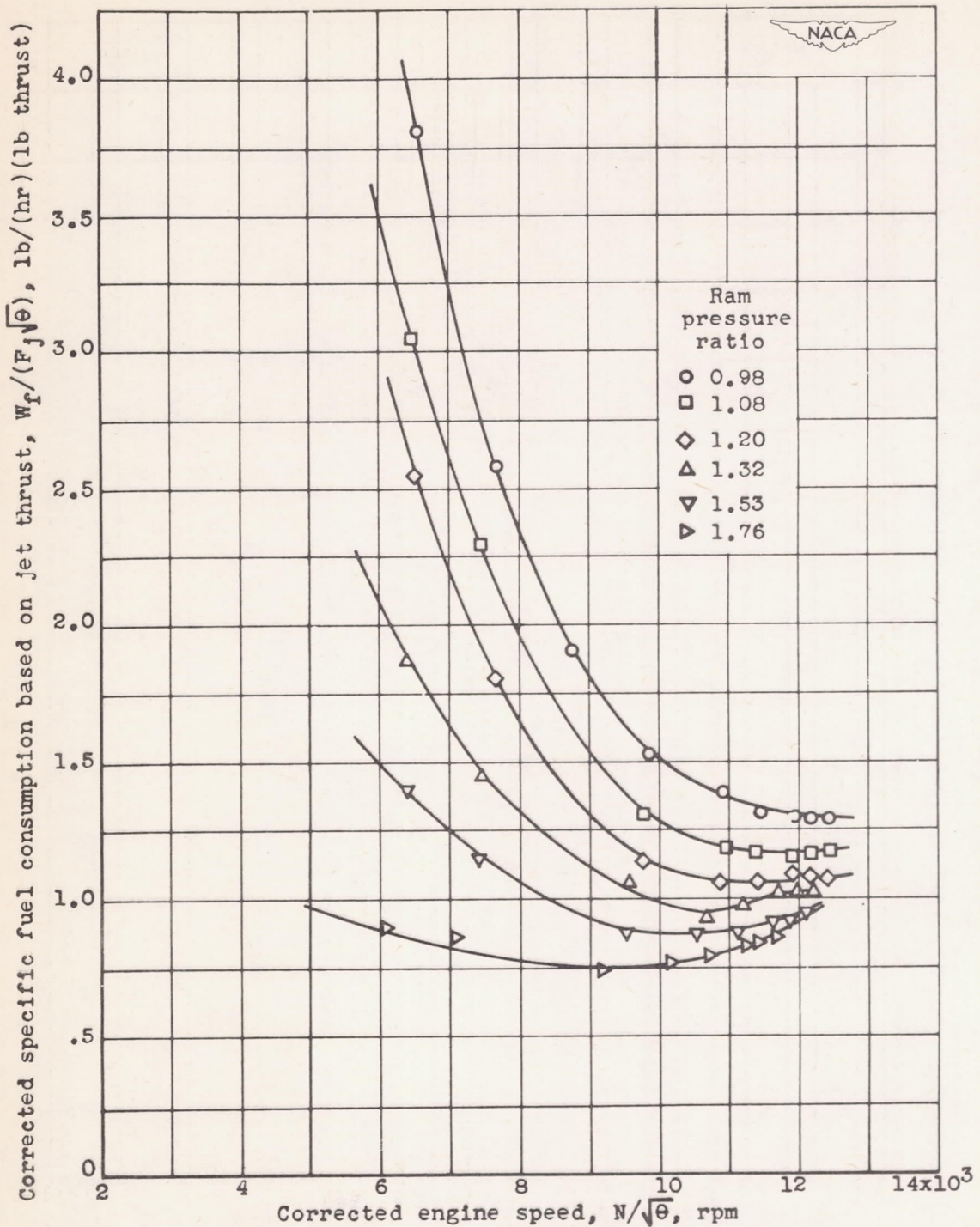NACA standard atmospheric conditions at sea level.

Figure 46.- Effect of corrected engine speed and ram pressure
ratio on corrected specific fuel consumption based on net
thrust at altitude of 30,000 feet. Engine speed and specific
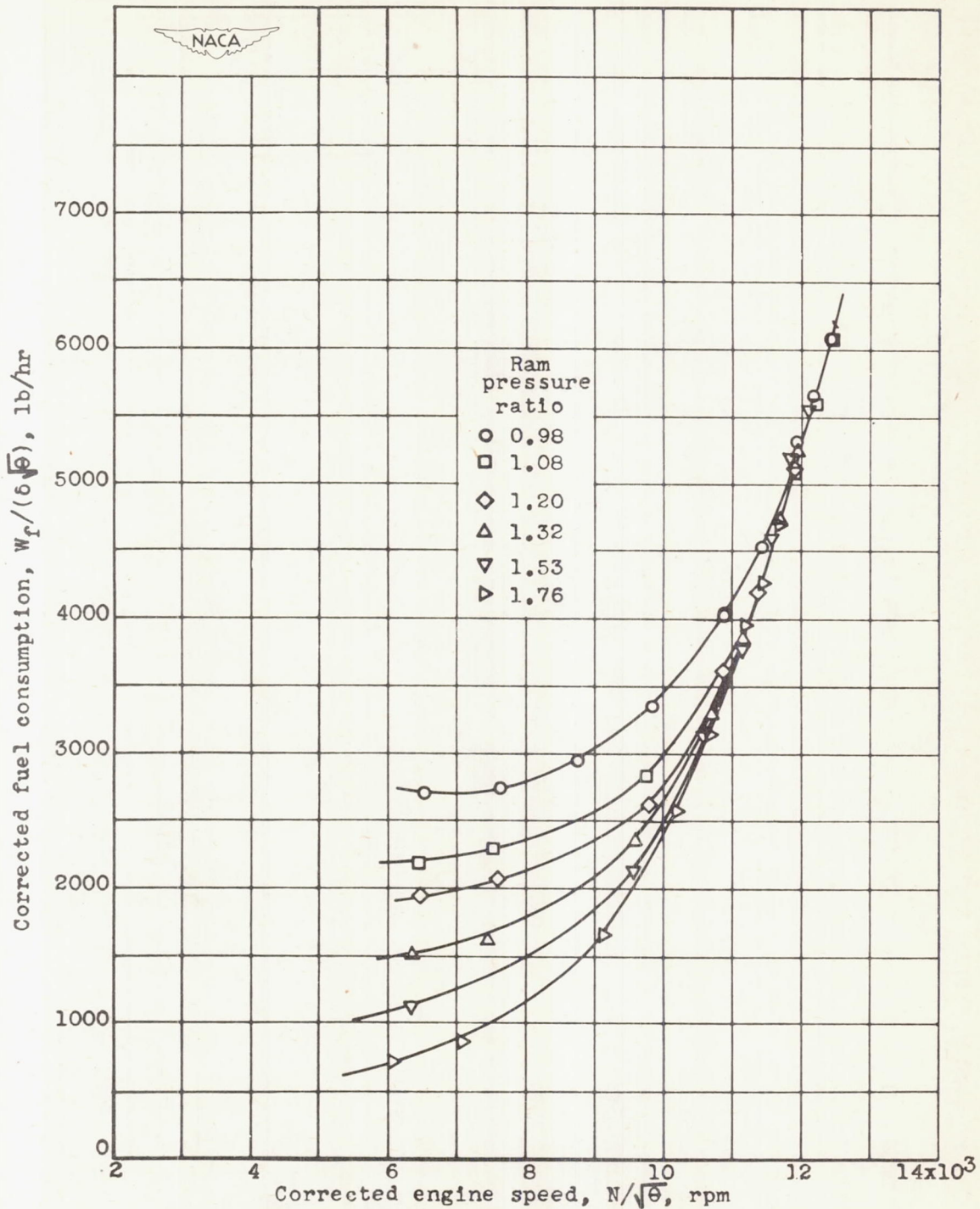fuel consumption corrected to NACA standard atmospheric con-
ditions at sea level.

Figure 47.— Effect of corrected engine speed and ram pressure
ratio on corrected specific fuel consumption based on jet
thrust at altitude of 30,000 feet. Engine speed and specific
fuel consumption corrected to NACA standard atmospheric con-
ditions at sea level.

Figure 48.- Effect of corrected engine speed and ram pressure
ratio on corrected fuel consumption at altitude of 30,000
feet. Engine speed and fuel consumption corrected to NACA
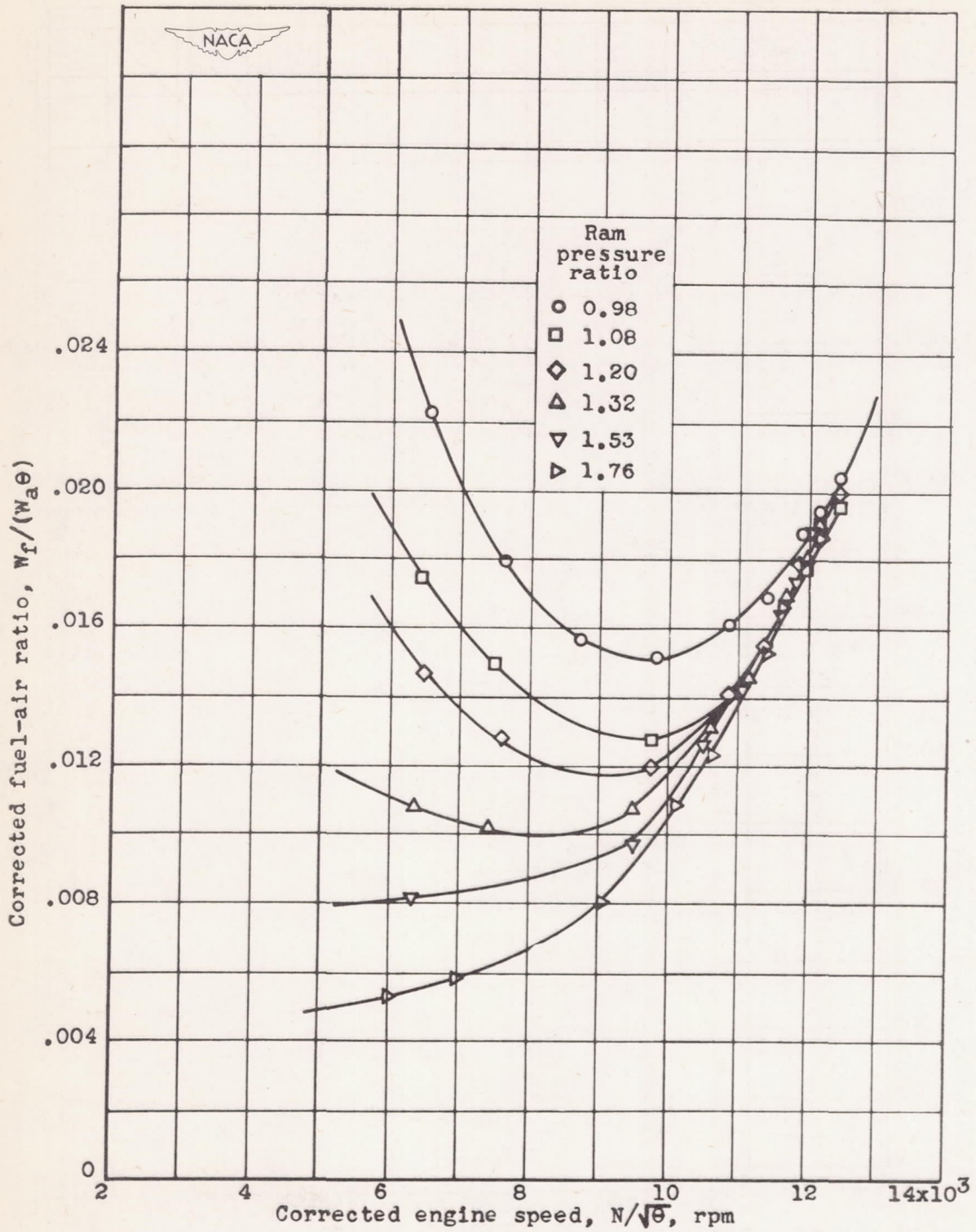standard atmospheric conditions at sea level.

Figure 49.- Effect of corrected engine speed and ram pressure ratio on corrected fuel-air ratio at altitude of 30,000 feet. Engine speed and fuel-air ratio corrected to NACA standard atmospheric conditions at sea level.
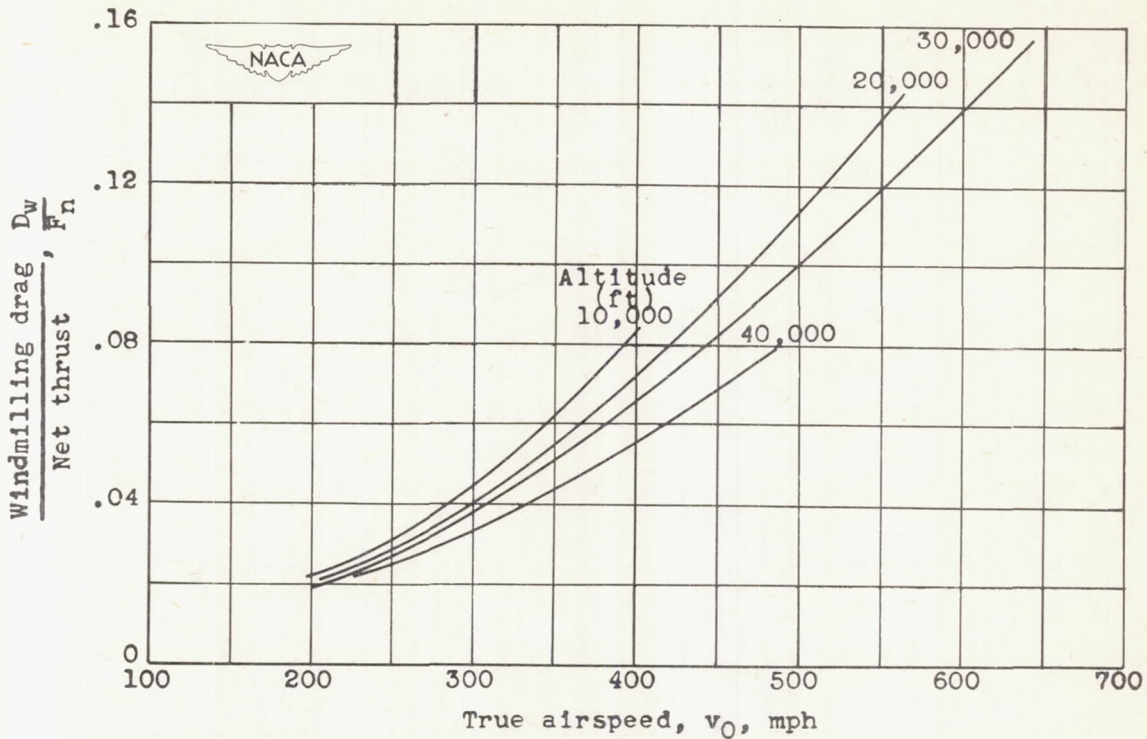
Figure 50.- Effect of altitude and true airspeed on ratio of windmilling drag to net thrust at engine speed of 11,500 rpm.
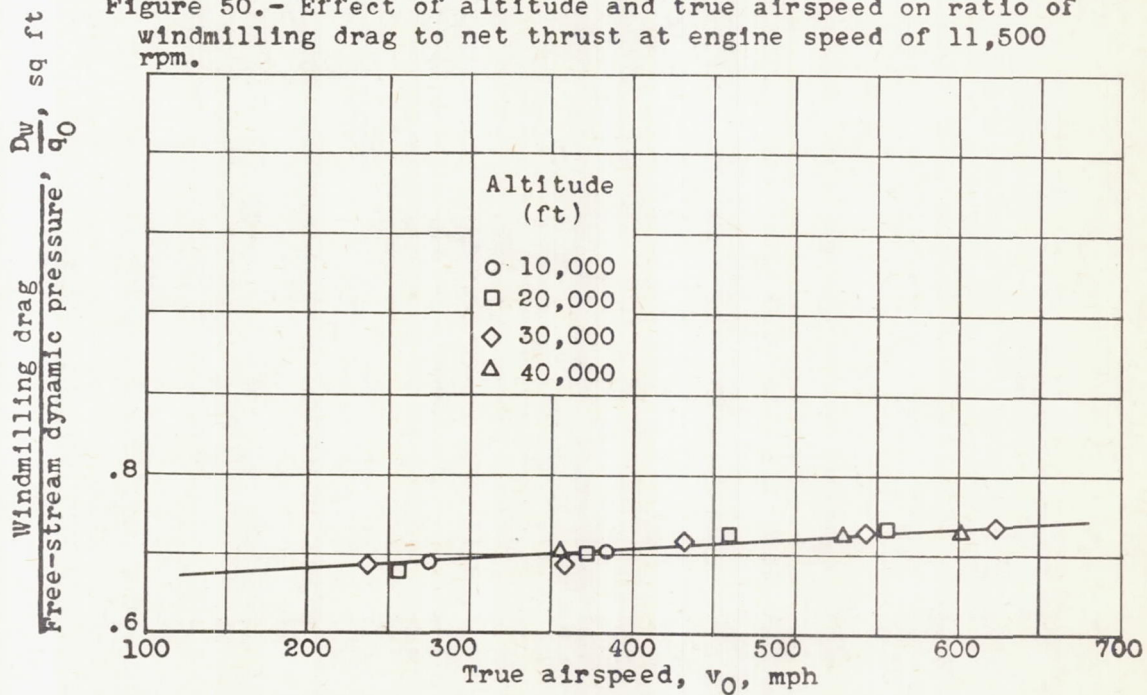


Figure 51.- Effect of pressure altitude and true airspeed on ratio of windmilling drag to free-stream dynamic pressure.
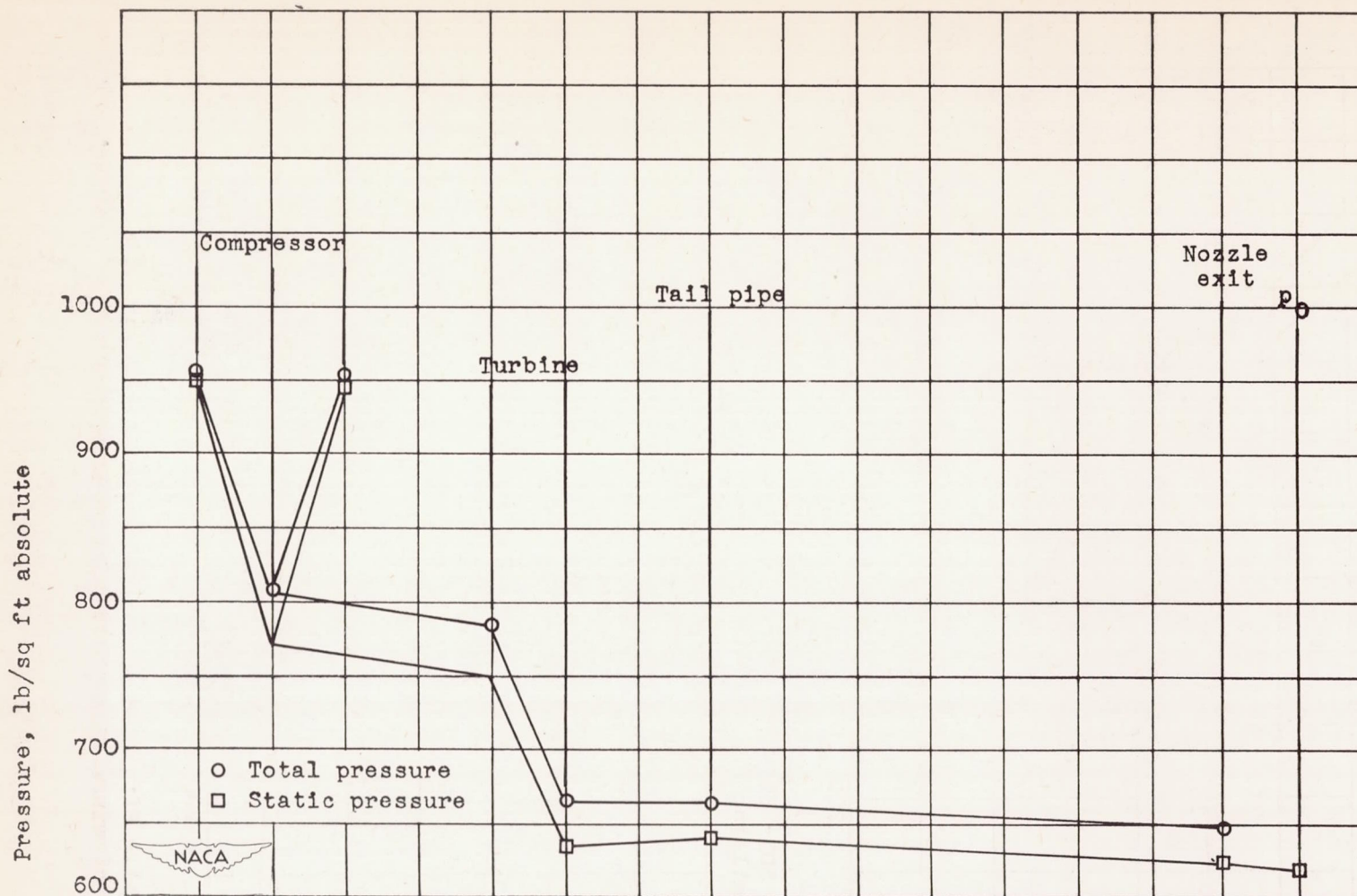
Figure 52.- Windmilling pressure survey of I-40 jet-propulsion engine.  Pressure altitude, 30,000 feet; true airspeed, 543 miles per hour; ram pressure ratio, 1.53.